For Whom the Bridge Tolls:
Congestion, Air Pollution, and Second-Best Road Pricing

Matthew Tarduno[†]

December 2024

Click here for the latest version

Abstract

Real-world congestion zones are imperfect because they charge heterogeneous road users uniform prices, and invite externality spillovers in space and time. I show that given these imperfections, calculating optimal prices requires (i) individual-level externalities, (ii) individual elasticities, and (iii) cross-price elasticities between priced and unpriced trips. Using bridge toll microdata and a natural experiment where peak-hour pricing was imposed on one of the San Francisco Bay Area's 4 trans-bay bridges, I estimate a discrete choice model of driving demand that yields these parameters. I then use this model to estimate optimal prices for proposed congestion zones in three U.S. cities. I find that leakage pushes second-best prices below trip-level externalities, and that optimal peak pricing recovers just 10-41% of the welfare gains of a first-best policy.

[†] University of Illinois at Chicago; tarduno@uic.edu. I thank James Sallee, Michael Anderson, and Reed Walker for their support throughout this project. I also thank Lucas Davis, Meredith Fowlie, Marco Gonzalez-Navarro, Alan Auerbach, Josh Apte, Max Auffhammer, Sofia Villas-Boas, Severin Borenstein, James Sears, Jenya Kahn-Lang, Marshall Blundell, Matthew Suandi, Elif Tasar, Eva Lyubich, Sara Johns, Matt Woerman, and Marcus Casey. Seminar participants at UC Berkeley, Williams College, The World Bank, Resources for the Future, NOVA SBE, the University of Rochester, the NYU Institute for Policy Integrity, NC State's Camp Resources, the 11th European Meeting of the Urban Economics Association, and OSWEET provided helpful feedback. Lastly, I would like to thank Jeff Gerbracht for invaluable assistance in accessing and understanding the tolling data used in this paper.

1. Introduction

On June 5$^{\text{th}}$, 2024, in a dramatic reversal, New York Governor Kathy Hochul made the decision to pause New York City's planned Congestion Pricing Program. Although the decision to halt congestion pricing was ultimately political, it reignited the policy debate over how New York's policy ought to be designed. Was the $15 toll originally favored by the MTA the right price? Or was Hochul right to suggest lowering the charge? Similarly, a number of policy attributes that appeared settled, from peak-hour toll designs to alternative exemption schemes, suddenly seemed in play again.

Surprisingly, existing research in urban and environmental economics offers limited prescriptions for New York policymakers. While economists have long advocated for charging road users to address the negative externalities associated with urban driving (Vickrey, 1963; Parry, 2002), the economics literature offers little insight on how to implement road pricing in practice, especially given that real-world policy instruments differ significantly from the first-best policies prescribed by economists.

A first-best road pricing policy would charge drivers for the marginal social damages (the time cost imposed on others plus the social cost of pollution generated) associated with every vehicle trip. Practical constraints, however, render first-best road pricing infeasible in most settings. Implementing a first-best policy would require detailed information about each driver's routes and emissions, as well as real-time traffic data. It is typically too costly to collect this information through a passive sensor network, and proposals for GPS-based pricing schemes are often rejected on privacy grounds (Lehe, 2019; Selmoune et al., 2020). Consequently, city-wide road pricing often takes the form of *cordon zones* — regions in the center of a city where drivers are charged for entry. Real-world road pricing schemes therefore deviate from the first-best policy along two important dimensions: First, feasible cordon systems cannot account for all of the heterogeneity in congestion and pollution externalities across trips that all enter the cordon. Second, cordon zones leave nearby roads unpriced, allowing for externality leakage. As a result, it is generally unclear how to set cordon prices even if policymakers have perfect information about the social damages associated with trips that pass through the city center (Parry, 2009).

In this paper, I adapt models from public finance to characterize optimal cordon prices in the face of these policy imperfections. I then generate empirical estimates of how drivers would respond to road pricing, and use these estimates together with formulas derived from the theoretical framework to calculate second-best cordon prices.

The second-best pricing framework I build stipulates a set of parameters necessary for calculating second-best road prices accounting for both leakage and imperfect pricing (i.e., many vehicle trips with different externalities are charged the same price). Calculating optimal prices requires information about (i) the heterogeneity in marginal trip-level externalities, (ii) the relationship between these externalities and individual price-responsiveness, and (iii) the elasticity of substitution between priced and unpriced trips. Outside of road pricing, this framework can be applied to any setting where externality heterogeneity and leakage simultaneously prevent the implementation of a first-best corrective policy (e.g., electricity markets, or sin taxes).

In theory, the two policy imperfections — leakage and heterogeneity — have an ambiguous effect on optimal cordon prices relative to prices in a first-best policy. Depending on the correlation between social damages and driver elasticities, heterogeneous externalities could imply optimal prices that are either above or below social damages (Diamond, 1973). The discrete spatial and temporal cutoffs in cordon pricing incentivize some drivers to shift trips in time and space to avoid tolls. Absent heterogeneity, this leakage would imply optimal prices that are unambiguously below social marginal damages (Green and Sheshinski, 1976). Whether second-best prices are above or below average Pigouvian prices therefore depends on the sign and strength of the correlation between price-responsiveness and individual externalities, as well as the size of the leakage effect.

In the empirical section of this paper, I use a natural experiment from the San Francisco Bay Area to recover estimates of each of the parameters necessary to calculate optimal cordon prices. In 2010, bridge tolls increased on all of the region's bridges, and peak-hour pricing was implemented on the region's busiest bridge. In my main set of empirical results, I use this variation in road prices together with administrative microdata from the region's electronic tolling system to estimate a discrete choice model of driving demand. Additionally, I corroborate a subset of the parameter values from the discrete choice model using a bunching estimator: The temporal cutoff in the Bay Area's peak-hour tolls yields a notched budget constraint for drivers; the size of the bunching just outside of peak hours is proportional to the willingness of drivers to substitute trips in time.

Taking a discrete choice approach simplifies the information required to apply the second-best tax framework (items (i)-(iii), above). Namely, it allows me to populate a substitution matrix between alternative driving times and routes based on a small number of parameters that describe driving choices rather than individually estimating substitution between each hour of day and possible route taken by a driver.

I use this model of driving demand to calculate the second-best optimal prices for New York's cordon zone and proposed zones in San Francisco and Los Angeles. I find that leakage is the dominant consideration in calculating second-best cordon prices. The possibility of drivers substituting their trips in time or space leads to second-best optimal prices that are below the average social damages associated with trips that enter the cordon. In San Francisco, for example, when cordon prices are constrained to peak hours, the second-best optimal prices that account for both heterogeneity and leakage are \$5.90 for the morning peak and \$8.50 for the evening peak. These prices are below the average social damages generated by trips that use the cordon during those periods ($7.66 and $10.43, respectively). Unsurprisingly, peak-hour cordon pricing performs poorly relative to the (infeasible) Pigouvian prescription. The second-best optimal road pricing scheme in San Francisco, for example, achieves only 41% of the total welfare gains relative to a policy where drivers are charged according to the marginal damages of each trip. Notably, these results are driven by the policy's ability to address congestion externalities, which tend to be 2 to 10 times larger on a per-trip basis than pollution externalities. Second-best peak-hour pricing performs even more poorly in New York (28% of the welfare gains of the first-best) and Los Angeles (10% of the welfare gains of the first-best).

To conclude, I investigate the prospects for improving cordon pricing policies. Allowing a policymaker to set a fixed schedule of hourly prices between 6 a.m. and 7 p.m. generates sizable welfare gains relative to a cordon policy constrained to charge prices only during peak hours. I estimate that these welfare gains range from $132 million annually in San Francisco to $514 million annually in New York. In each city, however, a cordon zone with second-best hourly prices would still leave a substantial portion (roughly 20 to 40%) of the possible welfare gains unrealized due to remaining issues of spatial leakage and imprecise pricing.

This paper makes three primary contributions. First, this paper provides the first empirical estimates of optimal cordon prices that account for both pollution and congestion. I recover optimal peak-hour cordon prices that range from $5.90 - $8.50 in San Francisco to $11.30 - $16.30 in New York. While there are robust literatures documenting the reduced-form relationship between road pricing and traffic speeds (Yang, Purevjav, and Li, 2020; Gibson and Carnovale, 2015; Leape, 2006), as well as traffic and local air pollution (Currie and Walker, 2011; Anderson, 2020; Gibson and Carnovale, 2015), these results have yet to be combined into optimal cordon prices that account for both of these externalities, as noted by Parry (2009). Importantly, the optimal road prices presented in the paper also account for imperfections in real-world policies. Both theoretical and empirical studies suggest that while price or quantity-based cordons can ameliorate pollution and congestion in some settings (Zhong, Cao, and Wang, 2017; Börjesson et al., 2012), policies designed without regard to agent re-optimization and heterogeneity may lead to poor or perverse policy outcomes (Davis, 2008; Zhang, Lawell, and Umanskaya, 2017; Hanna, Kreindler, and Olken, 2017; Green, Heywood, and Paniagua, 2020). Calculating optimal cordon prices through a second-best tax framework explicitly accounts for these considerations.

Second, this paper contributes to the literature on externality taxation by characterizing second-best prices in the presence of both heterogeneous externalities *and* externality leakage. This framework combines two canonical models of second-best pricing: the "Diamond" model (Diamond, 1973; Knittel and Sandler, 2018), which shows that second-best uniform prices are a weighted average of heterogeneous externalities, and the "leakage" model, where second-best optimal prices reflect marginal damages, less a term that captures leakage (substitution) to other unpriced goods that also generate externalities (Green and Sheshinski, 1976, see also Davis and Sallee, 2020; Holland, 2012). Specifically, I consider the setting where there are many externality-generating goods, the externalities vary across consumers and goods, and only a subset of the goods are taxable. I show that in the presence of both heterogeneity and substitution, the optimal second-best tax formula combines characteristics of the canonical Diamond and leakage models. Holding fixed all other taxes, the optimal tax on any *one* good is the Diamond-weighted marginal damages associated with the consumption of the good, less a term governed by the Diamond-weighted leakage to other goods. The optimal second-best tax vector solves a system of equations where terms in this system reflect individual externalities, own-price elasticities, and cross-price elasticities. This characterization is most closely related to Allcott, Lockwood, and Taubinsky (2019), who characterize the optimal vector of taxes on sugary drinks in the setting with welfare weights that reflect a planner's distaste for inequality.

This extension of optimal second-best pricing is applicable in settings outside of transportation. In energy markets, for example, the externalities associated with electricity generation differ based on the location of power plants (urban or rural; upwind or downwind of population centers), and policies implemented by states or utilities may allow for externality leakage if electricity is imported from other jurisdictions. Sin taxes (e.g., cigarette taxes) similarly have heterogeneous impacts on consumers, and taxing any single product may induce consumers to substitute towards related (and under-taxed) sin products (Fleissig, 2021).

Lastly, this paper presents a new bunching-based approach for estimating the willingness of commuters to reschedule their trips. Scheduling costs are key parameters in transportation economics (Vickrey, 1963; Arnott, De Palma, and Lindsey, 1990) and an important factor in determining the possible welfare gains from peak-hour congestion pricing (Kreindler, 2024). Adapting tools from the public finance literature on bunching, I develop an estimator that infers scheduling costs from the excess density of trips taken during times of day that fall just outside a peak pricing window. Because peak pricing is used to alleviate congestion in bridges and tunnels in many cities, this estimation approach can be applied to understand scheduling in other metro areas. Indeed, a close re-examination of existing empirical work shows this type of temporal bunching is quite common. As I detail in the results section, bunches around notches in congestion prices are visible in time-of-day plots of Milan (Gibson and Carnovale, 2015), Bergen (Isaksen and Johansen, 2021), Stockholm (Kristoffersson, 2013), and London (Transport for London, 2008).

2. Theory: Externality Taxation Under Heterogeneity and Leakage

Public economics provides an unambiguous prescription for addressing market externalities: apply a (Pigouvian) tax equal to the marginal damages associated with consuming the externality-generating good. In practice, policy instruments typically lack the precision and coverage to execute this prescription. When corrective taxation cannot account for heterogeneous externalities or leakage (substitution) to other externality-generating goods, the second-best optimal tax on any given good may differ substantially from the tax instituted in the ideal policy. In Sections 2.1 and 2.2, I outline canonical models of optimal taxation under each of these separate imperfections (heterogeneity and leakage). Then, in Section 2.4, I present a model that can be applied to instances where heterogeneity and leakage simultaneously prevent the implementation of the first-best.

2.1. Heterogeneity

For practical or legal reasons, policymakers are often constrained to apply a uniform corrective price to a good where the consumption externalities associated with that good are not uniform. In cordon zones, for example, drivers typically face a single charge for daytime trips or a toll that charges one price for peak-hour trips, and a lower price for off-peak trips.

Under these pricing schemes, many trips that generate different externalities are charged the same price. Sources of congestion heterogeneity include the total length of the trip, the time that the trip is taken, and the specific roads used within and outside of the cordon. Sources of pollution heterogeneity include vehicle attributes, travel speed, and trip length.

Diamond (1973) characterizes the second-best optimal uniform tax on a good which generates heterogeneous externalities when consumed by different agents: The optimal tax is a weighted average of the individual externalities, where the weights (henceforth *Diamond weights*) are the individual own-price elasticities.

Setup: consider n consumers that derive utility from their consumption of an externality-generating good, α_i, and disutility from other's consumption of this good: $U^i = U(\alpha_1, ..., \alpha_n) + \mu_i$. The second-best optimal uniform tax in this setting is:

$$\tau^* = \frac{-\sum_i \sum_{h \neq i} \frac{\partial U^h}{\partial \alpha_i} \alpha'_i}{\sum_h \alpha'_h} \tag{1}$$

Where α'_i is the derivative of consumer i's demand for α with respect to the price of α, and $\frac{\partial U^h}{\partial \alpha_i}$ is the marginal external cost that consumer i imposes on consumer h by consuming α.

This expression captures an important principle in second-best corrective taxation: If individual elasticities are positively (negatively) correlated with idiosyncratic externalities, the second-best uniform tax on the externality-generating good will be larger (smaller) than the naive average of marginal damages. Intuitively, the role of corrective taxes is to move individuals to adjust their consumption of a product to the level where private marginal benefit equals the social marginal cost. If a given group is unresponsive to price, however, the second-best optimal tax described above will provide the correct incentive for the responsive group to consume at the level that balances private and social marginal costs.

2.2. Leakage

Just as legal or practical constraints prevent policymakers from perfectly targeting externalities, these constraints often also prevent policymakers from pricing all related externality-producing goods. Cordon prices, for example, price only trips that pass over the cordon's boundary, leaving trips that avoid the cordon unpriced.

Green and Sheshinski (1976) show that in the case of two externality-generating goods (where one is taxable and the other is not) and homogeneous marginal damages, the second-best prescription is to tax the taxable good at its marginal damages, less a term that is increasing in both the substitutability of the two goods, and the marginal damages of the untaxable good.

Consider a setting with two goods, x and y, and associated marginal external damages ϕ_x and ϕ_y, respectively. A representative consumer with an exogenous income derives utility from these two goods, and a quasilinear numeraire: $U = U(x, y) + z$. If a social planner is constrained to only tax x, then the optimal tax is:

$$\tau_x^* = \phi_x + \frac{dy/dp_x}{dx/dp_x}\phi_y \tag{2}$$

The second-best optimal price balances the direct social damages associated with consumption of the taxable good (ϕ_x), with the leakage-associated social damages that result from an increase in the price of the taxable good ($\frac{dy/dp_x}{dx/dp_x}\phi_y$). In this paper, I will refer to the first term in this expression ($\frac{dy/dp_x}{dx/dp_x}$) as the *leakage share* between x and y.

In the remainder of this section, I cover two extensions to the above models, the second of which characterizes optimal cordon prices.

2.3. Leakage with Many Goods

Before characterizing second-best optimal taxes under both heterogeneity and leakage, I first extend the two-good model in Section 2.2 to the case of many (homogeneous) externality-generating goods, some of which are untaxable. This intermediate setting provides intuition useful for understanding the model with heterogeneity presented in Section 2.4.

Setup: A representative consumer chooses quantities of M goods, $(h_1, ..., h_M)$ and a numeraire, z. Each non-numeraire good has an associated (homogeneous) externality, ϕ_m that is linear in the consumption of m. A policymaker can choose tax levels τ_j for goods $j \in \{1, ..., J\}$ where $J < M$. I assume goods $k \notin \{1, ..., J\}$ are un- or under-taxed.

In Appendix A, I show that under these constraints the optimal tax for good j holding fixed the taxes on all other taxable goods k is:

$$\tau_j = \phi_j + \frac{1}{\frac{\partial h_j}{\partial p_j}} \left(\sum_{k \neq j}^{J} \frac{\partial h_k}{\partial p_j} [\phi_k - \tau_k] + \sum_{l=J+1}^{M} \frac{\partial h_l}{\partial p_j} \phi_l \right) \tag{3}$$

This intermediate result is a generalization of the two-good case. Holding fixed all taxes other than τ_j, the optimal value for the final tax is its externality, ϕ_m, plus a term that captures consumer substitution to other goods, and the level of unpriced externality of those goods. Identifying the optimal tax vector requires simultaneously solving J equations in the form of Equation 3. To do so, one can rewrite Equation 3 to separate the tax and externality terms:

$$\tau_j + \frac{1}{\frac{\partial h_j}{\partial p_j}} (\sum_{k \neq j}^{J} \frac{\partial h_k}{\partial p_j} \tau_k) = \phi_j + \frac{1}{\frac{\partial h_j}{\partial p_j}} \sum_{l=1}^{M} \frac{\partial h_l}{\partial p_j} \phi_l$$

This yields J equations, each linear in the J tax levels:

$$a_1^j \tau_1 + ... + a_l^j \tau_l + ... + a_J^j \tau_J = b_j \qquad \forall \quad j \in [1, J] \tag{4}$$

Where a_l^j and b_j are defined as: $$a_l^j = \frac{\frac{\partial h_l}{\partial p_j}}{\frac{\partial h_j}{\partial p_j}} \qquad \text{and} \qquad b_j = \phi_j + \sum_{m=1}^{M} \frac{\frac{\partial h_m}{\partial p_j}}{\frac{\partial h_j}{\partial p_j}} \phi_l$$

The a and b terms have intuitive interpretations. a_l^j is the share of the reduction in overall consumption of good j that shifts to good l as a result of an increase in the price of good j. That is, each a term is a leakage share between two taxable goods. b_j is the overall reduction in externalities that results from the increase in the price of good j; this consists of a direct component, ϕ_j, plus the sum of leakage terms: $\sum_{m=1}^{M} \frac{\partial h_m}{\partial p_j} / \frac{\partial h_j}{\partial p_j} \phi_l$, which are negative if j is a normal good and m is a substitute for j. This system can be written compactly as:

$$\underbrace{\begin{bmatrix} a_1^1 & ... & a_J^1 \\ & ... & \\ a_1^J & ... & a_J^J \end{bmatrix}}_{\boldsymbol{A}} \underbrace{\begin{bmatrix} \tau_1^* \\ ... \\ \tau_J^* \end{bmatrix}}_{\boldsymbol{\tau}} = \underbrace{\begin{bmatrix} b_1 \\ ... \\ b_J \end{bmatrix}}_{\boldsymbol{b}}$$

The optimal tax vector with taxable J goods out of M total externality-generating goods is:

$$\boldsymbol{\tau} = \boldsymbol{A}^{-1} \boldsymbol{b} \tag{5}$$

Equation 5 shows that solving for the second-best optimal vector of corrective taxes in a setting with incomplete tax coverage and substitution between many externality-generating goods requires a) the consumption externalities associated with each good, and b) the substitution matrix between all goods. Note that this substitution matrix contains cross-price *derivatives* and not cross-price *elasticities*. $\boldsymbol{A}$ contains 1's along the diagonal; when all j goods are substitutes, the off-diagonal terms of $\boldsymbol{A}$ fall in the interval $[0, -1]$.

2.4. Heterogeneity and Leakage

Finally, I characterize second-best taxes where a) there are many externality-generating products, b) policymakers can tax only a subset of these products, and c) externalities are heterogeneous in the consumption of the products.

Although I apply this model to urban driving externalities in this paper, many markets feature externalities and policy instruments that fit this description. Electricity generation, for example, produces externalities that vary by location (Muller and Mendelsohn, 2007), and local pollution policies may induce leakage if utilities or states import electricity across borders. Similarly, "sin" goods have externalities or internalities that vary across consumers, and taxing any one product (e.g., cigarettes) may induce leakage towards other products (e.g., vape pens) that do not fall under a policymaker's purview (Herrnstadt, Parry, and Siikamäki, 2015).

Lastly, as I introduce heterogeneity, it is worth noting that I assume that the social planner acts to maximize aggregate welfare, as in Diamond (1973). The formulae that follow do not account for redistributive preferences — heterogeneity is included in the model to reflect the implications of differences in externalities, rather than the interaction between externality and inequality aversion.

Setup: N heterogeneous consumers choose between M externality-generating goods and a numeraire, z. I denote individual i's consumption of good m as h_i^m. Each individual has an exogenous income μ_i. I assume that each consumer's utility is a function of their consumption of these M goods and a quasilinear numeraire, as well as other's consumption of these goods (which generate externalities and decrease i's utility): $U_i(h_1^1, ...h_1^M, ..., h_i^1, ...h_i^M, ...h_N^1, ...h_N^M) + z_i$.

As in Section 2.3, a policymaker can choose tax levels for goods $j \in \{1, ..., J\}$ where $J < M$. I assume goods $m \notin \{1, ..., J\}$ are un- or under-taxed. I denote τ^j as the tax on good j. In Appendix A, I show that the optimal tax on τ_j as a function of the k other tax levels is:

$$\tau_j = \frac{\sum_{i=1}^N \sum_g^N (\frac{\partial U^i}{\partial h_g^1} \frac{\partial h_g^1}{\partial p_j} + ... + \frac{\partial U^i}{\partial h_g^M} \frac{\partial h_g^M}{\partial p_j})}{\sum_{i=1}^N \frac{\partial h_i^j}{\partial p_j}} + \frac{\sum_{k \neq j}^J \frac{\partial h_i^k}{\partial p_j} \tau_k}{\sum_{i=1}^N \frac{\partial h_i^j}{\partial p_j}} \tag{6}$$

This expression resembles the homogeneous case (Equation 3), but each of the externality terms is replaced by a Diamond-weighted term that accounts for individual-level heterogeneity in externalities. As in the previous case, the optimal tax vector solves a system of J equations:

$$\underbrace{\begin{bmatrix} a_1^1 & ... & a_J^1 \\ & ... & \\ a_1^J & ... & a_J^J \end{bmatrix}}_{\boldsymbol{A}} \underbrace{\begin{bmatrix} \tau_1^* \\ ... \\ \tau_J^* \end{bmatrix}}_{\boldsymbol{\tau}} = \underbrace{\begin{bmatrix} b_1 \\ ... \\ b_J \end{bmatrix}}_{\boldsymbol{b}} \tag{7}$$

Now, a_l^j and b_j are defined as:

$$a_l^j = \frac{\sum_{i=1}^N \frac{\partial h_i^l}{p^j}}{\sum_{i=1}^N \frac{\partial h_i^j}{\partial p_j}} \qquad b_j = \underbrace{\frac{\sum_i^N \sum_{g\neq i}^N \frac{\partial U_i}{\partial h_g^j}\frac{\partial h_g^j}{\partial p_j}}{\sum_i^N \frac{\partial h_i^j}{\partial p_j}}}_{\text{Diamond-weighted externality of } j} + \underbrace{\sum_{l\neq j}^M \frac{\sum_i^N \sum_{g\neq i}^N \frac{\partial U_i}{\partial h_g^l}\frac{\partial h_g^l}{\partial p_j}}{\sum_i^N \frac{\partial h_i^j}{\partial p_j}}}_{\text{Diamond-weighted leakage shares}} \tag{8}$$

Solving for the second-best optimal corrective taxes therefore requires (i) the (heterogeneous) externalities associated with each good, (ii) the relationship between these heterogeneous externalities and individual price elasticities, and (iii) individual-level substitution matrices between goods.

These are considerable information requirements. In what follows, I demonstrate how to use a discrete choice model to reduce the dimensionality of this problem. Specifically, rather than estimating how each driver substitutes between each possible trip, I use a discrete choice model over routes and times of day to populate the substitution matrix of options facing drivers based on the attributes of those trips.

3. A Discrete Choice Model of Driver Behavior

The theory outlined in Section 2 stipulates that calculating the second-best optimal cordon prices requires information about the heterogeneity in the price responsiveness of different types of trips that cross a cordon, as well as the rates of substitution between trips that can and trips that cannot be priced. To recover these parameters, I estimate a canonical "bottleneck" model of driving demand (Arnott, De Palma, and Lindsey, 1990, 1993).

Formally, imagine drivers i who choose between departure times $h \in H$ and routes $r \in R$ to satisfy their demand for travel. Included in this choice set is the outside (no trip) option. Each driver has an exogenous ideal arrival time, $\tilde{h^i}$. Drivers are atomistic and face travel times $T^i(h,r)$ and tolls $p(h,r)$ that may vary by route and time of day. A driver arriving before or after their ideal arrival time incurs disutilities γ_e and γ_l per hour, respectively. Drivers also incur disutility α from each hour spent commuting. Lastly, each driver has idiosyncratic preferences for routes and travel times, $\varepsilon^i_{h,r}$.[1] Driver i thus receives the following indirect utility from traveling via route r at time h:

$$u^i(h,r) = -\alpha T^i(h,r) - \gamma_e \underbrace{|h + T^i(h,r) - \tilde{h^i}|_-}_{\text{time early}} - \gamma_l \underbrace{|h + T^i(h,r) - \tilde{h^i}|_+}_{\text{time late}} - \beta p(h,r) + \varepsilon^i_{h,r} \tag{9}$$

[1] Whether idiosyncratic preferences are identically and independently distributed or correlated within nests of trips carries implications for substitution patterns implied by this model. In the empirical section, I present results under both of these assumptions, and adopt the nested approach as my preferred specification when using this model to estimate substitution patterns. See Section 6.1 for further discussion.

To clarify the mapping between this discrete choice model and the optimal tax formula (Equation 7), a "good" (h^j in the notation used in Section 2) is a trip taken on a given *route* at a given *time of day*: $g \in H \times R$. Typical cordon zones have discrete spatial and temporal cutoffs.[2] The possibility of leakage reflects the ability of drivers to adjust trips in time (h) and space (r) to avoid tolls. Heterogeneity in externalities results from the fact that trips that enter a cordon zone during the same time of day are charged the same price, but differ in pollution externalities (a function of trip length, vehicle characteristics, and travel speed) as well as congestion externalities (a function of trip length and traffic density along the trip). To estimate the relationship between idiosyncratic externalities and price-responsiveness, I allow β, the coefficient on price, to vary across externality quantiles during estimation.

The value of estimating a discrete choice model is that it reduces the number of parameter estimates required for applying the optimal tax formula outlined in Section 2. A purely reduced-form approach would require exogenous variation in congestion tolls for each possible route and hour of day to estimate how drivers substitute between available options. Alternatively, Equation 9 implies a matrix of own and cross-price elasticities between any choice set. These elasticities are a function of model primitives (α_e, γ_e, γ_l, β) and trip attributes ($T^i(h,r)$, p, *time late*, and *time early*). In Section 4 through 7, I use tolling data to recover estimates of each of these parameters using a multinomial logit model. I also apply a bunching estimator to the introduction of peak-hour pricing in the Bay Area to produce separate estimates of scheduling parameters, γ_e and γ_l.

4. Natural Experiment: Traffic Tolling in the San Francisco Bay Area

I use administrative tolling data from the San Francisco Bay Area together with changes in regional bridge tolls to estimate the model of driving demand outlined above.

4.1. Bay Area Bridge Tolls

FasTrak is an electronic tolling system used in California. Drivers are charged for using certain roads (bridges and high-occupancy toll lanes) via transponders mounted to the car's dash. Drivers can pay with cash if they do not purchase a FasTrak device. Between 2010 and 2019, cash payers represented roughly 10% of all trips on Bay Area bridges. In the San Francisco Bay Area, tolls are collected on each of the region's trans-bay bridges (mapped in Figure 1) for westbound trips only.

[2] The London Cordon Zone, for example, charges road users £15 between 7 am and 10 pm. The Milan Cordon Zone charges users €2 to €5 based on vehicle type between 7:30 am and 7:30 pm. San Francisco's proposed zone would only charge drivers during morning and evening peak hours.

Figure 1 — San Francisco Bay Area Bridges

Before 7/1/2010 *After 7/1/2010*

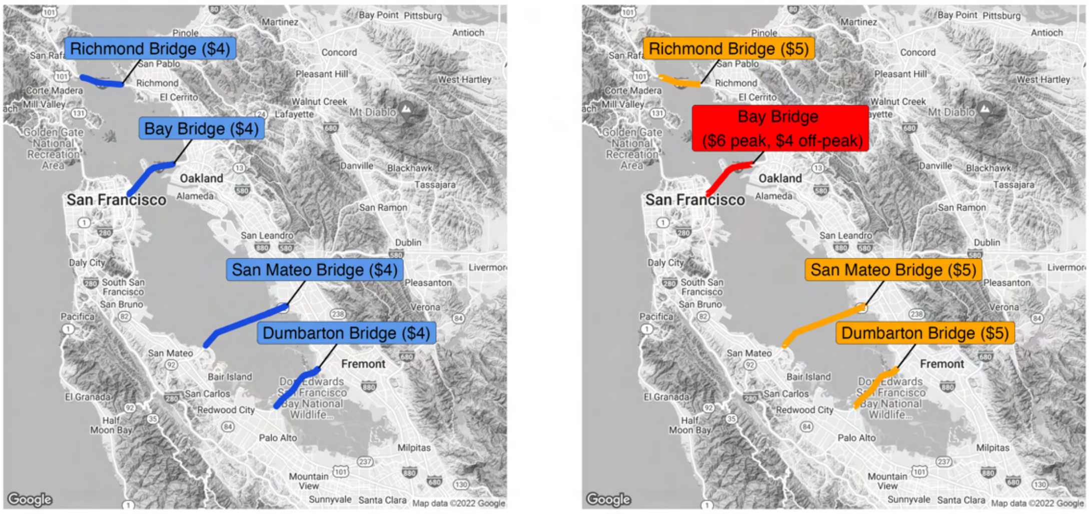

Figure 1: This map shows the four San Francisco Bay Area bridges used to estimate driver responses to toll prices in this paper. The *Richmond Bridge* connects Richmond and the eastern Bay Area to San Rafael and Marin County. The *Bay Bridge* connects Oakland to San Francisco. The *San Mateo Bridge* connects Hayward to San Mateo. The *Dumbarton Bridge* connects Fremont to Palo Alto. Each of these bridges charges drivers for westbound trips (as detailed in Figure A2).

4.2. Variation in Toll Prices

Bay Area FasTrak tolls vary by bridge, vehicle type, and time of day. I focus on passenger vehicles (as opposed to light and heavy-duty trucks), which constitute roughly 97% of vehicle trips on Bay Area bridges. Currently, passenger vehicles are charged between $3 and $7, depending on the time of day, the number of occupants, and whether or not the vehicle is electric/hybrid.

In this paper, I leverage several changes in the tolling structure that occurred on July 1, 2010, to identify the parameters necessary to calculate optimal road prices. In 2009, the Bay Area Toll Authority (BATA) adopted Resolution 90, which increased the base prices for passenger vehicles from $4 to $5 beginning on July 1, 2010, and established peak-hour pricing on the Bay Bridge (detailed below). This intertemporal variation in toll prices is plotted in Figure A2.

4.3. Peak-hour Pricing on the Bay Bridge

To address acute congestion on the region's busiest bridge, the Bay Area Toll Authority imposed peak hour pricing on the Bay Bridge (which connects San Francisco and Oakland) beginning on July 1, 2010. Passenger vehicles crossing westbound through the Bay Bridge toll plaza on weekdays between 5 a.m. and 10 a.m., or between 3 p.m. and 7 p.m. (*peak hours*) were charged $6. Tolls for all other hours (*off-peak*) remained at the pre-2010 price of $4.

Before July 1, 2010, passenger vehicles with two or more passengers, as well as eligible electric and hybrid electric vehicles were not subject to tolls on any Bay Area bridges. Starting in 2010, these vehicles were subject to the full toll value during off-peak hours, but retained a discount during peak hours: EV/carpool trips were charged $2.50 to use Bay Area bridges between July 1, 2010 and January 1, 2019.

Foreman (2016) uses reduced-form approaches to provide valuable estimates of the responses of Bay Area drivers to this change in bridge prices. They estimate the number of vehicle trips during peak hours on the Bay Bridge decreased by 6 to 8% (400 to 550 vehicles per hour) following the imposition of peak hour pricing. Travel during off-peak hours on the Bay Bridge increased by 4 to 20% (225 to 400 vehicles per hour). Point estimates suggest the $1 increase on the San Mateo and Dumbarton bridges led to modest decreases in bridge use (15 to 48 vehicles per hour). Notably, Foreman also finds that crossings on the San Mateo Bridge *increased* by 100 to 200 vehicles (around 5%) during peak hours, implying that some drivers switched from the Bay Bridge to its closest substitute in response to the peak-hour price difference across routes.

To summarize this variation in road prices in this empirical setting, the 2010 revision to bridge tolls in the San Francisco Bay Area replaced uniform prices with prices that varied across bridges and times of day. Reduced-form analyses of this policy suggest that drivers responded to pricing by reducing the overall number of trips, as well as shifting their trips in time and space. In the following sections, I use this variation in prices together with microdata on driver choices to estimate the model of personal vehicle travel described in Section 3.

5. Data

5.1. Reconstructing Choice Sets

Estimating the discrete choice model outlined in Section 3 requires individual-level data on travel choices, travel times, and road prices. To construct this choice set, I combine administrative microdata from the FasTrak tolling system with historic travel time data purchased from TomTom's *Historic Traffic Stats* database.

FasTrak Toll Data: I use administrative microdata from the FasTrak tolling system to create a panel of individual-level driving choices. These microdata record any electronic transactions that occurred on the four trans-bay bridges between January 1, 2009, and July 1, 2019. A single observation in this data set includes the date, time, and location of the vehicle crossing, as well as the vehicle class (axle number), the price paid, and an indicator for whether the vehicle used the EV/carpool lane. For vehicles with registered FasTrak devices (vehicles that did not pay cash), the microdata also include a unique FasTrak ID number. Roughly 40% of observations that use a FasTrak device also list the home zip code associated with the FasTrak holder.

In estimating the discrete choice model, I restrict the dataset on several dimensions. First, I include only devices with a valid Bay Area zip code. Second, for the purposes of estimation, I consider only weekday trips taken in a 2-week window before and after the 2010 change in toll prices (i.e., June 15th, 2010 to July 15th, 2010). Third, in estimation, I use only the morning commute hours (4 a.m. to 12 p.m.). Lastly, I drop devices with infrequent use (fewer than 2 weekday trips per week in the year prior to the 2010 price change), or users that take multiple westbound cross-bay trips per day during the 30-day study period. The resulting pool consists of 8,927 FasTrak devices and 78,226 bridge crossings.

These sample restrictions reflect the information requirements of the discrete choice model of driving demand. Recall that this model specifies driver utility as a function of trip attributes: travel time, time late or early, and price. Zip code information is necessary for assigning travel times to vehicle trips based on the distance between households and bridges. The restrictions based on the frequency of trips reflect the need to infer ideal arrival times for drivers. For FasTrak devices associated with daily commuters, ideal arrival times can be inferred based on bridge crossing times prior to July 1, 2010 (detailed below). Drivers that infrequently use bridges, or that use bridges many times a day, are not well-described by the discrete choice model I employ in this paper, as it is unclear how to assign these trips an ideal arrival time and trip termini. While imposing these sample restrictions comes at the cost of comprehensiveness, estimating the discrete choice model provides a distinct benefit relative to a reduced-form approach: For any given choice set (e.g., driving options subject to cordon prices) the structure of the discrete choice model directly implies the substitution parameters required for calculating optimal prices.

Travel Time Data: Because the FasTrak microdata include only the device zip code and bridge used, I must infer trip travel times. I do so in two steps.

First, based on the zip code and travel behavior of a given vehicle, I use data from the 2012 California Household Travel Survey (CHTS) to infer a probability distribution over destinations for that vehicle. For example, if I observe a driver from Oakland traveling via the Bay Bridge, I enumerate the destination cities of all CHTS drivers from Oakland who reported using the Bay Bridge. I repeat this for all of the driver's trips, resulting in a probability distribution over endpoints for each FasTrak device.

Second, I use TomTom's Historic Traffic Stats data to reconstruct the travel time between an individual's home zip code and each of the possible destination endpoints. The FasTrak data provide hourly traffic speeds for major roads in the 12 months before and the 12 months after the July 2010 adjustment to Bay Area tolls. Importantly, I also use the TomTom data to estimate counterfactual travel times. The result is a reconstruction of each driver's choice set, namely the travel time and price for each trip that the driver took, as well as the price and travel time if they had taken that same trip at a different time of day, or using a different bridge. This choice set construction is described in full detail in Appendix E.

Ideal Arrival Times: Ideal arrival times, $\tilde{h}^i$ in Equation 9, are not directly observed, and therefore must be inferred from each driver's activity. For each driver, I assign $\tilde{h}^i$ as the modal bridge crossing time of each individual during weekdays between January 1, 2010, and July 1, 2010, plus the weighted average travel time between the bridge toll plaza and each of the possible endpoints for that driver.

For example, consider a driver who exclusively uses the *Bay Bridge* during the pre-period, and who most commonly crosses this bridge at 9 in the morning. A trip taken by this individual that crosses the bridge at 9 a.m. would be assigned a value of zero for *time late* and *time early.* A trip taken by this individual that crosses the bridge at 10 a.m. would be assigned a value of *time late* of 1, plus any difference in expected after-bridge travel time between 9 a.m. and 10 a.m.

Lastly, it is worth noting that pre-period bridge crossing times may not indicate actual ideal crossing times if within-day traffic conditions provide sufficient incentive for drivers to shift their trips in time to reduce overall commute times. The estimates of scheduling elasticities that I recover from responses to peak-hour pricing on the Bay Bridge, however, are inconsistent with this type of strategic scheduling. If Bay Area drivers have schedule costs low enough to induce them to strategically reschedule trips in the absence of peak-hour pricing, a much higher portion of drivers should have responded to the imposition of peak-hour pricing by rescheduling trips to just outside of the peak pricing window.

5.2. Externalities

Although data on trip-level externalities is not necessary for estimating a model of driving demand, second-best optimal road prices depend on the correlation between the price elasticity of a given trip and the idiosyncratic externalities associated with that trip (see Section 2). I therefore estimate the congestion and pollution externalities associated with each FasTrak trip.

I do not include accident externalities when calculating trip-level externalities. Although most estimates of per-mile externalities in the economics literature suggest that accident externalities constitute a significant portion of the overall social costs of driving (Parry and Small, 2005; Anderson and Auffhammer, 2014), empirical evidence suggests that the social benefits from reduced accidents in cordon zones are an order of magnitude smaller than the benefits associated with reduced congestion and air pollution (Green, Heywood, and Paniagua, 2020). Broadly, this empirical evidence reflects the fact that the type of driving curtailed by cordon pricing—slow, daytime trips in cities—results in relatively few fatal traffic accidents. I provide further discussion of accidents and optimal cordon prices in Appendix H.

Congestion Externalities: Congestion externalities vary significantly in space and time. The transportation economics literature canonically presents congestion externalities as a function of traffic *density*, measured in vehicles per lane-mile (Small, Verhoef, and Lindsey, 2007). To assign congestion externalities to trips in the FasTrak dataset, I re-scale the congestion cost curve from Yang, Purevjav, and Li (2020). These authors use license-plate-based restrictions in Beijing to estimate the relationship between density and speed for different levels of baseline traffic density. I take this density-speed relationship and apply a setting-specific value of travel time ($20 value, which reflects research by Goldszmidt et al. (2020)) to produce a marginal external congestion cost curve for this paper (Figure A3). Note that although the shape of this curve is derived from Yang, Purevjav, and Li (2020), this is not equivalent to directly using per-mile congestion costs from Beijing to calculate congestion prices in the US, because I assign congestion costs to trips according to the specific density along that route. I further discuss the choice of congestion cost curves and present results using an alternative congestion cost curve in Appendix F.

The process of assigning congestion costs to trips is as follows: Using a network of traffic sensors on roadways in the Bay Area (the California Performance Measurement System, "PeMS"), I infer the density along the route for each FasTrak trip. These traffic sensors are mapped in Figure A12. For each trip, I use HERE Technology's *Routes* API to identify the likely route between the zip code associated with the device and the bridge crossing. For each traffic sensor along the driver's route, I use the marginal external congestion cost curve described above to assign a marginal external congestion cost (in dollars/mile) to this point based on the average traffic density at that sensor at that time of day. A trip's total congestion externality is then the average of the external congestion costs (in dollars/mile) along the route, times the length of the trip.

As noted above, because one trip termini is missing from the FasTrak data, I impute the congestion externalities for the missing segment of the trip (between the bridge and the place of work) using the likely destination locations conditional on observable characteristics (home zip code, bridge used). Note that the majority of variation in externalities is driven by the choice of bridge and time of day, suggesting any noise in this imputation process should not meaningfully impact estimates of the relationship between idiosyncratic externalities and price responsiveness.

Lastly, the endogeneity of traffic externalities bears discussion. The goal of this paper is not to develop a model of urban travel with endogenous congestion (as in Kreindler, 2024), but rather to study the implications of imperfections — leakage and heterogeneity — in cordon pricing. For simplicity, the main results use exogenous congestion externalities. Appendix F further discusses endogenous congestion. This Appendix (a) discusses how much one might expect the marginal cost of congestion to fall given reasonable demand responses, and (b) uses a fixed-point exercise to provide a lower bound for congestion prices in the face of endogenous congestion externalities.

Emissions Externalities: Fuel combustion and brake wear in passenger vehicles generate several air pollutants. These include "global" pollutants like CO_2 and methane, which contribute to climate change, as well as "local" pollutants like particulate matter (PM), nitrogen oxides (NO_x), and reactive organic compounds (ROCs), which negatively impact the health of nearby residents (Anderson, 2020; Currie and Walker, 2011). Vehicle emissions factors—the amount of a particular pollutant that a vehicle emits while traveling a mile—depend on a number of variables, including type of fuel consumed, fuel economy, vehicle age, and vehicle speed.

I estimate emissions for FasTrak trips using data from the California Air Resource Board's Emissions Factor Database (EMFAC). This database contains estimates of the average emissions rates of vehicles registered in each county as a function of vintage and vehicle speed. I then assign social costs to these trip-level emissions. For global pollutants, I use the EPA's 2021 social cost of carbon ($51 per ton) and methane ($1,500), respectively. Local pollutant damages reflect the cost of emitting each pollutant at ground level in San Francisco, according to the EASIUR model of local pollution damages. See Appendix C for details on individual pollutant costs.

Together, the data outlined in this section allow me to recreate the choices and choice sets facing a sample of FasTrak users, as well as the social costs associated with these choices.

6. Empirical Strategy

I use two strategies to recover the primitives that determine driving behavior. First, I use changes in toll prices together with the FasTrak microdata to estimate 9 via ordinary multinomial logit regression and nested logit regression. As a check for these results, I apply a bunching estimator to the Bay Bridge's notched tolling, producing a second estimate of scheduling costs.

6.1. Multinomial Logit and Nested Logit Regressions

As described in Section 5, the FasTrak microdata and the TomTom historic traffic data allow me to reconstruct the attributes of alternatives in the daily choice set for each driver. Namely, the different bridges, travel times, and prices facing trans-bay commuters. I then use these reconstructed choice sets to estimate the discrete choice model of driving decisions outlined in Section 3. Specifically, the commuter's latent utility on a given day, d, is:

$$V_{r,h,d} = \alpha \cdot time^i_{r,h,d} + \gamma_e \cdot early^i_{r,h,d} + \gamma_l \cdot late^i_{r,h,d} + \beta \cdot price_{r,h,d} + X_{r,h,d} + \epsilon^i_{r,h,d} \tag{10}$$

Following the notation from section 3, $time^i_{r,h,d}$ is the travel time associated with a route r and time of day h for individual i, $early^i_{r,h,d}$ is the time early at arrival, and $late^i_{r,h,d}$ is the time late. The $price_{r,h,d}$ variable does not vary by individual, but varies by bridge, time, and date. $X_{r,h,d}$ is a set of fixed effects for peak hours on each bridge, which I discuss below. $\epsilon^i_{r,h,d}$ is an extreme value error term. It is either independent and identically distributed (multinomial logit) or correlated within groups of alternatives (nested logit). The former yields the following simple choice probabilities, where j and k acts as shorthand for a route-time tuple, and y^i is the individual's choice on day d:

$$P(y^i = k|d) = \frac{e^{V^i_{k|d}}}{\sum_j e^{V^i_{j|d}}} \tag{11}$$

My preferred specification includes two adjustments to equations 10 and 11 made to meet the demands of the optimal tax formula: First, I interact the *price* variable with the externality quartile. Doing so produces estimates of price-responsiveness that are different for drivers who generate different amounts of externalities on their trips. Second, to allow for more flexible substitution patterns than those assumed by an ordinary logit model, I estimate a nested logit model with two nests: one degenerate nest that includes the outside "no trip" option, and a second nest that includes all possible bridges and times of day.[3] I further discuss the IIA assumption in this context in the following subsection.

Identification of the parameters of interest (β, γ_e, and γ_l) requires that the idiosyncratic error term is uncorrelated with choice attributes. The design of the peak-hour pricing on the bay bridge serves as a potential threat to identification: if trips during peak hours are popular for reasons other than the distribution of ideal arrival times (e.g. if there is a benefit to agents to having a similar schedule to other members of their household), then the peak-hour pricing in the post period could create a mechanical correlation between bay-bridge prices and idiosyncratic errors. To address this concern, I include peak-hour fixed effects for each bridge, which would subsume any temporal correlation between idiosyncratic errors and prices. These fixed effects do not absorb all of the variation in trip price; after the inclusion of these fixed effects, the price coefficient reflects differences in trip behavior before versus after the change in tolls, as well as extensive margin responses.

6.2. Own and Cross-Price Derivatives

The empirical strategies described above yield estimates of each of the primitives in Equation 9. Recall from Section 2 that the optimal cordon price formula requires information about how individuals substitute between available trip options. Given a set of routes and trip attributes, these parameter estimates imply a matrix of own- and cross-price derivatives. I can therefore use the parameter estimates from Equation 10 to predict substitution behavior in counterfactual settings. For goods x_j and x_k, the own and cross-price derivatives implied by a multinomial logit regression within an externality quantile are:[4]

[3] The two-nest logit model with a degenerate nest is a common approach in settings when there is a concern that cross-price elasticities between goods may differ from the cross-price elasticity of goods and the outside option. See, for example, Bertoli, Moraga, and Ortega (2013), Sheu (2014), or Kovach and Tserenjigmid (2022).

[4] See Train (2009) and Conlon and Mortimer (2021) for ordinary and nested logit derivatives, respectively.

Ordinary multinomial logit:

$$\partial s_j/\partial p_k = \begin{cases} \beta s_j(1-s_j), & \text{if } j=k \\ \beta s_j s_k, & \text{otherwise} \end{cases} \tag{12}$$

Nested logit logit:

$$\partial s_j/\partial p_k = \begin{cases} \beta s_k(\frac{-1}{1-\sigma} + \frac{\sigma}{1-\sigma} s_{j|G} + s_j), & \text{if } j=k \\ \beta s_k(\frac{\sigma}{1-\sigma} s_{j|G} + s_j), & \text{if } j,k \text{ in the same nest, G} \\ \beta s_j s_k, & \text{otherwise} \end{cases} \tag{13}$$

Where s_k is good k's share of choices, and σ is the degree of correlation in error terms in the non-degenerate nest (Berry, 1994).

Independence of irrelevant alternatives: Ordinary multinomial logit regressions are correctly specified when the independence of irrelevant alternatives (IIA) assumption holds. In my preferred specification, I use a nested logit model with a degenerate nest for the outside option to partially relax the IIA assumption. I also present results with three nests: "no trip," "Bay Bridge," and "other bridges."

It is also worth discussing why the IIA assumption may not be as pernicious in this setting as in other instances where discrete choice models are used to study substitution. Broadly, this is because the optimal tax formula relies on own and cross-price *derivatives*, not *elasticities.* Under IIA, cross-price elasticities are equal across goods, but derivatives are not. Holding fixed the good experiencing a price change, the cross-price elasticity between that good and a candidate substitute is proportional to the choice probability of the substitute.

Said differently, nesting structure may be very important when many goods have very similar choice probabilities. In these cases, an ordinary logit may incorrectly predict very similar cross-price derivatives because shares are similar when in reality substitution depends more subtly on attributes. In the setting of peak-hour transportation with a popular outside option, however, the large differences in choice shares mean that in practice, the predicted cross-price derivatives are similar for nested and ordinary logit. Specifically, most of the mass in cross-price derivatives is focused on the outside good and prime-hour trips, regardless of the specification.

6.3. Bunching Estimator

Below I outline how I use notches in the peak-hour tolling on San Francisco's Bay Bridge to recover the scheduling costs of drivers. This alternative empirical approach not only acts as a check for the results from the logit regressions, but it is also a novel approach to estimating scheduling costs.

Bunching estimators are used to infer elasticities or other structural parameters from the empirical density of choice variables around kinks or notches in a budget set (Chetty et al., 2011; Saez, 2010; Kleven and Waseem, 2013).[5]

Generally, bunching estimators use changes in the density of choice variables to identify characteristics of a "marginal buncher" — an individual who is indifferent between two positions along a notched/kinked budget set. Before presenting the bunching estimator, it is therefore useful to characterize the marginal bunching individual in this setting.

Consider a group of drivers with homogeneous scheduling costs and perfect control over when they cross a bridge that charges different tolls during peak and off-peak hours. A "buncher" is a driver who would cross the bridge during peak hours in the absence of peak-hour pricing, but who would adjust their travel time to just avoid the extra toll in a world with peak-hour pricing. For the *marginal* buncher, the utility from the lower price is equal to the scheduling costs of adjusting their trip to cross outside of peak hours. Equation 14 shows this indifference condition in terms of parameters from the discrete choice model, Equation 9. For simplicity, I examine the case of a driver who faces a decision of whether or not to shift their trip earlier:

$$\underbrace{\beta \Delta p}_{\text{Benefit from shifting}} = \underbrace{\gamma_e \Delta h}_{\text{Cost of shifting}} \tag{14}$$

Following the notation from Equation 9, β is the marginal utility of a dollar, Δp is the change in price at the notch, γ_e is the cost (in utils/hour) of shifting a trip earlier, and Δh is the number of hours between the price notch and the time of day when the marginal buncher would have crossed the bridge in the absence of a price notch. The scheduling cost, γ_e, can then be written as a function of the size of the price notch, and the time that the marginal buncher would have to adjust their trip in order to cross the bridge before peak hours:

$$\gamma_e = \frac{\beta \Delta p}{\Delta h} \tag{15}$$

If travel times also differ significantly in the neighborhood of the price notch, this condition becomes:

$$\gamma_e = \frac{\beta \Delta p + \alpha \Delta T}{\Delta h} \tag{16}$$

Where ΔT is the difference between a driver's total travel time if they cross the bridge just before the beginning of peak hours, and a driver's total travel time if they cross the bridge at the time of day when the marginal buncher would have crossed the bridge in the absence of a price notch. The characterization of a marginal buncher is plotted in Figure 2.

[5] Blomquist et al. (2021) note that under unrestricted preference heterogeneity, the size of bunching does not identify an elasticity of taxable income. Although I do not explicitly model the distribution of preference heterogeneity (following Kleven and Waseem (2013)), there are two characteristics of my empirical setting that limit potential biases. First, using pre-period data, I directly observe the counterfactual density of Bay Bridge trips. Second, there is a limit to how far drivers reschedule: The peak-hour periods are 4-5 hours long. This provides an upper bound for how far drivers reasonably shift to "bunch."

Figure 2 — The Relationship Between Scheduling Costs and Bunching

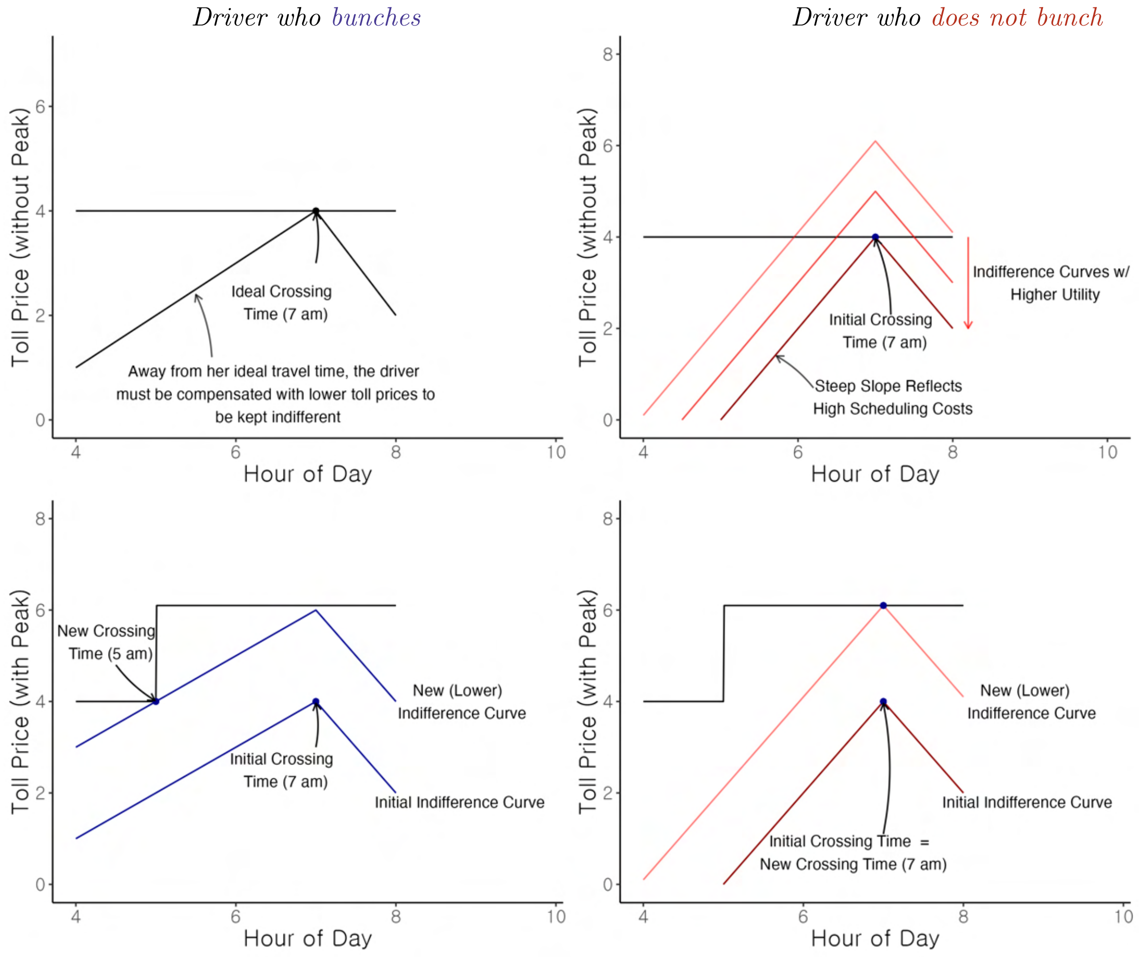

Figure 2: This figure illustrates the relationship between scheduling costs and bunching behavior in peak-hour toll schemes, as predicted by the discrete choice model outlined in Section 3. For expositional ease, this figure plots the case where travel times are constant throughout the day. The triangular shape of the indifference curves reflects the fact that the further a trip is from a given driver's ideal crossing time, the higher the compensation (via a lower toll price) required to maintain any given level of driver utility. In the right two panes, I plot indifference curves (red) of a driver with *high* scheduling costs, who does not shift their trip in response to peak pricing. In the left two panes, I plot the indifference curves of a diver with *low* scheduling costs, who does shift their trip in response to peak pricing. All else equal, when scheduling costs are lower, drivers are more willing to adjust their travel times in response to peak pricing, implying a larger mass of trips around price notches.

Equations 15 and 16 imply that the relevant scheduling cost (either γ_e or γ_l) is inversely proportional to the width of the density trough on the relatively expensive side of the peak-hour price notch. Intuitively, the width of the density trough reflects how far the marginal buncher moves their trip in response to a price incentive. All else equal, decreasing scheduling costs makes drivers more willing to shift their trips further from their ideal travel time for a given level of compensation. A wider density gap therefore implies lower scheduling costs.

Because the peak-hour pricing on the Bay Bridge (see Figure A1) creates *notches* rather than *kinks* in the budget sets of drivers, the region immediately adjacent to the price notch is strictly dominated under any scheduling cost. The fact that there is still a positive density of crossings during this dominated period suggests frictions may prevent drivers from perfectly optimizing (Kleven, 2016). In this setting, these 'frictions' may reflect inattentiveness (as in Finkelstein 2009) or the inability to perfectly time bridge crossings due to traffic shocks en route.

To account for these optimization frictions and allow for heterogeneous [6] scheduling costs, I use an estimator similar to Kleven and Waseem (2013). I first compare the density of trips in the dominated region before and after the imposition of peak pricing to identify the fraction of individuals with crossing times in the vicinity of the notch who are unresponsive to the price signal. I then estimate the excess trip mass on the relatively inexpensive side of the price notch:

$$B = \int_{\gamma_e} \int_{h*}^{h^*+\Delta h} (1-a) f_0(h, \gamma_e) dh d\gamma_e \simeq (1-a) f_0(h^*) E[\Delta h] \tag{17}$$

Where B is the excess bunching mass on the relatively inexpensive side of the notch, a is the fraction of drivers in the strictly dominated region, and $f_0(h)$ is the counterfactual (no-notch) density of vehicle crossings as a function of the time of day, h. $E[\Delta h]$ is the average adjustment among drivers who bunch at the price notch. Solving Equation 17 for Δh and plugging into Equation 16 yields the bunching estimator:

$$\gamma_e = \frac{\beta \Delta p}{{}^{B}\!/\!{}_{((1-a) f_0(h^*))}} \tag{18}$$

Relaxing the assumption that travel times are relatively flat around the notch point is straightforward but necessitates the value of travel time:[7]

$$\gamma_e = \frac{\beta \Delta p + \alpha \Delta T}{{}^{B}\!/\!{}_{((1-a) f_0(h^*))}} \tag{19}$$

7. Results

7.1. Reduced-form results

Before discussing the results from the discrete choice model that I use to calculate second-best cordon prices, this subsection briefly presents reduced-form evidence of drivers' responsiveness to the change in tolls in the four major trans-bay bridges in the Bay Area. The reduced-form regressions I estimate should not be taken as the main empirical results in the paper. They serve to motivate the

[6] Blomquist et al. (2021) note that under unrestricted preference heterogeneity, the size of bunching at kink/notch points does not identify an elasticity of taxable income. There are two characteristics of my empirical setting that limit potential biases: First, using pre-period data, I directly observe the counterfactual density of Bay Bridge trips. Second, there is a natural limit to how far drivers are willing to shift their trips: The peak-hour periods are 4-5 hours long. This provides an upper bound for how far drivers shift to "bunch."

[7] In all bunching estimates, I use a $20 value of travel time, which reflects San Francisco specific findings from Goldszmidt et al. (2020). I also present estimates of scheduling parameters that ignore time savings (Equation 18) in Appendix D.

approach that follows, and are broadly similar to previous reduced-form evaluations of this policy (see Foreman, 2016), which suggest reduced bridge crossings and substitution between bridges.

Figure A5 plots estimates of changes in total traffic on each bridge, by hour of day. Each point and confidence interval reflects the results of estimating a regression discontinuity (RD) around July 1, 2010 (equation 20) using aggregate traffic data from the corresponding bridge-hour. Table 1 displays the results of RD models where traffic data are aggregated up to the day level; Table 2 performs the same exercise, but restricts the aggregation to peak hours (6-10 am, and 3-7 pm).

$$count_d = \alpha_0 + \beta_1 \mathbb{1}(d > c) + \beta_2 \mathbb{1}(d > c)(d - c) + \beta_3 \mathbb{1}(d \leq c)(d - c) + \Gamma X_d + \epsilon_d \tag{20}$$

Above, d is the running variable in days and X is a set of fixed effects for the day of week.

Two high-level conclusions emerge from these reduced-form exercises. First, point estimates suggest that traffic volumes decreased in response to increased toll prices. The only large positive point estimates are for off-peak hours on the Bay Bridge (prices for trips taken on the Bay Bridge during these hours did not change before versus after July 1, 2010). Second, the closest substitutes for the Bay Bridge are the San Mateo Bridge and Dumbarton Bridge. Although point estimates for peak-hour traffic changes are negative for each of these bridges, these estimates are not statistically significant. The point estimates are also smaller in relative magnitude than the decrease observed on the San Rafael Bridge, which experienced the same 1-dollar increase in prices.

While these results are consistent with a story where commuters substitute between routes and times of day in addition to extensive margin responses to tolls, we cannot distinguish between these responses from the aggregate toll crossing data alone. This shortcoming motivates the discrete choice approach that follows.

Table 1 — Reduced-form estimates of changes in hourly bridge traffic

	Bay Bridge	San Mateo Bridge	Dumbarton Bridge	San Rafael Bridge
Post	-5349**	-2643	-2976*	-2606**
	(1984)	(1852)	(1557)	(993)
Linear Trend (Pre)	17	-29	-61***	-45**
	(34)	(27)	(14)	(18)
Linear Trend (Post)	350***	298**	259**	182***
	(114)	(113)	(96)	(65)
Mean	107287	34298	25872	29261
Day of Week FE	✓	✓	✓	✓

$^{***}p < 0.01$; $^{**}p < 0.05$; $^{*}p < 0.1$

Table 1: This Table shows estimates of change in westbound traffic on each of the San Francisco Bay Area's four trans-bay bridges following the July 2010 change in tolls. Each coefficient reflects applying equation 20, a regression discontinuity specification, to hourly data from the corresponding bridge. The coefficient in each column is the estimated change in total hourly trips. For reference, the mean number of hourly trips is included in the final row of the table. Heteroskedasticity-robust standard errors are reported in parentheses. The bandwidth for each regression is 26 days, which comes from applying the symmetric optimal bandwidth procedure described by Calonico, Cattaneo, and Farrell (2020) to data from the Bay Bridge.

Table 2 — Reduced-form estimates of changes in traffic, peak hours only

	Bay Bridge	San Mateo Bridge	Dumbarton Bridge	San Rafael Bridge
Post	-4993**	-2285	-2078	-1988*
	(2377)	(1827)	(1475)	(1073)
Linear Trend (Pre)	-34	-8	-43***	-41**
	(40)	(24)	(15)	(17)
Linear Trend (Post)	344**	215*	209**	164**
	(136)	(112)	(90)	(67)
Mean	47148	19218	15165	15560
Day of Week FE	✓	✓	✓	✓

$^{***}p < 0.01$; $^{**}p < 0.05$; $^{*}p < 0.1$

Table 2: This Table repeats the regressions from Table 1, but restricts the sample to only peak hours. Recall that peak hours — 6 a.m. to 10 p.m. and 3 p.m. to 7 p.m. — are the hours where prices on the Bay Bridge increased from \$4 to \$6. The variation in bridge tolls is explained in detail in Section 4. Each coefficient reflects applying equation 20, a regression discontinuity specification, to hourly data from the corresponding bridge. The coefficient in each column is the estimated change in total hourly trips. The mean number of hourly trips during the peak period is included in the final row of the table for reference. Heteroskedasticity-robust standard errors are reported in parentheses. The bandwidth for each regression is 26 days, which comes from applying the symmetric optimal bandwidth procedure described by Calonico, Cattaneo, and Farrell (2020) to data from the Bay Bridge.

7.2. Discrete Choice Model Results

Table 3 presents the parameter estimates for the discrete choice model of driving demand (Equation 9) estimated via multinomial logit and nested logit regressions. The first column shows the model estimated with a uniform price-responsiveness. The coefficient on *travel time*, *time early*, and *time late* can be converted into units of dollars per hour by dividing the point estimate by the coefficient on *price*. Column 1 therefore suggests that drivers are indifferent between saving roughly \$23.06 and saving an hour of travel time; they are indifferent between saving roughly \$15.94 arriving an hour early, and they are indifferent between saving roughly \$11.75 arriving an hour late.

In Column 2 of Table 3, I allow price responsiveness to vary with road users' idiosyncratic externalities. To do so, I break FasTrak devices into quantiles based on the average estimated externality (both pollution and congestion) of each device's choices in the month prior to the study period. I find little evidence that price elasticity varies systematically with idiosyncratic externalities in this sample.

Column 3 of Table 3 is my preferred specification. It is a nested logit model with two nests — a degenerate nest that includes the outside option (no trip) and a second nest that includes all bridges and routes. The results are similar to those from the multinomial logit. Because of the unidentified scale parameter, the reported coefficients are different sizes across specifications, but the *ratio* of the coefficient on price to the coefficient on travel time, time early, and time late are similar.[8] The implied value of travel time estimates are roughly \$20 to \$30 per hour, depending on the externality quantile, and the per-hour scheduling costs are between half and two-thirds of the per-hour value of travel time. The final specification, Column 4, adds a third nest for the region's busiest bridge, the Bay Bridge. The parameter estimates are similar, with somewhat larger price coefficients in relative terms. As a result, the implied value of time (\$14.95 to \$16.81 per hour) and scheduling elasticities (\$10.85 to \$6.67 per hour) are lower.

[8] This is well put by Train (2009), who writes " ...for interpretation it is useful to recognize that these estimated parameters are actually estimates of the "original" coefficients divided by the scale parameter σ... the scale parameter does not affect the ratio of any two coefficients, since it drops out of the ratio; for example, $\beta_1/\beta_2 = (\beta_1^*/\sigma)/(\beta_2^*/\sigma) = \beta_1^*/\beta_2^*$" (page 45).

Table 3 — Discrete Choice Model Estimates

	Multinomial (Pooled)	Multinomial	Nested (2 Nests)†	Nested (3 Nests)
Travel Time	-3.69^{***}	-3.69^{***}	-0.65^{***}	-2.69^{***}
	(0.01)	(0.01)	(0.03)	(0.02)
Time Early	-2.55^{***}	-2.55^{***}	-0.38^{***}	-1.74^{***}
	(0.01)	(0.01)	(0.02)	(0.03)
Time Tate	-1.88^{***}	-1.88^{***}	-0.27^{***}	-1.20^{***}
	(0.01)	(0.01)	(0.01)	(0.02)
Price	-0.16^{***}			
	(0.02)			
*Price * Quantile 1*		-0.16^{***}	-0.03^{***}	-0.18^{***}
		(0.03)	(0.00)	(0.01)
*Price * Quantile 2*		-0.18^{***}	-0.02^{***}	-0.17^{***}
		(0.03)	(0.00)	(0.01)
*Price * Quantile 3*		-0.12^{***}	-0.02^{***}	-0.16^{***}
		(0.03)	(0.00)	(0.01)
*Price * Quantile 4*		-0.19^{***}	-0.03^{***}	-0.17^{***}
		(0.03)	(0.00)	(0.01)
Nest: Any Trip			0.15^{***}	
			(0.01)	
Nest: Other Bridge				0.70^{***}
				(0.01)
Nest: Bay bridge				0.83^{***}
				(0.01)
Peak x Bridge FE	✓	✓	✓	✓

$^{***}p < 0.01$; $^{**}p < 0.05$; $^{*}p < 0.1$

Table 3: This Table contains parameter estimates for variations Equation 9, a discrete choice model of travel behavior described in Section 6. The dependent variable is whether an individual i elects to take a trip on route r at time of day h. *Travel time* is the travel time (in hours) that driver i would incur by traveling via route r at time h. *Time early* is the number of hours that driver i would arrive before their ideal arrival time if they were to travel via route r at hour h. *Time late* is analogously defined. *Price* is the toll that driver i would incur by traveling via route r at hour h. The choice data used to estimate these equations are individual-level FasTrak records from the San Francisco Bay Area; the travel time data are derived from historical TomTom traffic data. † is an indicator for my preferred specification, and the specification I rely on when calculating optimal cordon prices.

7.3. Bunching Estimator Results

Applying a bunching estimator to notches in the pricing schedule on the Bay Bridge, I recover scheduling costs (which I report as γ_e/β and γ_l/β for interpretability) that range from \$6 to \$15 per hour.

Figure 3 plots the density of trips by time of day before vs. after the imposition of peak-hour pricing for the 5 a.m. price notch on San Francisco's Bay Bridge. The 5 a.m. bunch in the post-period density of trips is consistent with a model of driving demand where drivers are willing to shift their trips in response to price incentives, but scheduling costs (a) prevent all drivers from doing so, and (b) lead drivers that do shift to adjust their travel time by the minimum amount necessary to receive the incentive.

Figure A8 plots the frequency of vehicle trips before versus after the imposition of peak hour pricing for all hours of day. Qualitatively, the bunches appear to be most pronounced during the early morning (5 a.m.) and early afternoon (3 p.m.) price notches. Intuitively, this suggests that it is less costly to arrive early than to arrive late for both morning and evening trips.

Using Equation 19, I estimate that during morning commute hours, the marginal driver is roughly indifferent between saving \$6 being an hour early, and indifferent between saving \$15 and being an hour late. During evening commute hours, the marginal driver is roughly indifferent between saving \$9 being an hour early, and indifferent between saving \$13 and being an hour late. These estimates are summarized in Table 4.

Table 4 — Estimating Scheduling Costs via Bunching

Parameter	**Estimate (\$\hour)**
Time Early (5 a.m. notch)	6.195
	(0.419)
Time Early (3 p.m. notch)	9.744
	(1.545)
Time Late (10 a.m. notch)	15.498
	(2.593)
Time Late (7 p.m. notch)	13.759
	(1.306)

Table 4: This table shows estimates of the costs to drivers of scheduling trips earlier or later than the driver's ideal trip time (γ_e/β and γ_l/β in notation from equation 9). I recover these estimates using Equation 19, which relates scheduling costs to the number of additional vehicle trips observed in the period just outside of the peak-hour pricing period on San Francisco's Bay Bridge. In addition to the number of extra trips, Equation 19 reflects scheduling frictions, as well as any time savings that result from drivers adjusting their trips to fall just outside of peak hours, assuming a \$20 value of travel time for Bay-Area travelers, as estimated by Goldszmidt et al. (2020). The additional bunching mass at price notches is estimated by comparing the number of trips in the neighborhood of the threshold time before vs. after the imposition of peak-hour pricing (see Equation 17) using administrative tolling data from the Bay Area Toll Authority. Bootstrapped standard errors are in parentheses.

Figure 3 — Bunching in Response to Peak-Hour Pricing

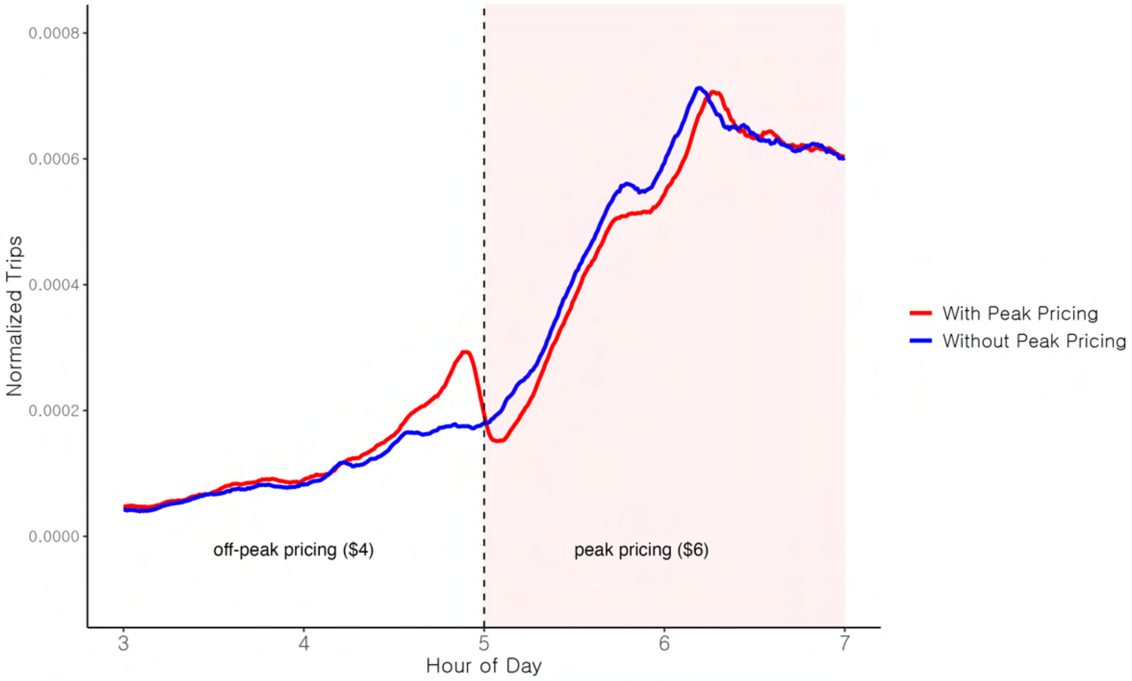

Figure 3: This figure plots the difference in the number of trips in the 6 months before (blue) vs the 6 months after (red) the imposition of peak-hour pricing on the Bay Bridge on July 1, 2010. To facilitate comparison, the number of trips at each time of day is normalized (divided by the total number of daily pre or post-period vehicle trips). The red shaded region demarcates times of day that were subject to peak-hour pricing after July 1, 2010. The vehicle trip counts reflect administrative tolling microdata collected by the Bay Area Toll Authority. Excluded from this graph are trips using the carpool/EV lane, which face a different pricing scheme. Figures A8 and A10 plot bunches for the other price notches (10 a.m., 3 p.m., and 7 p.m.) in the peak-hour pricing scheme on the Bay Bridge. See also Figure A8 for bunches at other hours.

Appendix B contains figures that examine the persistence of bunching behavior and the role of tax salience in determining bunching. Figure A11 shows that the bunching behavior is more extreme for drivers who pay in cash than it is for drivers who pay electronic tolls, corroborating findings by Finkelstein (2009). The scheduling cost estimates in Table 4 and elsewhere in this paper reflect the behavior of drivers using electronic toll systems, as this is the technology that would be used in many of the world's proposed cordons. The difference in cash vs. non-cash responses to time-of-day toll systems suggests that factors that increase the salience of electronic tags (e.g., variable message signs displaying cordon costs) may lead to larger temporal adjustment. Figure A10 compares bunching behavior at 6 months, 1 year, and 5 years after the beginning of peak hour pricing: the bunches become smaller over time, and the additional density is spread over a larger off-peak time zone at year 5 than it is at six months. Thus, while some drivers may be able to adjust their ideal arrival times in the long run, the parameters that drive bunching (schedule costs and ideal arrival times) appear stable for a large fraction of road users.

7.4. Comparisons to Parameter Estimates from the Literature

Several studies from the transportation economics literature provide valuable context for the logit and bunching estimator results presented in this subsection. A common heuristic for the value of travel time is 50% of the wage rate, which reflects seminal work by Lave (1969), as well as research collated by Small (2012). According to the 2010 - 2012 California Household Transportation Survey, the median Bay Area household earned roughly \$66,000 per worker, equivalent to \$31.74 per hour. The 50% heuristic therefore implies a median value of travel time of just under \$16. Recent empirical estimates suggest slightly higher travel time: using a field experiment among Lyft riders, Goldszmidt et al. (2020) recover estimates of the value of travel time in San Francisco equal to roughly \$20, or roughly 75% of the 2017 after-tax wage rate (\$17.79 in 2010 dollars). Broadly, the implied value of time in Table 3 is similar to, if slightly larger than, similar estimates from the literature.

Estimates of scheduling costs (γ_e and γ_l, or $\gamma_e\beta$ and γ_l/β) are less common in the economics literature. In general, existing studies accord with analysis by Small (1982), which found that a) it is more costly for drivers to be late than early, b) on a per-hour basis, the cost of being early is lower than the value of travel time, and c) the cost of being late can be higher or lower than the value of travel time depending on the setting. Kreindler (2024), for example, estimates that for drivers in Bangalore, India, early-arrival schedule costs are roughly a quarter of the value of travel time, and late arrival is more costly than early arrival. In a 2005 choice experiment, Tseng, Ubbels, and Verhoef (2005) find that for drivers in the Netherlands, the cost of early arrival (€4.9/hour) is roughly half of the value of travel time (€9.8/hour), but late arrivals are very costly (€19.7/hour).

The scheduling costs I recover using discrete choice and bunching estimators are qualitatively similar to previous findings: the bunching estimator suggests that drivers prefer being early to being late, and both sets of results suggest that early and late costs are lower than the value of travel time on a per-hour basis.[9]

Finally, it is worth highlighting the potential usefulness of a bunching estimator for studying scheduling costs in other settings. A re-examination of existing empirical work shows this type of temporal bunching is common: Figure A9 shows that bunches around notches in congestion prices are visible in time-of-day plots of traffic in Milan (Figure 4 of Gibson and Carnovale, 2015), Bergen (Figure 4 of Isaksen and Johansen, 2021), Stockholm (Figure 2 of Kristoffersson, 2013, and London (Figure 3.8 of Transport for London, 2008). Many bridges and toll roads in the US have similar cutoffs, including roads in Boston, Washington D.C., Seattle, and New York City.

[9] Although the bunching estimator and the discrete choice approach yield scheduling costs that are similar in magnitude, they differ in which direction (early or late) is more costly. This discrepancy arises because these methods use slightly different variation. Scheduling elasticities from the discrete choice model reflect both the price variation induced by the peak-hour tolling period as well as differences in travel times across hours of day.

8. Second-Best Optimal Cordon Prices

In this section, I use the discrete choice model estimated in Section 7 together with the tax framework from Section 2 to calculate optimal cordon prices. I first demonstrate this procedure using San Francisco's proposed cordon, and then consider New York and a proposed zone in Los Angeles.

At a high level, calculating optimal cordon prices in any city takes four steps: First, I use travel survey data (e.g., the National Household Travel Survey) to identify a representative sample of trips that pass through a city's proposed cordon. Second, I assign externalities to those trips using information about the vehicle driven in each trip, and the traffic density along the trip. This process is similar to the process described in Section 5. Third, I use the discrete choice model estimated in Section 7 to calculate substitution elasticities between different trips available to drivers. And fourth, I apply the optimal tax formula outlined in Section 2 to the ingredients from steps 1-3.

I refer to the cordon zones in San Francisco and Los Angeles as "proposed" cordon zone. In light of the recent pause in New York's Congestion Pricing Program, it is worth briefly discussing the status of each of these proposed congestion zones. In each city, I take the cordon zone boundary directly from the local transportation agencies planning documents. There are, however, differences across cities in the likelihood that congestion pricing exist future.

New York City's congestion pricing program is set to begin in January of 2025, but legal challenges and the incoming Trump administration mean that it is possible that the congestion charge may be suspended at some point. San Francisco's Downtown Congestion Pricing Study was paused in 2022 due to changing traffic and urban conditions in the city following the COVID-19 pandemic. As of 2024, the San Francisco Country Transportation Authority website suggests that the ability to restart the congestion pricing planning process in San Francisco rests with the Transportation Authority Board, and that any potential start date is still at least 4 years out. Of the three cities, Los Angeles is the city furthest from implementing congestion pricing. LA Metro has been studying congestion pricing and receiving public comment since at least 2019, but as of writing, there is not an official congestion pricing study timeline, nor do the proposed plans explicitly discuss how expensive congestion tolls would be under a hypothetical policy.

8.1. San Francisco's Proposed Cordon Zone

Figure 4 shows a map of the proposed cordon zone in San Francisco and Table A1 contains the proposed tolling schedule. Both the Figure and the Table reflect the San Francisco Country Transportation Authority's 2021 report on downtown congestion pricing (San Francisco County Traffic Authority, 2021).

In the main results presented in this section, I treat as fixed the shape of the cordon and the time periods where prices will be charged. Doing so accords with the setup of the second-best tax problem described in Section 2, where the set of taxable goods is an exogenous constraint. Here the set of taxable goods, J, includes only two goods: morning and evening peak-hour trips that pass through the cordon zone. I present results from expanding the set of taxable goods in Section 8.8.

For simplicity, I also assume that all passenger vehicles will be charged the same price for using the cordon zone. This assumption abstracts from the low-income cordon price exemptions being considered by many cities. In Appendix K, I show that because the majority of commuters would not qualify for this exemption, the changes in welfare, congestion, and pollution that would result from exempting low-income drivers in the San Francisco Bay Area are second-order. As acknowledged in Section 2, the setup of this problem also assumes that policymakers do not weigh marginal utility across income groups. For a characterization of optimal corrective taxation under preferences for redistribution, see Allcott, Lockwood, and Taubinsky (2019).

FIGURE 4 — SAN FRANCISCO'S PROPOSED CONGESTION PRICING ZONE

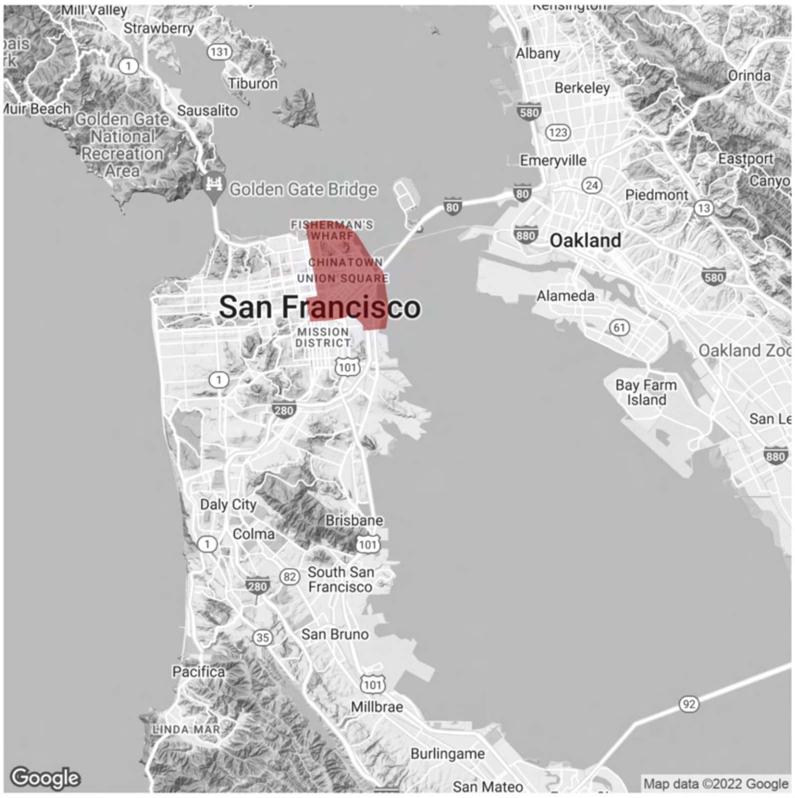

Figure 4: San Francisco's proposed cordon pricing scheme (San Francisco County Traffic Authority, 2021). Under the 2021 plan outlined by the San Francisco County Transit Authority, trips that enter the cordon would be charged during peak hours using toll readers mounted on gantries that span roadways on the border of the cordon region.

8.2. Personal Vehicle Trips in the San Francisco Area

The National Household Travel Survey (NHTS) is a survey of US individual travel habits administered by the Federal Highway Administration. Participants in this survey are recruited via mail;

survey responses are incentivized by small ($5 to $20) rewards, and can be completed through mail-back forms or online. The 2017 NHTS garnered responses from 381,975 individuals, each of whom filled out "Travel Diaries" that detailed their travel habits during one randomly selected 24-hour period. In addition to information about the attributes of the trip taken, the NHTS also collects demographic information about surveyed persons and their households.

I use the 2017 NHTS California Add-On to build a representative dataset of trips that cross San Francisco's proposed cordon zone.[10] Each *trip* in this dataset consists of a start location (zip code or Census Block), an end location (zip code or Census Block), information about the vehicle that took the trip (make, vintage, fuel type), and the time of day that the trip was taken. I determine whether or not a trip passes through the cordon using the HERE Technology's *Routes* API. The resulting dataset contains 1,891 trips that cross the cordon zone during weekdays between the hours of 4 a.m. and 10 p.m., which I plot in the left pane of Figure A6.

To predict substitution in time and space under San Francisco's cordon, I construct a set of alternatives for each trip. For every cordon trip in the NHTS, I construct alternative departure times at 12-minute intervals throughout the day. Using HERE Technology's *Routes* API, I can assign travel times to each of these alternative trips by varying the departure time. For trips with termini that lie outside of the cordon zone (i.e., trips that only pass through the cordon zone en route to their destination), I identify the most direct detour that circumvents the cordon zone. I then calculate travel times for this non-cordon route for each 12-minute interval throughout an average traffic day. These detour routes are plotted in the right pane of Figure A6.

The result of this data collation is a set of trip endpoints for the San Francisco area, where drivers can choose over *route* $\in$ {cordon, non-cordon} and *time of day* $\in \{4.0, 4.2, \ldots, 22.0\}$, as well as a generic outside option. This choice set allows me to predict how drivers would choose between options based on the attributes (travel time, time early, time late, and toll price) specified by the discrete choice model estimated in Section 3.

8.3. Trip-Level Externalities

For each trip described above (trips in the NHTS with suggested routes that pass through the cordon, as well as alternative trips in space and time), I assign traffic and pollution externalities in a manner similar to the process described in Section 5. The detail of the NHTS survey data, however, allows for more precise estimation of both congestion and pollution externalities relative to trips observed in the FasTrak tolling data.

As shown in Figure A4, emissions vary by vehicle attributes as well as travel speed. The NHTS

[10] Note that the FasTrak microdata used in Section 7 are ill-suited for this task because many of the trips that cross San Francisco's proposed cordon do not use any bridge.

includes information about the vehicle used on each trip, including the vehicle vintage, make, and fuel type (gasoline, diesel, EV, or hybrid). Using the travel time and distance information for each trip returned by the HERE Routes API, I assign an average speed to each trip. I then merge emissions factors onto each trip based on vehicle vintage, fuel type, and travel speed, using data from California's EMFAC database. I plot the emissions externalities for the 1,891 NHTS trips that cross the proposed cordon in Figure A7.

To assign congestion externalities to trips, I use rescaled estimates from Yang, Purevjav, and Li (2020) as described in Section 5. I.e, I match routes to traffic sensors, and then assign externalities to the route according to the relationship between density and marginal external cost. I plot the trip-level externalities for the NHTS trips that cross the proposed cordon in Figure A7.

8.4. Substitution Between Trips

The last set of parameters necessary for calculating optimal cordon prices are the parameters that govern how substitutable trips are in time and space. Specifically, calculating optimal prices using Equation 7 requires *leakage shares* between trips: $\frac{dh_k}{dp_j} / \frac{dh_j}{dp_j}$. Recall that if j and k are trips (defined as a specific route $\in$ {cordon, non-cordon} at a specific hour of day $\in$ {4.0, 4.2, ..., 22.0}) the leakage share between trip k and trip j represents the share of the reduction in usage of trip k that shifts to trip j as a result of the increase of the price of taking trip j. For a concrete example, imagine that a one-dollar increase in the price of driving through a cordon zone between the hours of 8 a.m. and 9 a.m. reduces trips by 10%, with 6% of all trips shifting one hour earlier (call these trips y) and 4% of trips shifting to routes that circumvent the cordon (call these trips z). The leakage shares are $\frac{dh_y}{dp_x} / \frac{dh_x}{dp_x} = 0.6$ and $\frac{dh_z}{dp_x} / \frac{dh_x}{dp_x} = 0.4$, respectively.

Using Equation 13, leakage shares are implied directly from parameters of the multinomial or nested logit regressions estimated in Section 7. I use the latter in the results reported below.

8.5. Optimal Prices

Figure 5 plots three lines relevant for understanding optimal cordon prices. The blue line plots the average externalities for trips that pass through San Francisco's cordon zone by hour of day, estimated using the process detailed above. The purple line shows these externalities re-weighted as per Diamond (1973) to account for the correlation between the price-responsiveness of trips and idiosyncratic trip-level externalities, as reported in Table 3. Finally, the red (dashed) line plots the second-best optimal prices for San Francisco's proposed cordon when tolling is restricted to morning and evening peak hours (6-10 a.m. and 3-7 p.m., respectively). The second-best optimal scheme charges \$5.90 during morning peak hours, and \$8.50 during evening peak hours. These second-best optimal prices are calculated using Equation 7, and take into account both the correlation between externalities and elasticities, as well as the substitution to unpriced alternatives in time and space.

Figure 5 — Second-Best Optimal Cordon Prices

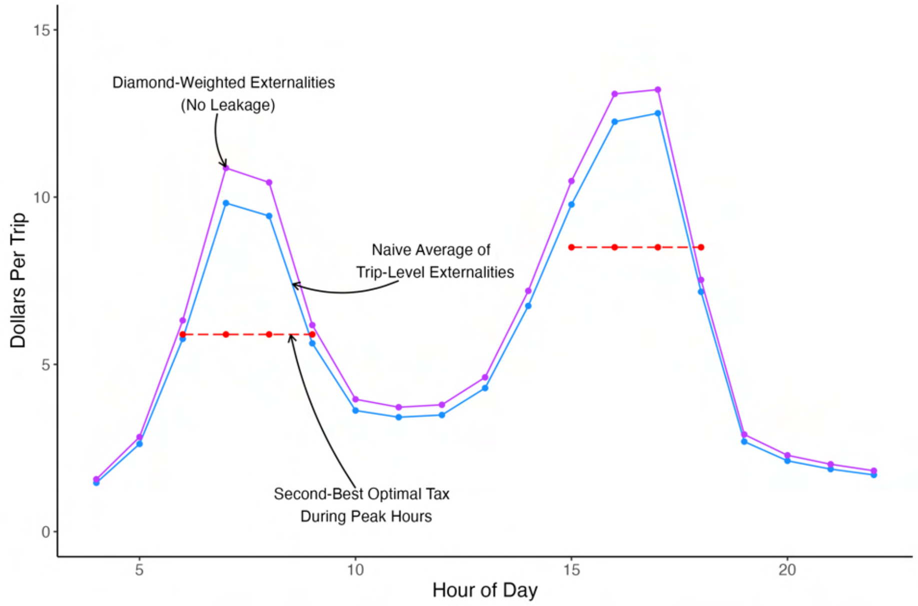

Figure 5: This figure plots three prices relevant for understanding optimal second-best cordon tolls. The blue line plots the average externality (pollution and congestion) for trips that cross San Francisco's cordon by hour of day, estimated using data from the 2017 NHTS (see Section 8.3). The purple line plots trip-level externalities re-weighted to account for the correlation between trip-level externalities and trip-level elasticities, as per Diamond (1973). The red (dashed) line plots the second-best optimal price for San Francisco's proposed cordon when tolling is restricted to morning and evening peak hours (6-10 a.m. and 3-7 p.m., respectively). These second-best optimal prices are calculated using Equation 7, and take into account both the correlation between externalities and elasticities ("Diamond weights"), as well as the substitution (leakage) to unpriced alternative trips in time or space.

The results plotted in Figure 5 reflect social damages calculated using driving conditions that exist in the current, untaxed equilibrium. Consistent with the literature on externality taxation, the second-best tax formula presented in Section 8 phrases optimal taxes as a function of externalities *at the optimum.* As shown in figures A3 and A19, the marginal damages associated with driving are non-constant in traffic density/speed, meaning that in general, damages at the taxed equilibrium will be different (lower) than those observed in the untaxed equilibrium. Whether or not the difference between marginal damages calculated at versus away from the optimum is a first-order concern depends on the slope of the marginal damages function and the responsiveness of drivers to taxation. In Appendix F, I use simulations where I iteratively calculate taxes and traffic density to bound the second-best optimal cordon prices in San Francisco. The fixed point from this exercise constitutes a lower bound because it ignores "induced demand", which will tend to attenuate the difference in traffic conditions between taxed and untaxed equilibria (Duranton and Turner, 2011). I recover lower bounds for the second-best toll of $4.29 and $5.90 for the morning and evening peak hours, respectively.

8.6. The Impact of Pricing on Congestion, Emissions, and Welfare

Figure 5 shows that because tolls would incentivize drivers to substitute to routes that avoid the cordon zone, where they would still cause congestion and pollution, the optimal peak-hour cordon prices are below the marginal social damages associated with the average vehicle trip using the cordon zone. In this subsection, I estimate counterfactual driving behavior under a number of tax scenarios to understand the extent to which the imperfections in cordon pricing policies undermine the congestion, pollution, and welfare gains engendered by road pricing policies. These three scenarios are:

1. **No congestion pricing**. This is the status quo; the only charges that trips may face are the existing Bay Area bridge tolls, set to 2020 levels.

2. **First-best (Pigouvian) pricing**. Every trip a driver could choose would be priced according to its social damages, which include both congestion and pollution externalities.

3. **Second-best optimal peak-hour cordon prices**. These prices are calculated using Equation 7. Trips that pass through the cordon area are charged \$5.90 during morning peak hours, and \$8.50 during evening peak hours (see Figure 5).

I summarize these results in Column 1 of Table 6. Two themes emerge. First, on all three outcome measures —– welfare, congestion externalities, and pollution externalities —– second-best optimal peak-hour pricing more closely resembles the status quo than the first-best policy. Second, the welfare results are largely driven by reductions in congestion externalities, as these externalities tend to be 2 to 10 times larger than pollution externalities.

8.7. Cordon Pricing in New York and Los Angeles

In this section, I calculate optimal peak-hour cordon prices for New york's congestion Zone and Los Angeles' proposed zone, and evaluate the performance of the second-best optimal cordon pricing scheme relative to a policy that prices every trip at social marginal damages.

Figure 6 — Proposed Cordons in New York and Los Angeles

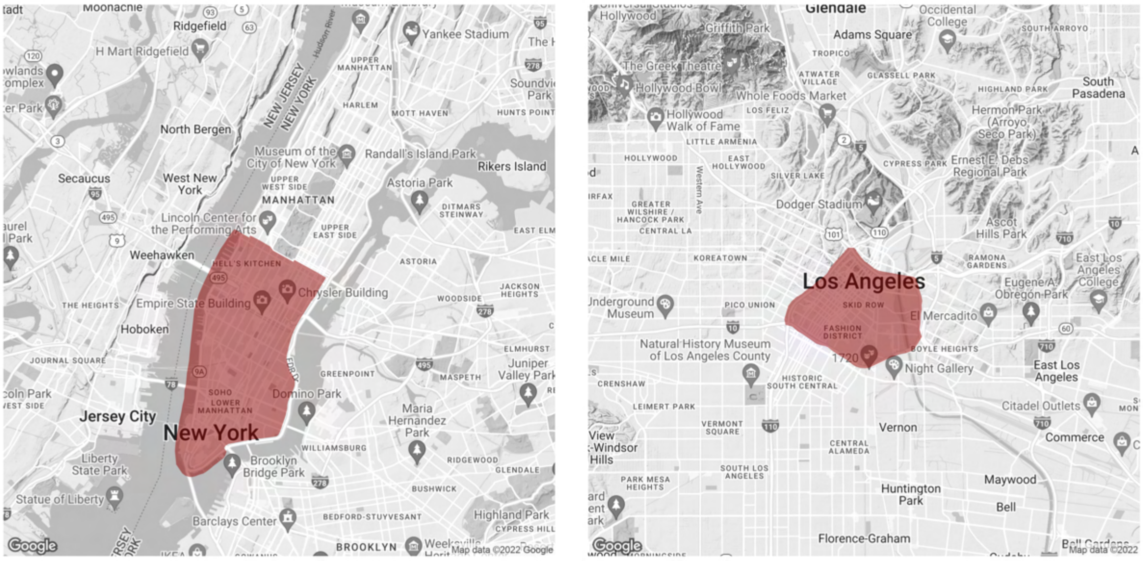

Figure 6: Proposed cordon pricing schemes in New York (Regional Plan Association, 2021) and Los Angeles (Southern California Association of Governments, 2019).

As outlined in Section 2, calculating the second-best optimal cordon prices requires information about the marginal damages of trips that cross through a cordon zone, as well as information about the elasticity and substitutability of these trips. For each of the above cities, I follow the same general template as in San Francisco (see Sections 8.2 through 8.4): First, I use survey data[11] and Here Technology's *Routes* API to identify trips where the fastest route passes through the city's proposed cordon. Second, I use vehicle attributes and travel speed to assign pollution externalities, and use traffic density data[12] from city roads to assign congestion externalities to those trips. Third, I calculate substitution parameters between those trips.

Ideally, there would be a natural experiment in each city that would allow for the estimation of city-specific driving demand primitives (price responsiveness, β, scheduling costs, γ_e and γ_l, and the value of travel time, α) that are used to calculate substitution parameters, as well as city-specific correlations between externalities and price responsiveness (Diamond weights). Absent such experiments, I calculate optimal cordon prices and welfare outcomes in New York and Los Angeles using the driving demand primitives and Diamond weights estimated in San Francisco (see Table 3). These results are reported in Tables 5 and 6.

In Appendix I, I use questions from the 2017 NHTS to examine the external validity of the

[11] The NHTS does not report detailed trip start and end locations for states that are not part of the NHTS Add-On program. As such, the trip data for New York come from the 2018 NY Citywide Mobility Survey.

[12] Traffic density data for Los Angeles is publicly available through California's PeMS database. Traffic density for NY is courtesy of the NYSDOT Traffic Monitoring Section.

model estimated in San Francisco. Specifically, the NHTS asks respondents to report their schedule flexibility (Yes/No) as well as their responsiveness to gasoline demand (Scale of 1 to 5). These proxies for demand primitives are broadly similar across the three cities I examine in this paper. In Appendix J, I document substitution to public transit in response to the increase in Bay Area bridge tolls, and discuss how optimal cordon prices may differ based on the availability of public transportation options. While estimates from a regression discontinuity performed on data from the Bay Area Rapid Transit (BART) system suggest that transit ridership increased after July 2010 (see Table A6), the implied magnitude of mode shifting is small: These estimates suggest that only 6% of drivers who chose not to drive in response to the higher toll prices substituted those trips with BART. In Table A7, I test whether access to public transit impacts the price responsiveness of Bay Area drivers. Point estimates suggest that drivers who live in zip codes near transit stations may be modestly more price-responsive than those who live far away from transit stations, but this difference is not statistically significant. Broadly, the public transit ridership patterns in the Bay Area imply that while some drivers do shift to public transit when the price of their commuting trips increases, these shifts are relatively small, even in transit-rich areas.

Table 5 — Comparing Second-Best Cordon Prices to Social Damages

	Value ($)		
	San Francisco	Los Angeles	New York
Second-Best Price, AM Peak (6-10)	5.90	10.29	11.26
Second-Best Price, PM Peak (3-7)	8.50	11.93	16.31
Average Marginal Damages, AM Peak (6-10)	7.66	14.80	17.60
Average Marginal Damages, PM Peak (3-7)	10.43	17.10	25.03

Table 5: This table compares second-best optimal peak hour prices for the proposed cordons in San Francisco, Los Angeles, and New York to the average social damages associated with trips that pass through the cordon zones during this period. "Social damages" include both congestion and pollution damages. The second-best optimal cordon prices were calculated using Equation 7 — they reflect both heterogeneity in trip-level externalities and leakage in time and space.

Table 6 — Congestion, Pollution, & Welfare Effects of Peak-Hour Cordon Pricing

	Performance Relative to the First-Best (%)		
Outcome	San Francisco	Los Angeles	New York
Welfare Gain	0.411	0.102	0.277
Congestion	0.379	0.11	0.251
Pollution	0.406	0.088	0.377

Table 6: This table compares the second-best optimal peak-hour cordon pricing scheme in 3 US cities to a first-best policy where all vehicle trips (all times of day; cordon and non-cordon) are charged based on the social damages they generate. "Peak hours" are defined as 6-10 a.m. and 3-7 p.m.; second-best cordon prices are constrained to be uniform during these hours. The three outcomes of interest are congestion externalities, pollution externalities, and total welfare (the utility of drivers, in dollars, less total externalities). The results in this table reflect the simulated choices of 1.18 million drivers in San Francisco, 953,000 drivers in LA, and 1.43 million drivers in New York. The number of drivers used in each simulation reflects reports from the respective cities. See page 27 of San Francisco County Transportation Authority (2020) for San Francisco, page 41 of Southern California Association of Governments (2019) for Los Angeles, and Table 4A-1 of Metropolitan Transportation Authority (2023). The choice probabilities for different alternatives (cordon vs. non-cordon trips at different times of day, and a generic outside option) were generated by applying the nested logit model shown in Column 3 of Table 3 to the driver choice sets constructed using transportation survey data (see Section 8).

8.8. Hourly Cordon Pricing

Tables 5, and 6 describe results where the policymaker is restricted to only price cordon trips during peak hours, as is proposed by the San Francisco County Traffic Authority. In this section I relax this constraint, allowing the policymaker to set a fixed hourly toll schedule during normal commuting times. In the notation of the second-best tax model outlined in Section 2, The set J now includes 13 taxable "goods," where each good covers all cordon trips for a given hour of day $\in \{6, 7, ..., 18\}$.

Table 7 displays estimates of welfare outcomes under second-best tax with hourly cordon pricing versus a first-best policy where every trip is charged according to the social damages associated with that trip. Relaxing this constraint leads to significant improvements, with welfare gains in each city roughly doubling with respect to the gains under uniform peak-hour pricing. In each city, however, a cordon zone with second-best hourly prices would still leave a substantial portion (roughly 20 to 40%) of the possible welfare gains unrealized due to remaining issues of spatial leakage and imprecise pricing.

Table 7 — Back of the Envelope Welfare Gains From Cordon Pricing

	Annual Welfare Gain Relative to Status Quo ($ Million)		
Policy	San Francisco	Los Angeles	New York
First-Best	339	689	1,671
Second-Best (Peak Only)	140	70	463
Second-Best (Fixed Hourly)	272	432	977

Table 7: This table displays back of the envelope calculations for the annual welfare gains under three road pricing policies: 1) The first-best policy where all trips (including those that re-route to avoid a city's cordon) are priced according to marginal congestion and pollution damages; 2) second-best peak hour (6-10 a.m. and 3-7 p.m.) prices (see Table 5); and 3) second-best-optimal time-of-day prices, which are allowed to vary by hour according to a fixed schedule between 6 a.m. and 7 p.m. The cordon prices in rows (2) and (3) are calculated using Equation 7 — they reflect both heterogeneity in trip-level externalities and leakage in time and space. The figures in this table reflect simulated choices using the nested logit model shown in Column 3 of Table 3. The results in this table reflect the simulated choices of 1.18 million drivers in San Francisco, 953,000 drivers in LA, and 1.43 million drivers in New York. The number of drivers used in each simulation reflects reports from the respective cities. See page 27 of San Francisco County Transportation Authority (2020) for San Francisco, page 41 of Southern California Association of Governments (2019) for Los Angeles, and Table 4A-1 of Metropolitan Transportation Authority (2023).

9. Discussion

Cordon prices differ from first-best driving taxes in two important ways: incomplete coverage invites leakage, and uniform prices do not reflect heterogeneity in trip-level damages. Whether second-best prices are above or below trip-level damages depends on the degree and sign of the correlation between price-responsiveness and externalities, and the strength of the leakage effect.

Figure 5 shows that leakage depresses second-best peak-hour congestion prices. In San Francisco, optimal prices are $5.90 for the morning peak period and $8.50 for the evening peak period — significantly below the social cost of trips that cross the cordon at those times.

My findings suggest that if the determinants of driver decisions (price responsiveness, value of travel time, schedule flexibility) are similar across large US cities, then optimal cordon prices are also below the average of social damages generated by downtown trips in New York and Los Angeles. Table 5 shows that in New York, for example, the second-best optimal cordon prices are about $11.26 and $16.31 for morning and evening peaks, respectively, which are below the average social damages associated with cordon trips in each of those periods ($17.60 and $25.03, respectively). In Los Angeles, the optimal morning and evening peak prices are $10.29 and $11.93, compared to average social damages of $14.80 and $17.10.

Cordon zones charging the second-best prices described in Table 5 would generate significant welfare gains in New York ($463 million annually) and San Francisco ($140 million annually), but modest benefits in Los Angeles ($70 million annually). To put these figures in perspective, the 2021 annual budget of the City of San Francisco is $13.7 billion, and the 2021 annual budget of New

York is $88.2 billion. These annual welfare gains are therefore on the order of half to one percent of city budgets in New York and San Francisco.

Despite these welfare gains, the results in Section 8 suggest that the blunt nature of cordon pricing limits their effectiveness relative to an ideal policy. In San Francisco, optimal peak-hour cordons achieve 41% of the welfare gains that would be realized under a first-best policy. This ratio is even lower in New York (28%) and Los Angeles (10%).[13]

What adjustments could improve the performance of the proposed cordon zones in the United States? Relative to a peak-only tolling scheme, allowing policymakers to set a fixed schedule of prices that vary by time of day (Table 6) provides sizeable welfare gains: $132 million in San Francisco, $362 million in Los Angeles, and $514 million in New York. In each city, however, this flexible pricing strategy still leaves a significant portion of the first-best welfare gains unrealized.

I take as given the cordon zone design. The difference in performance between the cordon zones across cities, however, highlights the central role of leakage in the effectiveness of congestion pricing. Because downtown LA lacks the bounding bodies of water seen in New York and San Francisco, the LA cordon zone appears more prone to spatial trip leakage. Indeed, the NHTS trip-level data suggest that roughly 57% of trips that pass through LA's proposed zone have viable detours that avoid the zone — higher than in New York (45%) or San Francisco (19%). These trips are also similar in damages to the cordon zone trips: On average, "detour" trips in LA have social costs that are 95% as high as the average cordon zone trip. In New York, this ratio is 41%. In San Francisco, detour trips have *higher* social damages than the average cordon trip, but as mentioned above, the majority of trips do not have a viable detour.

To summarize, the proposed cordon zone in Los Angeles is both easy to avoid for drivers *and* the substitute routes are associated with high social costs. As a result, even second-best optimal prices yield relatively small welfare gains.

What lesson does the above comparison hold for policy? Policymakers may want to set congestion zone boundaries to preempt spatial leakage. Depending on the idiosyncratic geography of a city, an optimal cordon zone may include outlying or relatively uncongested routes that provide close substitutes for congested central roads. Expanding cordon zones, however, comes at a cost. Regardless of the design of the tolling system at the boundaries, trips that remain entirely inside the cordon are not priced. Expanding the cordon too far may therefore undermine the policy's overall coverage. A full characterization of this tradeoff is beyond the scope of this paper, but may prove

[13] Notably, the welfare gains of peak-hour pricing policies largely track reductions in congestion externalities. This reflects the fact that on a per-trip basis, the estimated social damages associated with congestion tend to be much larger than the social damages associated with pollution (see Figure A7). This feature may not hold in non-US cities, especially those with large diesel vehicle fleets.

an interesting question for future research.

10. Conclusion

This paper makes three contributions. First, this paper generates the first estimates of optimal cordon prices that account for both pollution and congestion externalities. While optimal prices vary across proposed cordon zones in the US, several themes emerge: Congestion externalities constitute the bulk of marginal damages, outweighing pollution externalities two- to ten-fold. This finding accords with Parry and Small (2005), who suggest that congestion (rather than pollution) is the largest component of an optimal gasoline tax. Additionally, optimal peak-hour cordon prices tend to be *below* the average social damages associated with trips that cross through a cordon because of externality leakage in time and space. This leakage effect is larger than the heterogeneity effect (see Diamond, 1973), which increases second-best optimal prices.

Second, this paper presents the first estimates of the welfare losses that result from imperfections in real-world cordon policies. Back of the envelope calculations suggest that while a second-best peak hour cordon price in San Francisco would produce $140 million worth of welfare gains, this policy would fall short of the first-best policy by $132 million annually. This foregone welfare is significant: $132 million is roughly 1% of the City of San Francisco's 2020-2021 Budget. The predicted performance of proposed cordons in New York and Los Angeles are qualitatively similar. The role of leakage in this setting suggests that there may be large gains from designing cordon zones to preempt spatial leakage and that certain cities may see larger welfare gains due to cordon pricing because of idiosyncratic geography that makes spatial trip substitution more difficult.

Lastly, this paper contributes to the literature in public and environmental economics by extending existing models of second-best taxation to simultaneously account for leakage and heterogeneity in externalities. Accounting for these policy imperfections implies subtly different policy prescriptions than the canonical "Principle of Targeting" (Sandmo, 1975). When externality leakage and externality heterogeneity are present, the policy instrument that generates the largest welfare improvements may not be the tax that best targets the naive average of externalities. Instead, for each good, the optimal instrument balances the magnitude of externality reduction with the damages that would result from leakage. The results in this paper highlight a case where, due to policy imperfections, the optimal policy differs significantly from a tax that best targets the average of consumption externalities. While applying the second-best tax framework outlined in this paper requires detailed information about externalities and consumer demand, the increasing availability of microdata continues to lower the costs for credible estimation of demand systems. This trend, together with the ubiquity of imperfections in externality taxation, suggests that this framework will be useful for future research in settings outside of optimal road pricing.

References

Allcott, Hunt, Benjamin B Lockwood, and Dmitry Taubinsky. 2019. "Regressive sin taxes, with an application to the optimal soda tax." *The Quarterly Journal of Economics* 134 (3):1557–1626.

Anderson, Michael L. 2014. "Subways, strikes, and slowdowns: The impacts of public transit on traffic congestion." *American Economic Review* 104 (9):2763–2796.

———. 2020. "As the wind blows: The effects of long-term exposure to air pollution on mortality." *Journal of the European Economic Association* 18 (4):1886–1927.

Anderson, Michael L and Maximilian Auffhammer. 2014. "Pounds that kill: The external costs of vehicle weight." *Review of Economic Studies* 81 (2):535–571.

Arnott, Richard, Andre De Palma, and Robin Lindsey. 1990. "Economics of a bottleneck." *Journal of Urban Economics* 27 (1):111–130.

———. 1993. "A structural model of peak-period congestion: A traffic bottleneck with elastic demand." *The American Economic Review* :161–179.

Berry, Steven T. 1994. "Estimating discrete-choice models of product differentiation." *The RAND Journal of Economics* :242–262.

Bertoli, Simone, J Fernández-Huertas Moraga, and Francesc Ortega. 2013. "Crossing the border: Self-selection, earnings and individual migration decisions." *Journal of Development Economics* 101:75–91.

Blomquist, Sören, Whitney K Newey, Anil Kumar, and Che-Yuan Liang. 2021. "On bunching and identification of the taxable income elasticity." *Journal of Political Economy* 129 (8):000–000.

Börjesson, Maria, Jonas Eliasson, Muriel B Hugosson, and Karin Brundell-Freij. 2012. "The Stockholm congestion charges—5 years on. Effects, acceptability and lessons learnt." *Transport Policy* 20:1–12.

Calonico, Sebastian, Matias D Cattaneo, and Max H Farrell. 2020. "Optimal bandwidth choice for robust bias-corrected inference in regression discontinuity designs." *The Econometrics Journal* 23 (2):192–210.

Chetty, Raj, John N Friedman, Tore Olsen, and Luigi Pistaferri. 2011. "Adjustment costs, firm responses, and micro vs. macro labor supply elasticities: Evidence from Danish tax records." *The Quarterly Journal of Economics* 126 (2):749–804.

Conlon, Christopher and Julie Holland Mortimer. 2021. "Empirical properties of diversion ratios." *The RAND Journal of Economics* 52 (4):693–726.

Currie, Janet and Reed Walker. 2011. "Traffic congestion and infant health: Evidence from E-ZPass." *American Economic Journal: Applied Economics* 3 (1):65–90.

Davis, Lucas W. 2008. "The effect of driving restrictions on air quality in Mexico City." *Journal of Political Economy* 116 (1):38–81.

Davis, Lucas W and James M Sallee. 2020. "Should electric vehicle drivers pay a mileage tax?" *Environmental and Energy Policy and the Economy* 1 (1):65–94.

Diamond, Peter A. 1973. "Consumption externalities and imperfect corrective pricing." *The Bell Journal of Economics and Management Science* :526–538.

Duranton, Gilles and Matthew A Turner. 2011. "The fundamental law of road congestion: Evidence from US cities." *American Economic Review* 101 (6):2616–52.

Finkelstein, Amy. 2009. "E-ztax: Tax salience and tax rates." *The Quarterly Journal of Economics* 124 (3):969–1010.

Fleissig, Adrian R. 2021. "Estimating elasticities of substitution for sin goods." *Applied Economics* 53 (30):3549–3561.

Foreman, Kate. 2016. "Crossing the bridge: The effects of time-varying tolls on curbing congestion." *Transportation Research Part A: Policy and Practice* 92:76–94.

Gibson, Matthew and Maria Carnovale. 2015. “The effects of road pricing on driver behavior and air pollution.” *Journal of Urban Economics* 89:62–73.

Goldszmidt, Ariel, John A List, Robert D Metcalfe, Ian Muir, V Kerry Smith, and Jenny Wang. 2020. “The Value of Time in the United States: Estimates from Nationwide Natural Field Experiments.” Tech. rep., National Bureau of Economic Research.

Green, Colin P, John S Heywood, and Maria Navarro Paniagua. 2020. “Did the London congestion charge reduce pollution?” *Regional Science and Urban Economics* 84:103573.

Green, Jerry and Eytan Sheshinski. 1976. “Direct versus indirect remedies for externalities.” *Journal of Political Economy* 84 (4, Part 1):797–808.

Hanna, Rema, Gabriel Kreindler, and Benjamin A Olken. 2017. “Citywide effects of high-occupancy vehicle restrictions: Evidence from “three-in-one” in Jakarta.” *Science* 357 (6346):89–93.

Herrnstadt, Evan, Ian WH Parry, and Juha Siikamäki. 2015. “Do alcohol taxes in Europe and the US rightly correct for externalities?” *International Tax and Public Finance* 22 (1):73–101.

Holland, Stephen P. 2012. “Emissions taxes versus intensity standards: Second-best environmental policies with incomplete regulation.” *Journal of Environmental Economics and Management* 63 (3):375–387.

Isaksen, Elisabeth Thuestad and Bjørn Gjerde Johansen. 2021. “Congestion pricing, air pollution, and individual-level behavioral responses.” *Available at SSRN 3832230* .

Kleven, Henrik J and Mazhar Waseem. 2013. “Using notches to uncover optimization frictions and structural elasticities: Theory and evidence from Pakistan.” *The Quarterly Journal of Economics* 128 (2):669–723.

Kleven, Henrik Jacobsen. 2016. “Bunching.” *Annual Review of Economics* 8:435–464.

Knittel, Christopher R and Ryan Sandler. 2018. “The welfare impact of second-best uniform-Pigouvian taxation: evidence from transportation.” *American Economic Journal: Economic Policy* 10 (4):211–42.

Kovach, Matthew and Gerelt Tserenjigmid. 2022. “The focal Luce model.” *American Economic Journal: Microeconomics* 14 (3):378–413.

Kreindler, Gabriel. 2024. “Peak-Hour Road Congestion Pricing: Experimental Evidence and Equilibrium Implications.” *Econometrica* 92 (4):1233–1268.

Kristoffersson, Ida. 2013. “Impacts of time-varying cordon pricing: Validation and application of mesoscopic model for Stockholm.” *Transport Policy* 28:51–60.

Lave, Charles A. 1969. “A behavioral approach to modal split forecasting.” *Transportation Research UK* 3 (4).

Leape, Jonathan. 2006. “The London congestion charge.” *Journal of Economic Perspectives* 20 (4):157–176.

Lehe, Lewis. 2019. “Downtown congestion pricing in practice.” *Transportation Research Part C: Emerging Technologies* 100:200–223.

Mangrum, Daniel and Alejandro Molnar. 2017. “The marginal congestion of a taxi in New York City.” *Processed, Vamderbilt University* .

Metropolitan Transportation Authority. 2023. “Regional Transportation Effects and Modeling.” Tech. rep., Central Business District (CBD) Tolling Program Environmental Assessment.

Muller, Nicholas Z and Robert Mendelsohn. 2007. “Measuring the damages of air pollution in the United States.” *Journal of Environmental Economics and Management* 54 (1):1–14.

Parry, Ian WH. 2009. “Pricing urban congestion.” *Annu. Rev. Resour. Econ.* 1 (1):461–484.

Parry, Ian WH and Kenneth A Small. 2005. “Does Britain or the United States have the right gasoline tax?” *American Economic Review* 95 (4):1276–1289.

Parry, Ian William Holmes. 2002. “Comparing the efficiency of alternative policies for reducing traffic congestion.” *Journal of Public Economics* 85 (3):333–362.

Regional Plan Association. 2021. “Congestion Pricing in New York City.” Tech. rep., Regional Plan Association.

Saez, Emmanuel. 2010. “Do Taxpayers Bunch at Kink Points?” *American Economic Journal: Economic Policy* 2 (3):180–212.

San Francisco County Traffic Authority. 2021. “Downtown Congestion Pricing Study: Winter 2021 Update.” Tech. rep., San Francisco County Traffic Authority.

San Francisco County Transportation Authority. 2020. “San Francisco Mobility, Access, and Pricing Study.” Tech. rep., San Francisco County Transportation Authority.

Sandmo, Agnar. 1975. “Optimal taxation in the presence of externalities.” *The Swedish Journal of Economics* :86–98.

Selmoune, Aya, Qixiu Cheng, Lumeng Wang, and Zhiyuan Liu. 2020. “Influencing factors in congestion pricing acceptability: a literature review.” *Journal of Advanced Transportation* 2020 (1):4242964.

Sheu, Gloria. 2014. “Price, quality, and variety: Measuring the gains from trade in differentiated products.” *American Economic Journal: Applied Economics* 6 (4):66–89.

Small, Kenneth A. 1982. “The scheduling of consumer activities: work trips.” *The American Economic Review* 72 (3):467–479.

———. 2012. “Valuation of travel time.” *Economics of Transportation* 1 (1-2):2–14.

Small, Kenneth A, Erik T Verhoef, and Robin Lindsey. 2007. *The economics of urban transportation*. Routledge.

Southern California Association of Governments. 2019. “Mobility Go Zone Pricing Feasibility Study.” Tech. rep., Southern California Association of Governments.

Train, Kenneth E. 2009. *Discrete Choice Methods with Simulation*. Cambridge University Press.

Transport for London. 2008. “Central London congestion charging impacts monitoring sixth annual report, July 2008.” Tech. rep., Transport for London.

Tseng, Yin Yen, Barry Ubbels, and Erik Verhoef. 2005. “Value of time, schedule delay and reliability.” In *ERSA conference papers*.

Vickrey, William S. 1963. “Pricing in urban and suburban transport.” *The American Economic Review* 53 (2):452–465.

Yang, Jun, Avralt-Od Purevjav, and Shanjun Li. 2020. “The marginal cost of traffic congestion and road pricing: Evidence from a natural experiment in Beijing.” *American Economic Journal: Economic Policy* 12 (1):418–53.

Zhang, Wei, C-Y Cynthia Lin Lawell, and Victoria I Umanskaya. 2017. “The effects of license plate-based driving restrictions on air quality: Theory and empirical evidence.” *Journal of Environmental Economics and Management* 82:181–220.

Zhong, Nan, Jing Cao, and Yuzhu Wang. 2017. “Traffic congestion, ambient air pollution, and health: Evidence from driving restrictions in Beijing.” *Journal of the Association of Environmental and Resource Economists* 4 (3):821–856.

Appendix

A. Theory Appendix

A.1. Substitution with Many Goods

Setup: A representative consumer chooses quantities of M goods, $(h_1, ..., h_M)$ and a numeraire, z. Each non-numeraire good has an associated externality, ϕ_m. A policymaker can choose tax levels for goods $j \in \{1, ..., J\}$ where $J < M$. I assume goods $k \notin \{1, ..., J\}$ are un- or under-taxed.

The consumer's problem: An agent maximizes utility over M goods $(h_1, ..., h_M)$ and a numeraire good z.

$$max\{U(h_1, ..., h_M) + z\} \quad s.t. \tag{21}$$

$$(p_1 + \tau_1)h_1 + (p_J + \tau_J)h_J + p_{J+1}h_{J+1} + ... + p_M h_M + z \leq I \tag{22}$$

The first-order conditions for an interior solution to the consumer's problem are:

$$U_j = \lambda(p_j + \tau_j) \quad \forall \quad j \in \{1, ..., J\} \tag{23}$$

$$U_k = \lambda(p_k) \quad \forall \quad k \notin \{1, ..., J\} \tag{24}$$

$$\lambda = 1 \tag{25}$$

The planner's problem: I assume that the planner seeks to maximize aggregate welfare, which is the utility of the representative consumer less the aggregate social cost of consumption, $\sum_1^M \phi_m h_m$. The planner's choice variables are tax levels $\tau_1 ... \tau_J$, which are applied to the taxable goods $j \in \{1, ..., J\}$.

$$\begin{gathered} max\{U(h_1, ..., h_M) + z - \sum_1^M \phi_m h_m\} \; st. \\ p_1 h_1 + ... + p_N h_N + z \leq I \end{gathered} \tag{26}$$

Assuming an internal solution, first-order condition wrt p_j (where $j \in \{1, ..., J\}$) is:

$$0 = \frac{\partial h_j}{\partial p_j}[U_j - \phi_j - p_j] + \sum_{k \neq j}^{M} \frac{\partial h_k}{\partial p_j}[U_k - \phi_k - p_k] \tag{27}$$

Plugging in the consumer's first order conditions and solving for τ_m:

$$0 = \frac{\partial h_j}{\partial p_j}[\tau_j - \phi_j] + \sum_{k \neq j}^{J} \frac{\partial h_k}{\partial p_j}[\tau_k - \phi_k] + \sum_{l=J+1}^{M} \frac{\partial h_l}{\partial p_j}[\phi_l] \tag{28}$$

$$\tau_j = \phi_j + \frac{1}{\frac{\partial h_j}{\partial p_j}}(\sum_{k \neq j}^{J} \frac{\partial h_k}{\partial p_j}[\phi_k - \tau_k] + \sum_{l=J+1}^{M} \frac{\partial h_l}{\partial p_j}\phi_l) \tag{29}$$

This intermediate result is intuitive. Holding fixed all taxes other than τ_j, the optimal value for this final tax is its externality, ϕ_m, minus a term that captures the extent to which consumers switch to other goods, and the level of unpriced externality of those goods.

Identifying the optimal tax level for *all* taxable goods requires solving J equations simultaneously:

$$\tau_j + \frac{1}{\frac{\partial h_j}{\partial p_j}}(\sum_{k \neq j}^{J} \frac{\partial h_k}{\partial p_j}\tau_k) = \phi_j + \frac{1}{\frac{\partial h_j}{\partial p_j}}\sum_{l=1}^{M} \frac{\partial h_l}{\partial p_j}\phi_l \tag{30}$$

This gives us J equations, each linear in the J tax levels:

$$a_1^j\tau_1 + ... + a_k^j\tau_k + ... + a_J^j\tau_J = b_j \qquad \forall j \in \{1, ..., J\} \tag{31}$$

Where a_k^j and b_m are defined as:

$$a_k^j = \frac{\frac{\partial h_k}{\partial p_j}}{\frac{\partial h_j}{\partial p_j}} \tag{32}$$

$$\beta_j = \phi_j + \sum_{l=1}^{M} \frac{\frac{\partial h_l}{\partial p_j}}{\frac{\partial h_j}{\partial p_j}}\phi_l \tag{33}$$

The a and β terms have an intuitive interpretation. a_k^j is the share of the reduction in overall consumption of good j that shifts to good k as a result of an increase in the price of good j. β_j is the overall reduction in externalities that results from the increase in the price of good j; this consists of a direct component, ϕ_j plus a (negative) leakage term, $\sum_{l=1}^{M} \frac{\partial h_l}{\partial p_j} / \frac{\partial h_j}{\partial p_j}\phi_l$. This system can be written as:

$$\begin{bmatrix} a_1^1 & ... & a_J^1 \\ & ... & \\ a_1^j & ... & a_J^J \end{bmatrix} \begin{bmatrix} \tau_1 \\ ... \\ \tau_J \end{bmatrix} = \begin{bmatrix} b_1 \\ ... \\ b_J \end{bmatrix} \tag{34}$$

$$\boldsymbol{A\tau} = \boldsymbol{b} \tag{35}$$

$$\boldsymbol{\tau} = \boldsymbol{A}^{-1}\boldsymbol{b} \tag{36}$$

A.2. Heterogeneity and Leakage

Setup: N Heterogeneous consumers choose between M externality-generating goods and a numeraire, z. I denote individual i's consumption of good m as h_i^m. Each individual has an exogenous income μ_i. I assume that each consumer's utility is a function of their consumption of these M goods and a quasilinear numeraire, as well as other's consumption of these goods (which generate externalities and decrease i's utility): $U_i(h_1^1, ...h_1^M, ..., h_i^1, ...h_i^M, ...h_N^1, ...h_N^M) + z_i$.

As in section 2.3, a policymaker can choose tax levels for goods $j \in \{1, ..., J\}$ where $J < M$. I assume goods $k \notin \{1, ..., J\}$ are un- or under-taxed. I denote τ^j as the tax on good j.

The consumer's problem: Agent i maximizes utility over M goods $(h_i^1, ..., h_i^M)$ and their consumption of the numeraire good z_i.

$$\begin{gathered} max\{U_i(h_1^1, ...h_1^M, ..., h_i^1, ...h_i^M, ...h_N^1, ...h_N^M) + z_i\} \ st. \\ (p^1 + \tau^1)h_i^1 + (p^J + \tau^J)h^J + p^{J+1}h_i^{J+1} + ... + p^M h_i^M + z_i \leq \mu_i \end{gathered} \tag{37}$$

The first-order conditions for this problem are:

$$\begin{aligned} \frac{\partial U_i}{\partial h_i^j} &= \lambda(p^j + \tau^j) && \forall \ \ j \in \{1, ..., J\} \\ \frac{\partial U_i}{\partial h_i^k} &= \lambda(p^k) && \forall \ \ k \notin \{1, ..., J\} \\ & && \lambda = 1 \end{aligned} \tag{38}$$

The planner's problem: I assume that the planner seeks to maximize aggregate welfare, $\sum_1^N (U_i + z_i)$. The planner's choice variables are tax levels $\tau^1 ... \tau^J$, which are applied to the taxable goods $j \in [1, J]$.

$$\begin{gathered} max\{\sum_i^N (U_i(h_1^1, ...h_1^M, ..., h_i^1, ...h_i^M, ...h_N^1, ...h_N^M) + z_i) \\ st. \qquad (p^1)\sum_i^N h_i^1 + ... + (p^J)\sum_i^N h_i^J + (p^{J+1})\sum_i^N h_i^{J+1} + ... + (p^M)\sum_i^N h_i^M + \sum_i^N z_i \leq \sum_i^N \mu_i \end{gathered} \tag{39}$$

Assuming an internal solution, first-order condition wrt p^j (where $j \in [1, J]$) is:

$$0 = \sum_{i=1}^N \frac{\partial U_i}{\partial h_i^l}\frac{\partial h_i^l}{\partial p_j} + \sum_{i=1}^N \sum_{g \neq i}^N \frac{\partial U^i}{\partial h_g^1}\frac{\partial h_1^g}{\partial p_j} + ... + \frac{\partial U^i}{\partial h_g^M}\frac{\partial h_g^M}{\partial p_j} - p^1 \sum_i \frac{\partial h_i^1}{\partial p_j} - ... - p^M \sum_i \frac{\partial h_1^M}{\partial p_j} \tag{40}$$

Plugging in the consumer's first order conditions and solving for τ_j:

$$\tau_j = \frac{\sum_{i=1}^{N} \sum_{g}^{N} \big(\frac{\partial U^i}{\partial h_g^1} \frac{\partial h_g^1}{\partial p_j} + ... + \frac{\partial U^i}{\partial h_g^M} \frac{\partial h_g^M}{\partial p_j} \big)}{\sum_{i=1}^{N} \frac{\partial h_i^j}{\partial p_j}} + \frac{\sum_{k \neq j}^{J} \frac{\partial h_i^k}{\partial p_j} \tau_k}{\sum_{i=1}^{N} \frac{\partial h_i^j}{\partial p_j}} \tag{41}$$

This expression for the optimal level of a given tax is equivalent to the equation for substitutes with homogeneous damages where each of the marginal damages is replaced by a "Diamond" term which accounts for heterogeneity.

B. Additional Tables and Figures

Table A1 — San Francisco's Proposed Congestion Pricing Scheme

	Income Group			
Time Period	High	Middle	Low	Very Low
Peak Hours	6.50	4.33	2.17	Free
Off-Peak Hours	Free	Free	Free	Free

Table A1: San Francisco's proposed cordon pricing scheme, as per the San Francisco County Transportation Authority (San Francisco County Traffic Authority, 2021). Trips that enter the cordon (see Figure 4) would be charged during peak hours according to the income of the registered vehicle. Tolls will be levied using electronic tag readers mounted on gantries that span roadways on the border of the cordon region. An individual's income group depends both on income and family size. For single individuals, the annual income thresholds for high, middle, low, and very low income are \$150,000, \$116,000, \$66,000 and \$46,000, respectively. For a household of four, the thresholds are \$65,000, \$95,000, \$142,000, \$166,000.

Figure A1 — Peak Pricing on Bay Area Bridges

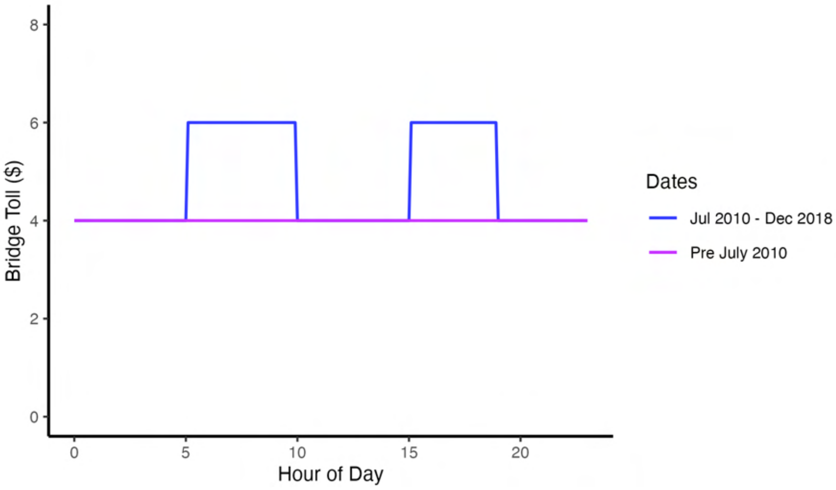

Figure A1: This figure displays peak-hour pricing schemes for passenger vehicles (vehicles with two axles) on California's Bay Bridge, which connects San Francisco and Oakland. Beginning on July 1, 2010, passenger vehicles crossing westbound on weekdays during peak hours (between 5 a.m. and 10 a.m., or between 3 p.m. and 7 p.m.) faced higher prices than vehicles crossing during off-peak hours. Peak-hour prices are displayed on a large variable-message sign about the Bay Bridge toll plaza. Weekend trips on the Bay Bridge and trips on the other major Bay Area bridges are not subject to peak pricing, instead charging the base rate for passenger vehicles ($4 for pre-2010 and $5 for July 2010 - December 2018).

Figure A2 — Variation in Passenger Vehicle Bridge Tolls

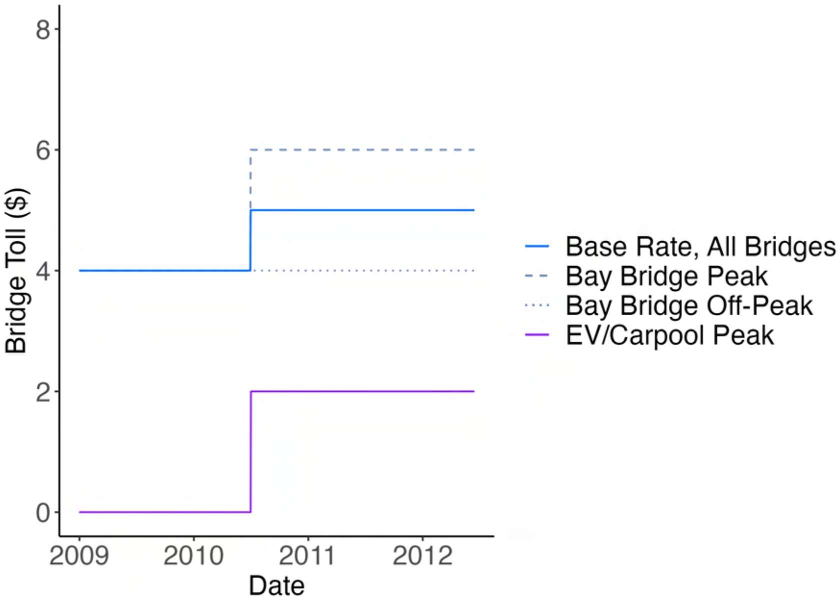

Figure A2: This figure shows Bay Area bridge tolls between 2009 and 2012 for passenger vehicles. Prices are uniform across bridges, with the exception of the Bay Bridge, which connects San Francisco and Oakland. Beginning in 2010, passenger vehicles crossing the Bay Bridge faced a two-dollar difference between peak and off-peak prices. The peak ($6) and off-peak ($4) prices are plotted above as dotted and dashed lines, respectively. EV and carpool trips were free on all bridges prior to 2010. Beginning in July of 2010, EV/carpool trips were charged the base rate ($5 on the San Mateo, Dumbarton, and Richmond Bridges; $4 on the Bay Bridge), except during peak hours, where they receive a discount ($2.5) on all bridges.

Figure A3 — Congestion Costs as a Function of Density, Re-Scaled from Yang et al. (2020)

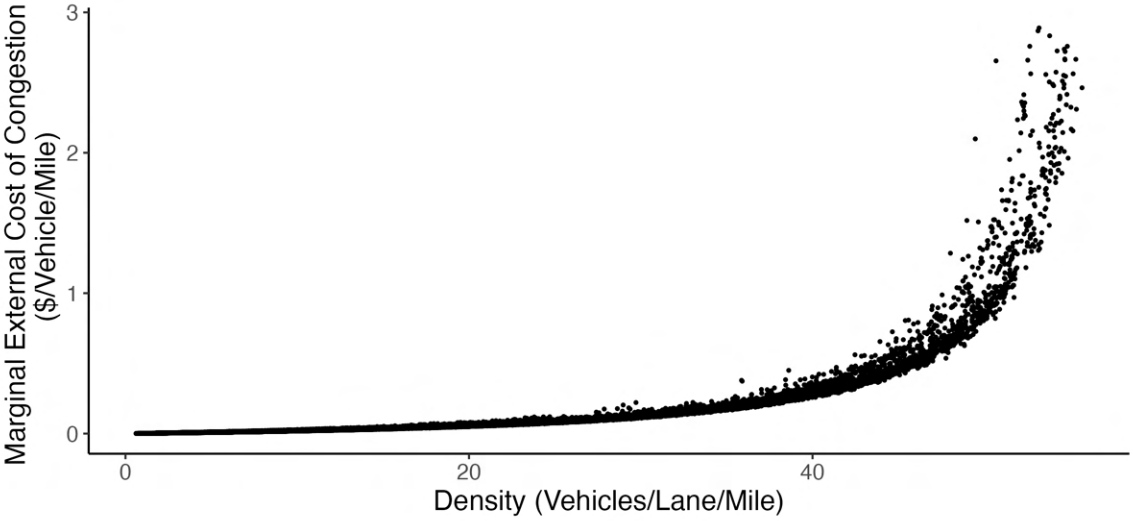

Figure A3: Congestion costs reproduced from Yang, Purevjav, and Li (2020), who exploit variation in traffic density generated by Beijing's driving restriction to estimate the relationship between traffic density and speed. The original results are presented in Yuan/Vehicle/km. I convert these values to dollars by a) converting currencies, and b) replacing the Beijing-specific value of time from (50% of the average wage rate in Beijing) with a $20 value of travel time, which reflects San Francisco-specific estimates from Goldszmidt et al. (2020).

Figure A4 — Average Pollution Externalities by Travel Speed

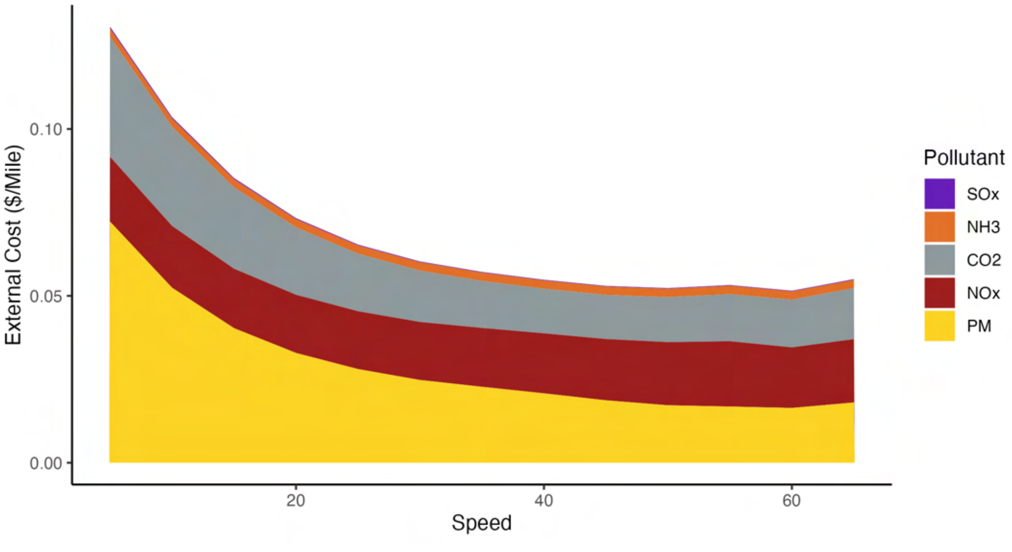

Figure A4: This figure plots per-mile pollution externalities at various speeds for an average passenger vehicle in the Bay Area. These costs reflect VMT-weighted average emissions factors (in grams/mile) of different pollutants at different speeds reported by California's Emissions Factor Model (EMFAC). The EMFAC emissions factor estimates reflect state DMV and smog check data. To convert these emissions factors to per-mile costs, I multiply the emission factor for each pollutant by the corresponding social cost of each pollutant. For local pollutants, the social cost is calculated using the Estimating Air Pollution Social Impact Using Regression (EASIUR) Online Tool, calibrated with coordinates from San Francisco. For global pollutants, I use the EPA's 2021 social costs of $51 per ton of CO_2 and $1,500 per ton of CH_4, respectively.

Figure A5 — Impact of the 2010 Toll Changes on Bay Area Bridge Traffic

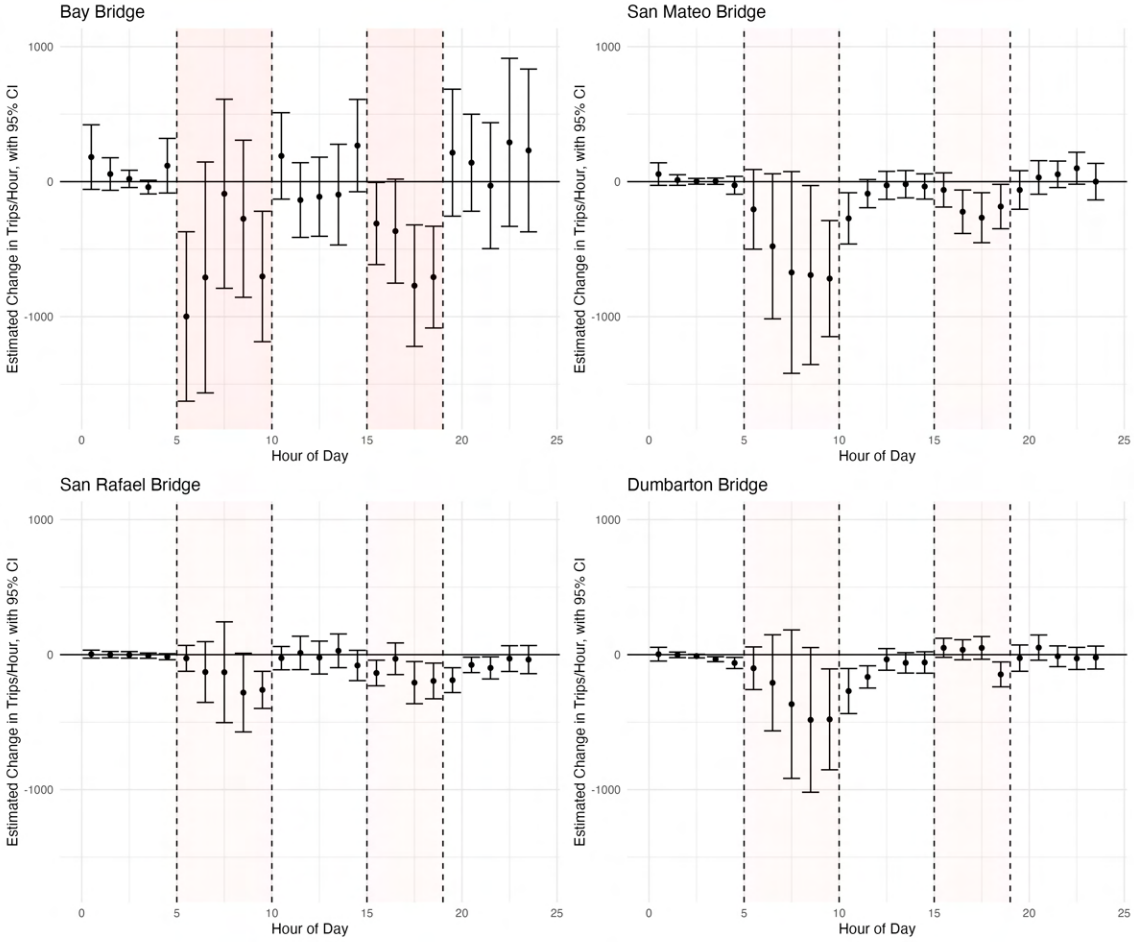

Figure A5: This figure displays hourly estimated changes in traffic volume on the four major trans-bay bridges after the 2010 change in toll prices. Each point represents the estimated coefficient for a given bridge an hour of the day, as per equation 20. The red shaded region corresponds to the peak hour pricing on the Bay Bridge; the other three bridges did not have peak hour pricing either before or after the toll change. The data used to arrive at these estimates are hour-by-date aggregate bridge crossing data courtesy of FasTrak.

Figure A6 — Cordon and Non-Cordon Routes for Bay-Area Trips

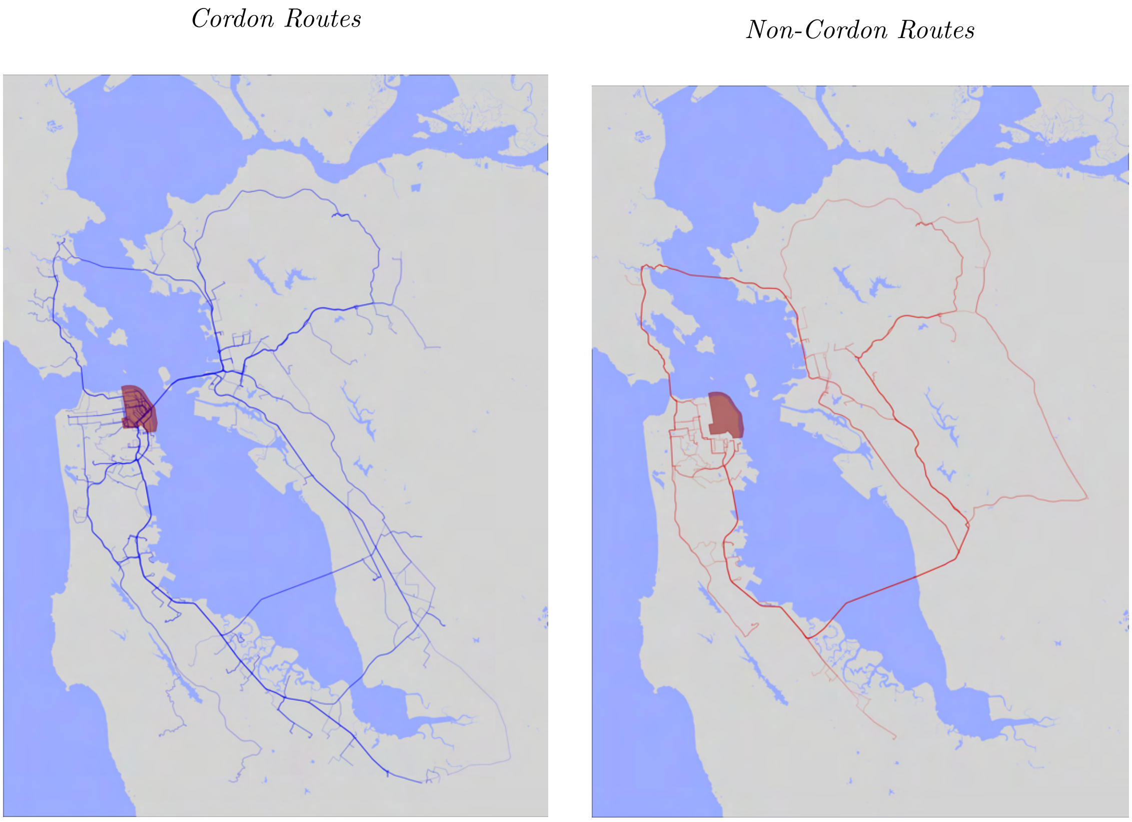

Cordon Routes

Non-Cordon Routes

Figure A6: This figure plots cordon and non-cordon routes constructed from the 2017 National Household Travel Survey (NHTS) California Add-On. The left pane plots 1,891 trips that cross San Francisco's proposed congestion zone, according to suggested routes generated with the HERE Technology's *Routes* API. The right pane plots detour routes for the subset of these trips where it is possible to circumvent the congestion zone (i.e., trips with both start and end points that are outside of the cordon). Each driver's choice set consists of a cordon route (the left pane) for every 12-minute time of day interval, as well as a non-cordon route (the right pane), if such a detour exists, for every 12-minute time of day interval. The choice sets of all drivers also include a generic outside option.

Figure A7 — External Costs for Trips Crossing San Francisco's Proposed Cordon

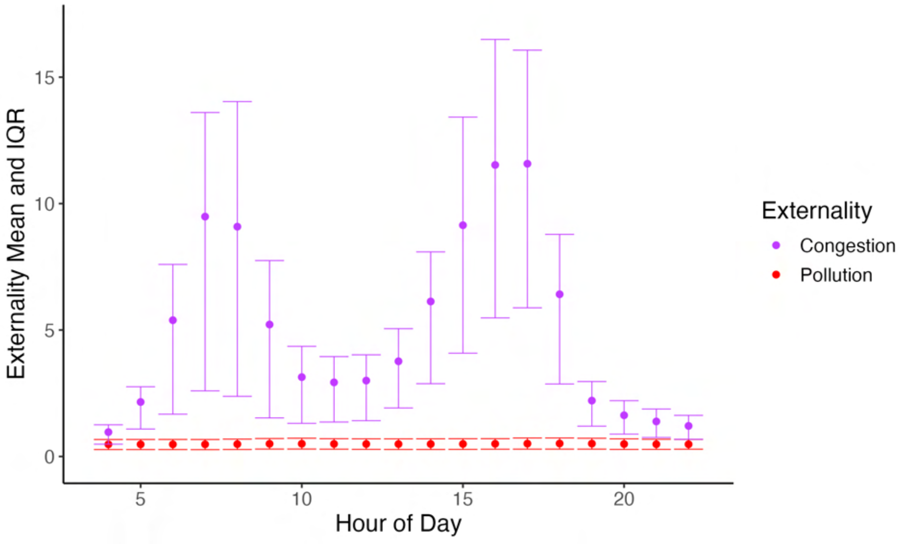

Figure A7: This Figure plots pollution (red) and congestion (purple) externalities by hour for trips in the 2017 National Household Travel Survey (NHTS) with suggested routes that pass through San Francisco's proposed cordon zone. The mean externality within any given hour is represented by a dot; the box spans the 25th to 75th externality percentile, and the bars span the 5th to 95th externality percentile. Trip routes reflect the suggested directions from HERE Technology's *Routes* API. Congestion costs were calculated by identifying traffic sensors along a given route and assigning per-mile congestion costs to each sensor using estimates of the density-congestion relationship from Yang, Purevjav, and Li (2020) and an average value of travel time of $20, as per Goldszmidt et al. (2020). Pollution emissions were calculated by merging emissions factors from California Air Resources Board's EMFAC database with trips based on vehicle fuel type, vehicle age, and average trip travel speed. I convert emissions to externalities using EPA social costs for global pollutants and EAISUR costs for local pollutant emissions in San Francisco.

Figure A8 — Bunching at Price Notches

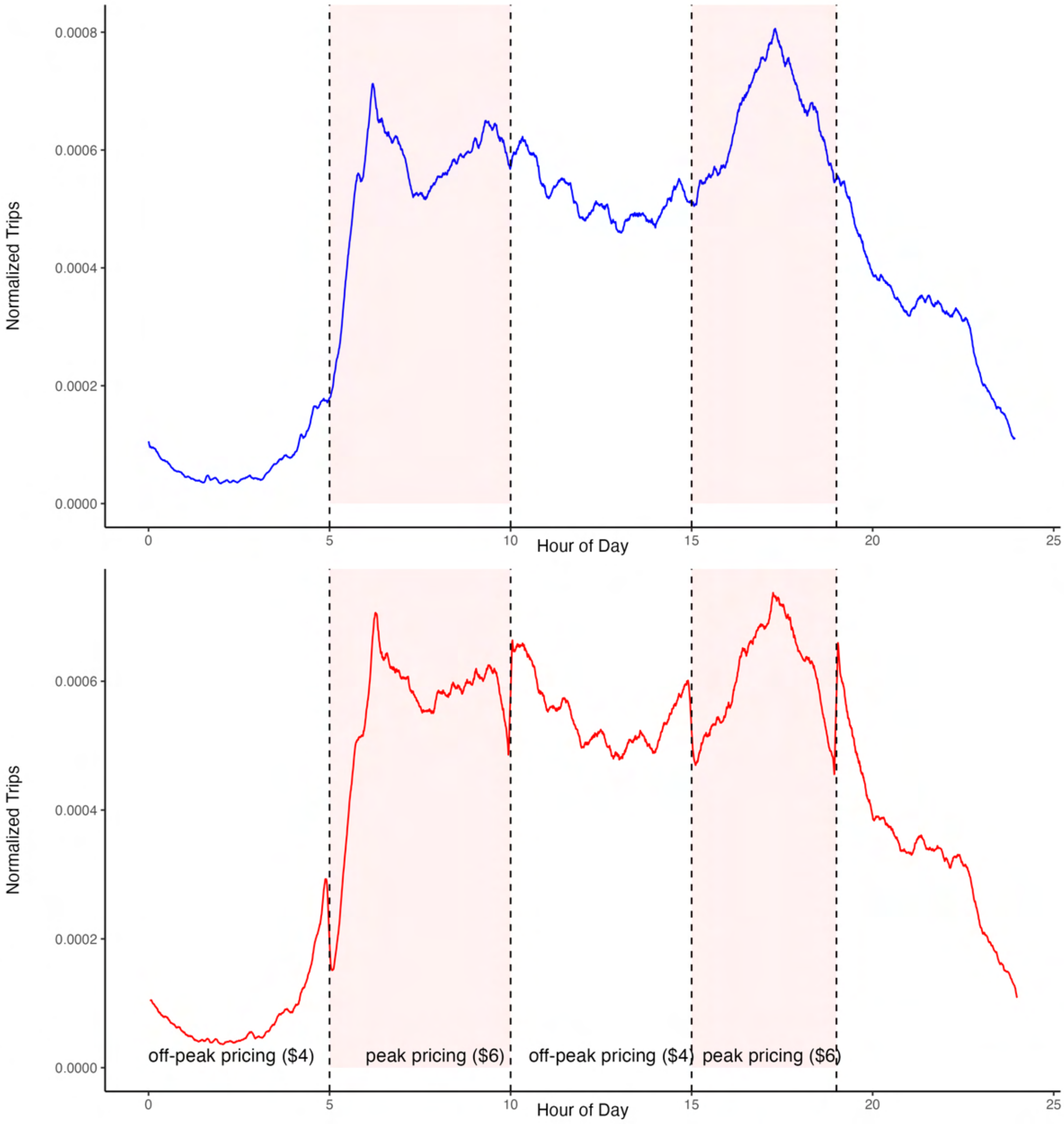

Figure A8: This figure plots the density (the share of total daily crossings) of passenger vehicle trips crossing San Francisco's *Bay Bridge* in the 6 months before (blue) and 6 months after (red) the imposition of peak hour pricing on July 1, 2010. This plot excludes trips that use the carpool lane, as well as eligible electric vehicles, each of which faced a different pricing scheme. The red shaded regions demarcate times of day that were subject to peak-hour pricing after July 1, 2010.

Figure A9 — Bunching at Temporal Toll Cutoffs in Other Settings

Figure 4: DiD estimates on traffic volume by 15 min. intervals. 2 years pre/post

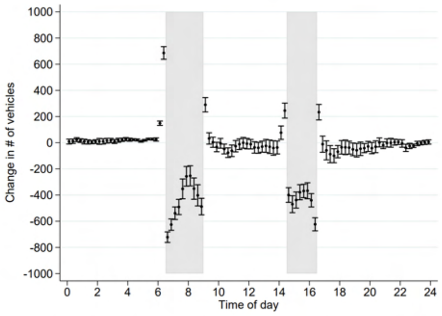

Notes: Figure plots treatment effects estimated from from equation 1, where regressions are run separately for each 15 minute increment. Whiskers indicate 95% confidence intervals. Standard errors are not adjusted for multiple hypothesis testing. Gray shaded areas indicate rush hours. Traffic is measured as the total number of cars passing the toll cordon every 15 minutes. Standard errors are clustered at the week level.

Figure 4 of Isaksen and Johansen (2021). Bergen, Norway.

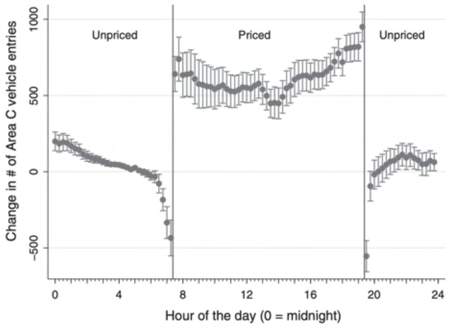

Fig. 4. Effect of Area C charge suspension on vehicle entries, by 15-min interval. Dependent variable is Area C entries by vehicles subject to charge. Estimates are from Eq. (1), estimated separately for each 15-min interval. Whiskers represent Newey-West standard errors multiplied by 1.96. The lag length is 35 for hours 23.5–5.25, 7 otherwise. "Unpriced" and "priced" labels refer to status of a given interval under the Area C policy, which prices entries 7:30AM–7:30PM.

Figure Gibson and Carnovale (2015). Milan, Italy. This figure plots point estimates of changes in traffic following the suspension of congestion pricing.

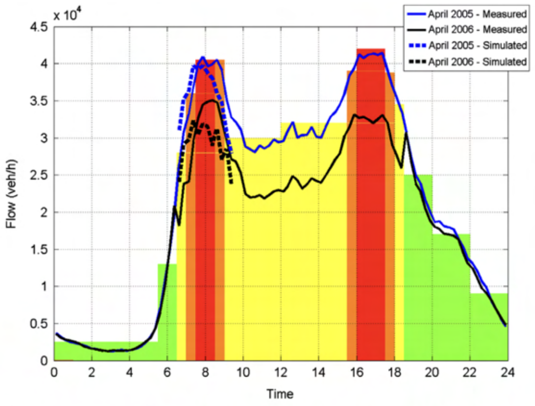

Fig. 2. Measured (solid) and simulated (dotted) daily flow variations (for interpretation of the references to colour in this figure, the reader is referred to the web version of this article).

Figure 2 of Kristoffersson (2013). Stockholm, Sweden.

Figure 3.8 Flows across the Thames screenline within the central London congestion charging zone, by time of day, 2004 to 2007.

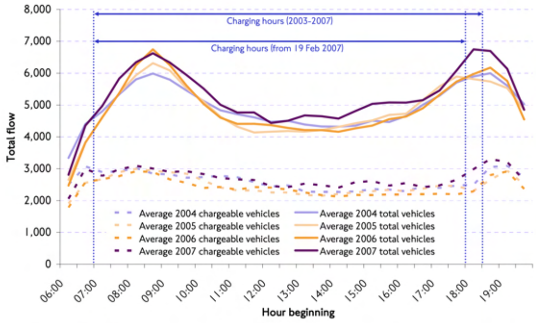

Figure 3.8 of Transport for London (2008). London, United Kingdom. The dotted lines show volumes for vehicles facing a toll.

Figure A9: These figures show that congestion pricing induces bunching in other settings, suggesting that a bunching estimator similar to the one described in Section 6 could be used to recover commuter scheduling elasticities elsewhere.

Figure A10 — Bunching in the Short and Long Run

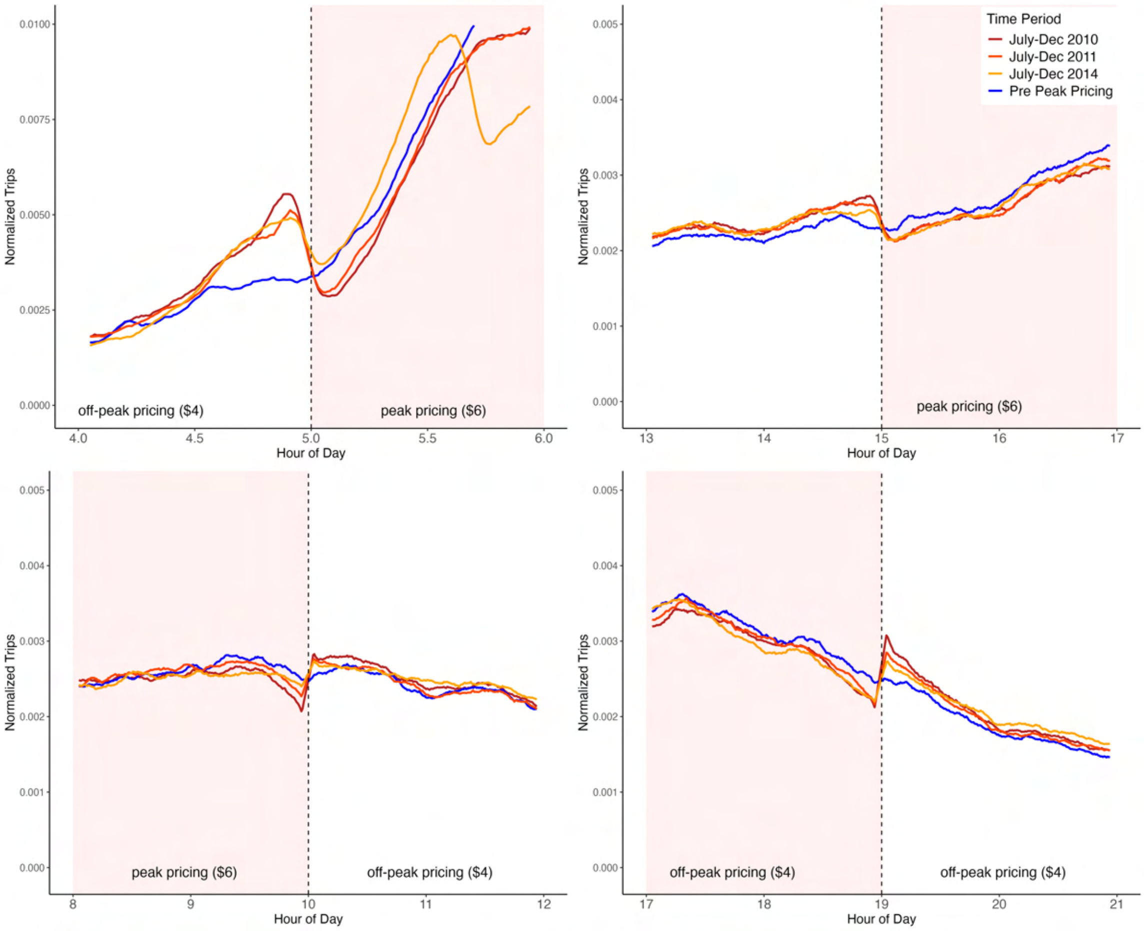

Figure A10: San Francisco's *Bay Bridge* imposed peak hour pricing on July 1, 2010 (see Section 4). This figure plots the density of passenger vehicle trips crossing the Bay Bridge in the hours surrounding each of the price notches in January-July of 2010 (blue) against three other time periods: July-December of 2010 (brown), July-December of 2011 (red), and July-December of 2014 (orange). This plot excludes trips that use the carpool lane, as well as eligible electric vehicles, each of which faced a different pricing scheme. The red shaded regions demarcate times of day that were subject to peak-hour pricing after July 1, 2010.

Figure A11 — Bunching in Electronic Tolls vs. Cash Tolls

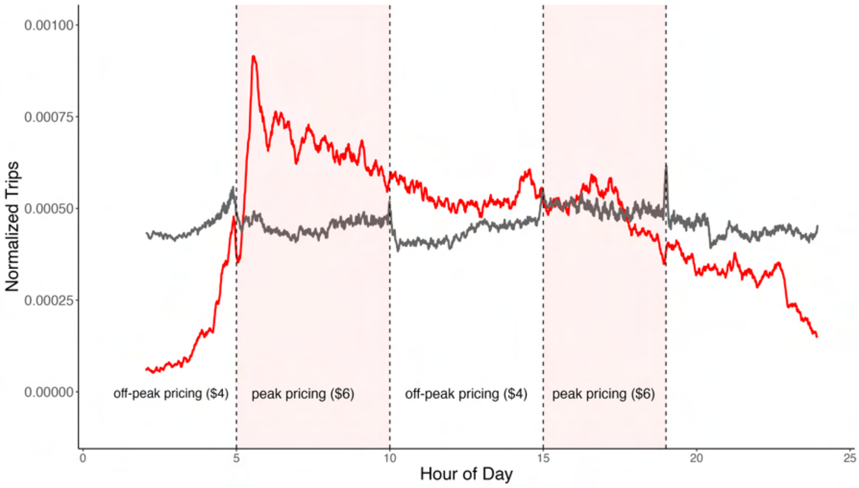

Figure A11: San Francisco's *Bay Bridge* imposed peak hour pricing on July 1, 2010 (see Section 4). This figure plots the density of passenger vehicle trips crossing the Bay Bridge in the hours surrounding each of the price notches in 2014 (records of cash payments are unreliable prior to 2014). The red line shows trips using an electronic FasTrak device; the grey line shows cash payments. This plot excludes trips that use the carpool lane, as well as eligible electric vehicles, each of which faced a different pricing scheme. The red shaded regions demarcate times of day that were subject to peak-hour pricing after July 1, 2010.

Figure A12 — Traffic Sensors in the Bay Area

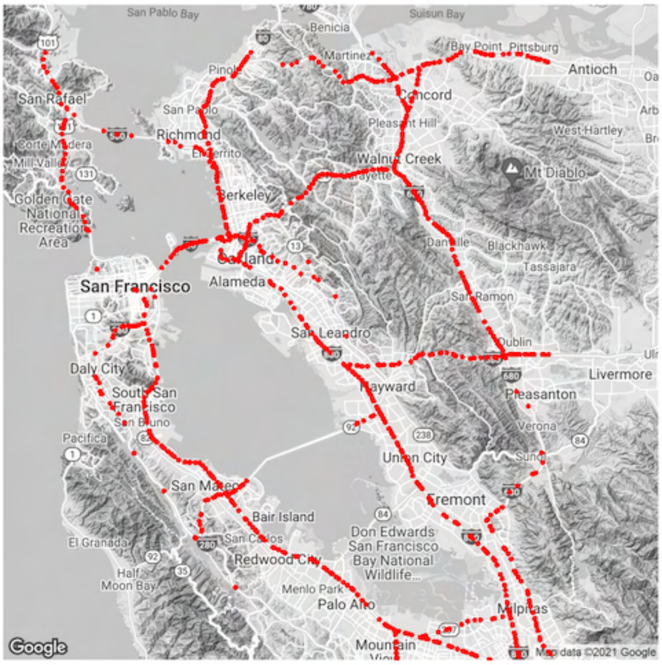

Figure A12: This figure plots traffic sensors from the Caltrans Performance Measurement System (PeMS). Each sensor reports hourly vehicle count and speed data that are converted to traffic density (vehicles/lane/mile) using the fundamental diagram of traffic flow. These traffic density readings are then used to assign congestion externalities to vehicle trips based on route and time of day, as described in sections 5 and 8.

C. Calculating Emissions Externalities

This section details the process of estimating emissions externalities for each trip in the FasTrak dataset.

The California Emissions Factor (EMFAC) fleet database reports average vehicle emissions rates (measured in grams per mile) by county. These data are stratified by vehicle fuel type, vehicle vintage, and vehicle travel speed. The EMFAC database reports the following pollutant species: particulate matter (PM2.5, or PM), nitrogen oxides (NO_x), nitrous oxide (N_2O), reactive organic compounds (ROC), ammonia (NH_3), carbon dioxide (CO_2), sulfur oxides (SO_2), and methane (CH_4). The data underlying EMFAC aggregates reflect state vehicle registrations and data from the California Bureau of Automotive Repair's (BAR) Smog Check database. For each FasTrak trip, I assign emission factors for each pollutant based on the average travel speed for that trip (see Appendix E) and the county where the FasTrak device is registered. The total emissions of any pollutant is the estimated emissions *rate* for that trip multiplied by the trip *length*. To convert trip-level emissions to costs, I use social cost estimates from two sources. For local pollutants, I use damages predicted by the EAISUR model (Heo, Adams, and Gao (2016)), which combines a state-of-the-art chemical transport model together with estimates from the economics and epidemiology literatures to predict the cost of emitting pollution in different areas of the United States. For global pollutants, I use social damages from the US EPA. These pollutant values are listed in Table A2.

Table A2 — Social Costs of Vehicle Pollution in San Francisco

	Damages ($/Ton Emitted)		
Pollutant	**SF**	**LA**	**NY**
$PM_{2.5}$	772, 000	1, 270, 000	1, 146, 000
SO_2	65, 800	44, 750	44, 125
NO_x	24, 200	52, 750	62, 875
NH_3	1, 24, 000	825, 750	561500
CO_2	51	51	51
CH_4	1, 500	1, 500	1, 500
N_2O	18, 000	18, 000	18, 000
ROC	2, 392	2, 392	2, 392

Table A2: This table displays the social costs of emitting 1 ton of various pollutants in San Francisco, Los Angeles, and New York, respectively. Estimates of local pollutants ($PM_{2.5}$, nitrogen oxides (NO_x), nitrous oxide (N_2O), reactive organic compounds (ROC), ammonia (NH_3), sulfur oxides (SO_2)) reflect annual averages from the EAISUR model (Heo, Adams, and Gao (2016)). Global pollutants (carbon dioxide (CO_2) and methane (CH_4)) are values used by the US EPA.

D. Bunching Estimator

This Appendix contains details of the bunching estimators used as a second empirical approach to recovering scheduling elasticities (see Section 6). The following two equations are bunching estimators that do, and do not account for changes in travel times for bunches, respectively:

$$\gamma_e = \frac{\beta \Delta p + \alpha \Delta T}{{}^{B}\!/\!_{((1-a)f_0(h^*))}}$$

$$\gamma_e = \frac{\beta \Delta p}{{}^{B}\!/\!_{((1-a)f_0(h^*))}}$$

Table A3 shows estimates of each of the component parts of these estimators for the 5 a.m. price notch. The change in price (Δp) is the same ($2) for all notches. The excess mass (B) is the integral of the difference in densities in the half-hour period[14] prior to the imposition of peak hour pricing. Following Kleven and Waseem (2013), I use the comparison of the pre and post July 2010 density within the 5 minutes after the beginning of peak-hour pricing to identify the fraction of unresponsive individuals (a, 76%). As an approximation for the change in travel time (ΔT), I use TomTom's Historic Traffic Stats to compute the difference in average travel travel times between 5:00 a.m. and 6:00 a.m. (see Figure A13 below) for FasTrak drivers using the Bay Bridge. The components of bunching estimators for the other three notches (10 a.m., 3 p.m., and 7 p.m.) follow this same procedure.

Table A3 — Bunching Estimator for Scheduling Costs (Shifting Earlier, 5 a.m.)

Parameter	**Estimate**
Fraction Unresponsive (a)	0.76058
Excess Mass at Notch (B)	0.00208
Baseline Density at Notch	0.00019
Mean Schedule Cost without Friction ($/hour)	18.65659
Mean Schedule Cost accounting for Frictions ($/hour)	4.46673
Mean Schedule Cost accounting for Frictions and Travel Time ($/hour)	6.19461

Table A3: Rows 1-3 of this table show estimates of parameters used to infer scheduling costs from the additional density of trips just after the end of peak-hour pricing on San Francisco's Bay Bridge (Equation 17). Rows 4-6 show estimates of scheduling costs. In Row 4, I calculate the naive average scheduling cost under the assumption that there are no optimization frictions. In row 5, I use the estimated fraction of non-responsive individuals from row 1 to account for optimization frictions. In row 6, I also account for the difference in travel times for drivers who reschedule their trips to avoid peak-hour pricing.

[14] This is the "excluded range" (Kleven and Waseem (2013) section II.C) where bunching leads the density of drivers to exceed the counterfactual density. See Figure 3 for a comparison of the bunching and counterfactual densities.

Figure A13 — Travel Times in the Vicinity Price Notches

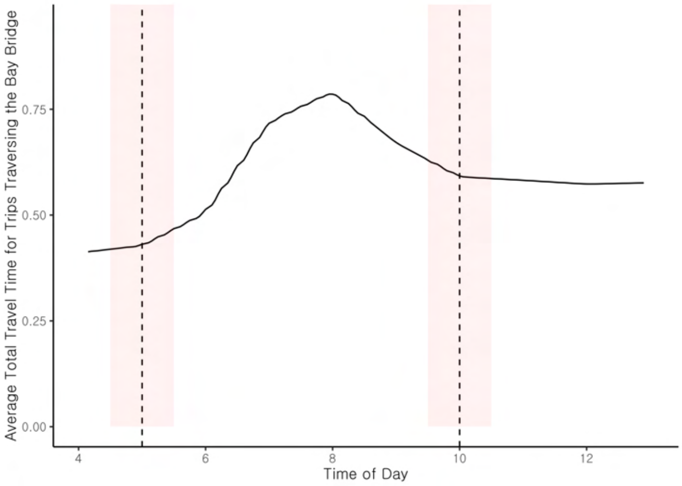

Figure A13: This figure plots average travel times for trips traversing the Bay Bridge during the morning hours. The average travel times in this figure were calculated by 1) identifying all drivers that primarily use the Bay Bridge and b) using TomTom Historic Traffic Stats to calculate travel times for each individual, for each hour of day as described in Section 5. The red shaded area represents the approximate range where individuals adjust in response to the imposition of peak-hour pricing, according to FasTrak toll data. The relatively flat profile of travel times in the price notch neighborhood suggests that the first-order decision facing drivers who travel at this time of day is between price and scheduling costs, as opposed to changes in total travel time. As shown in Table A3, estimates that account for differences in travel times in the bunching estimators are roughly 30% larger than estimates that ignore differences in travel times.

E. Imputing Travel Times

Travel times, T^i, are not directly observed for FasTrak trips, and therefore must be imputed. In this Appendix, I describe the process for inferring travel times, $T^i(h, r)$, for each trip in each individual's choice set.

The choice set of any individual consists of all *bridges* $\in$ {*Dumbarton Bridge, San Mateo Bridge, Bay Bridge, Richmond Bridge*} at all *times of day* $\in \{4.0, 4.2, ..., 22\}$. A *trip* in this choice set constitutes a *bridge-time* pair, (h, r). I estimate travel times for each trip in each individual's choice set in three steps:

***Step 1*: Infer the distribution of endpoints**. The FasTrak tolling data include information about the bridges used, as well as the home zip code associated with each FasTrak device. Before calculating travel times using historic traffic data, I must make inferences about the missing endpoints for each driver. To do so, I use survey data from the 2010-2012 California Household Travel Survey (CHTS). This survey constitutes a representative sample of Bay Area commuters, and contains detailed information on the driving habits of respondents. To generate a probability distribution of “work” endpoints for each individual, I subset the CHTS survey data to trips that match based on the home city and bridge used. The Bay Area is relatively unique in that it is a large metropolitan area that consists of many small cities. The 29 “cities” that serve as termini for travel time estimation are plotted in Figure A14.

***Step 2*: Calculate travel times**. I use TomTom’s Historic Traffic Stats to calculate the travel times. This traffic database contains detailed historic traffic data collected from TomTom devices, as well as data that TomTom purchases from other GPS providers. For each FasTrak device in the sample, I calculate the travel time between the device’s home city and each of the end cities assigned positive probability for that device in *Step 1.* Importantly, I estimate travel times for both trips that were taken, as well as counterfactual trips that used a different bridge or were taken at a different hour of day.

***Step 3*: Aggregate travel times by bridge and time of day**. Lastly, I collapse the distribution of possible travel times within each *bridge-time* pair by the probability weights from *Step 1.* That is, the result of *Step 2* contains travel times for each choice (a *bridge-time* pair), for each device based on possible “work” locations associated with that device. *Step 3* then assigns a single travel time to each bridge-time choice for each device by taking the probability-weighted sum of the travel times associated with these possible work locations, where those probability weights are based on the CHTS survey data (*Step 1*).

The result of Steps 1-3 is a data set that contains estimated travel times for each trip taken by each device, as well as the travel times that a driver would have faced for each trip, had they taken it at a different hour of day or using a different bridge.

Figure A14 — TomTom Traffic Segments

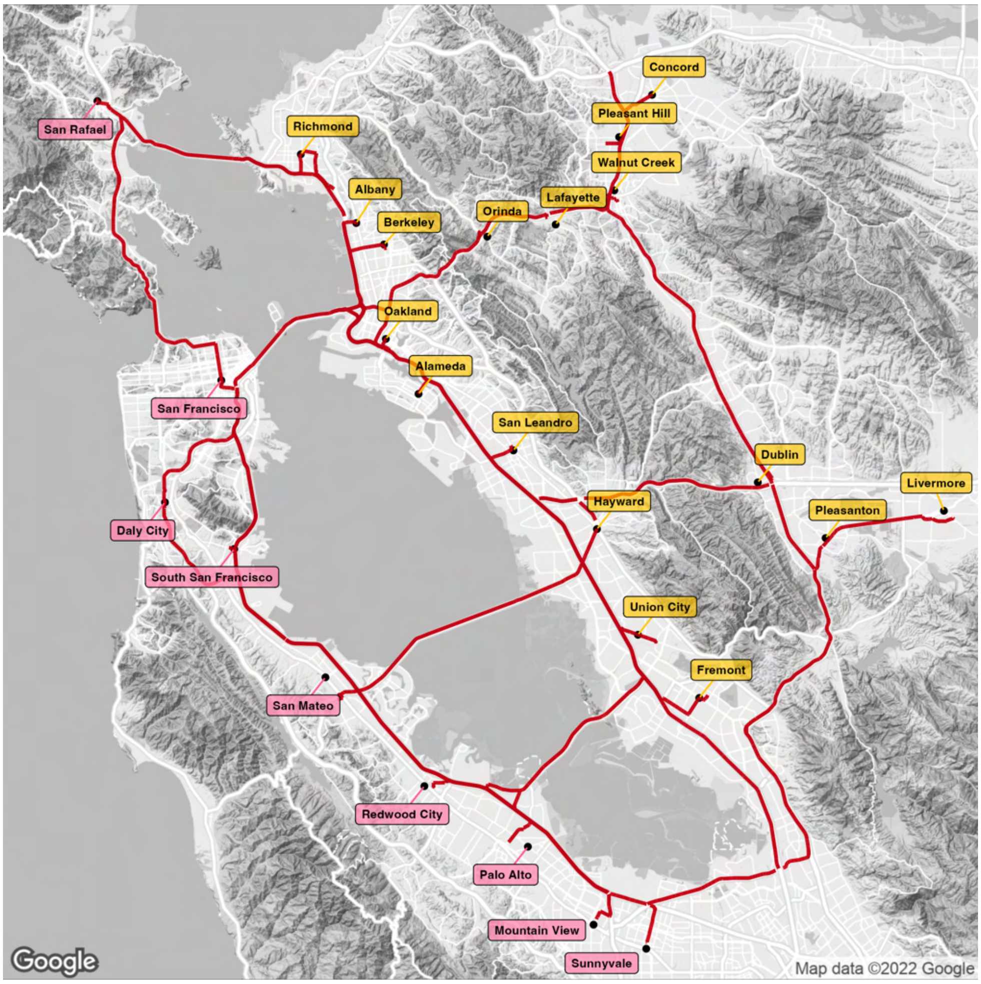

Figure A14: This figure plots the coverage of the historic travel time data purchased from TomTom (in red) together with the 29 most populous cities in the Bay Area. These road segments were selected using Google Maps suggested driving points between the origin and destination cities. These traffic data report the average weekday travel times for passenger vehicles traveling along each segment of road, by hour of day, for the year prior (July 1, 2009 - July 1, 2010) and the year following (July 1, 2010 - July 1, 2011) the 2010 adjustment to Bay-Area bridge tolls.

F. Alternate Congestion Cost Functions and Endogenous Congestion

In subsection F.1, I re-estimate the second-best optimal peak-hour congestion prices for San Francisco using an alternate speed-density relationship derived from California's PeMS traffic data system. In subsection F.2, I discuss endogenous congestion costs, and bound the impact of endogenous congestion on the second-best optimal congestion prices presented in the body of this paper.

F.1. Alternate Marginal External Cost of Congestion Estimates

The results presented in this paper use a density-speed function from Yang, Purevjav, and Li (2020). These authors use exogenous variation induced by a license-plate-based driving restriction in Beijing to estimate the relationship between traffic density and traffic speed, which can then be used to infer a marginal external congestion cost curve. I then re-scale this curve to account for differences in the value of travel time, and then assign costs to segment-hours according to that segment-hours' traffic density.

To address concerns that the density-speed relationship may look different in Beijing and the US,[15] I apply the procedure outlined by Yang, Purevjav, and Li (2020) to data from Los Angeles. This exercise yields a second estimate of the relationship between density and the marginal external cost of congestion, which I then use to re-estimate the paper's main congestion price result.

California's PeMS database (described in Section 5) reports traffic data, including speed and density, at 5-minute intervals. These data are reported for a network of road sensors on freeways and other major thoroughfares. To address endogeneity concerns in the speed-density relationship, I instrument for traffic density using the 2003 Los Angeles public transit strike, which lasted from October 14th through November 18th of that year. This is the same variation used by Anderson (2014), who argues that public transit plays an important role in congestion mitigation because the counterfactual trips for public transit users are already heavily congested.

To isolate changes in traffic density that are plausibly downstream of the public transit strike, I restrict my sample to sensors in downtown Los Angeles. I further restrict the sample to sensors that have complete coverage between September 1, 2003 and December 20, 2003. The result is a balanced panel of 761 traffic sensors.

Using these data, I estimate the following instrumental variables regression, following Yang,

[15] There are many setting-specific estimates of the marginal external cost of congestion (see for example Mangrum and Molnar (2017)), but few causally-identified estimates of an entire marginal external congestion cost curves to use as a robustness check.

Purevjav, and Li (2020):

$$Speed_{s,h,d} = \alpha + \beta * \hat{density}_{s,h,d} + \Gamma X_{s,h,d} + \epsilon_{s,h,d} \tag{42}$$

$$density_{s,h,d} = \alpha + \pi * strike_d + \Gamma X_{s,h,d} + \eta_{s,h,d} \tag{43}$$

The subscripts in this regression correspond to the traffic sensor, s, the time of day, h, and the date, d. The *strike* indicator, which equals one between October 14th and November 17th (inclusive), acts as an instrument for traffic density. X is a vector of fixed effects for the dow of week, the hour of data, and the traffic sensor. Note that the coefficient notation in this equation matches Yang, Purevjav, and Li (2020); α and β in these equations should not be conflated with the role that these symbols play elsewhere in the paper.

The results of this instrumental variables regression are in Table A4. The first-stage suggests that traffic density, measured in vehicles per lane-mile, increased by 1.8 vehicles per mile during the strike. This is roughly an 8% increase relative to the average of 22.7 vehicles per lane-mile. Speed was lower during strike days by 1.48 miles per hour. The IV estimate implies that an increase in traffic density of one vehicle per lane-mile slows traffic by roughly 0.82 miles per hour. This slope is similar to the slope reported by Yang et al., whose IV estimates range from −0.814 to −1.136.

Table A4 — Estimating the Density-Speed Relationship using LA's Transit Strike

	density (First Stage)	*mph* (Reduced Form)	*mph* (IV)
Density			-0.815***
			(0.087)
Strike	1.819***	-1.482***	
	(0.117)	(0.499)	
Sensor FE	✓	✓	✓
Day of Week FE	✓	✓	✓
Hour of Day FE	✓	✓	✓
Num. obs.	4012365	4012365	4012365

$^{***}p < 0.01$; $^{**}p < 0.05$; $^{*}p < 0.1$

Table A4: This Table contains the results of estimating the relationship between traffic density and traffic speed using 761 PeMS traffic sensors in Los Angeles. The data used in to estimate these regressions run from September 1, 2003 to December 20, 2003, and include only observations that occur between 6 am and 10 am. *Density* is measured in vehicles per lane-mile. *Strike* is an indicator which equals one between October 14th and November 18th (inclusive). Standard errors are clustered at the station level.

Given an estimate of the slope between traffic density and travel speed, I use equation (2) from Yang et al. to recover a marginal external cost of congestion (MECC) curve:

$$MECC_{s,h,d} = VOT * o * T_{s,h,d} \frac{\epsilon}{1-\epsilon} \tag{44}$$

Where $\epsilon = \frac{\partial S}{\partial D}\frac{D}{S} = \beta\frac{D}{S}$, VOT is the value of travel time, o is the vehicle occupancy rate, and T is travel time (i.e., the inverse of speed).

Figure A15 plots the results of this exercise alongside the replicated results from Figure 6 of Yang, Purevjav, and Li (2020). At high traffic densities, I estimate a higher MECC than do Yang et al. The bulk of road segment-hour observations in cities like San Francisco, however, have traffic densities that are below 30 vehicles per lane-mile, where the estimates I produce here are similar to existing estimates. For reference, I plot the mean peak and off-peak traffic densities for the PeMS data used to match traffic externalities to routes in Section 8.

Figure A15 — Comparing Marginal External congestion Cost Curves

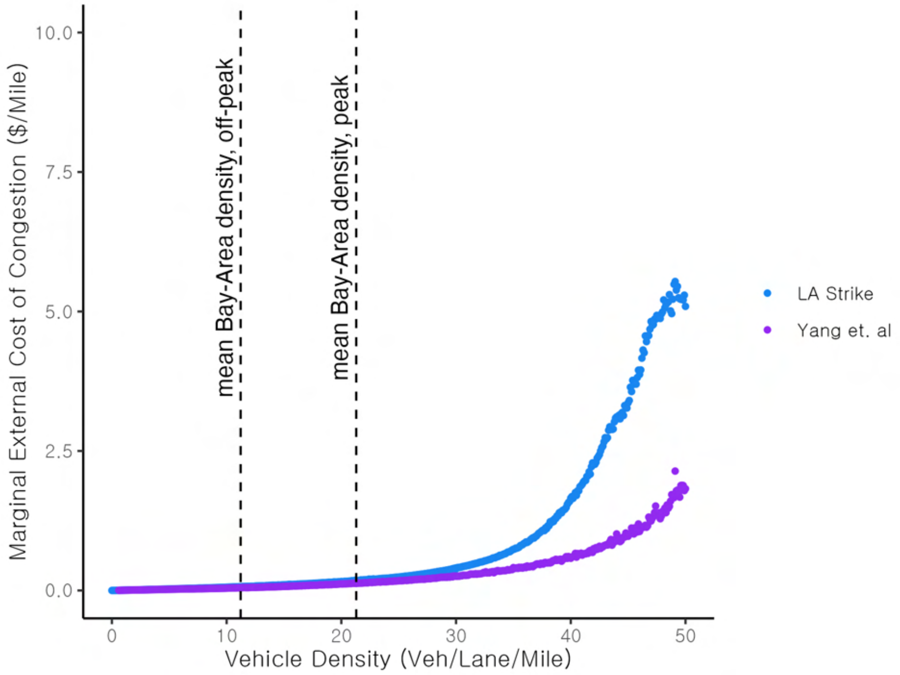

Figure A15: This figure plots two estimates of the marginal external costs of congestion, binned by increments of 0.1 vehicles per lane-mile. The purple curve is reproduced from Figure 6 of Yang, Purevjav, and Li (2020), re-scaled using US values of travel time. The blue curve reflects the results from plugging the IV coefficient in Table A4 into equation 44. The dotted vertical lines represent the mean peak and off-peak density for road-segment observations used to assign congestion externalities to Bay-Area routes in Section 8.

Armed with an alternative marginal external cost curve, I re-estimate San Francisco's peak-hour optimal taxes. Specifically, I use the LA-based MECC estimates from Figure A15 when assigning congestion externalities to routes in a driver's choice set. The remaining inputs to the optimal tax calculation — namely the discrete choice model of travel and the air pollution externality estimates

– are unchanged. Table A5 reports these results. Unsurprisingly, the PeMS-based marginal external cost curve yields higher estimates of per-trip externalities, and higher second-best optimal prices relative to the results in the body of the paper. The ratio of second-best prices to average marginal external costs per trip, however, is similar across specifications.

Table A5 — Second-Best Optimal Congestion Prices using Alternate Congestion Cost Functions

	Yang et al. MECC	LA MECC
Second-Best Price, AM Peak (6-10)	5.90	8.37
Second-Best Price, PM Peak (3-7)	8.50	11.76
Average Marginal Damages, AM Peak (6-10)	7.66	11.26
Average Marginal Damages, PM Peak (3-7)	10.43	14.67

Table A5: This Table compares optimal peak-hour congestion prices estimated using the density-speed relationship estimated by Yang, Purevjav, and Li (2020) and optimal peak-hour congestion prices estimated using the density-speed relationship estimated using the results from Table A4.

F.2. Endongenous Congestion

The second-best cordon price results presented in Section 8 reflect social damages calculated using traffic conditions in untaxed equilibrium. Consistent with the literature on externality taxation, the second-best tax formula in Section 2 phrases optimal taxes as a function of externalities *at the optimum*. As shown in figure A3, the marginal damages associated with driving are not constant in traffic density/speed, meaning that in general, damages at the taxed equilibrium will be different (lower) than those observed in the untaxed equilibrium. Whether the difference between marginal damages calculated at versus away from the optimum is a first-order concern depends on the slope of the marginal damages function and the responsiveness of drivers to taxation.

Figure A15 plots the average peak and off-peak densities on the marginal external cost curves from Yang et al., as well as a second marginal external cost curve used as a robustness check in the previous section. Although the marginal external cost of congestion is steep at high densities, even at peak times, the densities that typically occur on urban roads in the Bay Area fall on a relatively flat part of this curve. For example, reducing the density by 10% on every road segment used to calculate optimal congestion prices for San Francisco in Section 8 would reduce the marginal cost of congestion by roughly 17% on average. For reference, at $9 per trip, New York's congestion pricing policy is expected to reduce traffic by roughly 6.4% in the central business district.

Because it is not clear whether the optimal tax framework would magnify or mute these changes, I also take a simulation approach to understanding the potential impact of endogenous externalities. Specifically, I simulate changes in traffic density under taxation to estimate a lower bound for the second-best optimal cordon prices in San Francisco. To arrive at this lower bound, I iteratively calculate traffic density, driver choices, and taxes until I reach a fixed point where driver's decisions under a given tax vector, τ^*, imply traffic densities (and associated externalities) such that applying Equation 7 to these conditions again yields τ^*. I see this fixed point as a lower bound because it accounts for reductions in congestion, but not induced demand. I discuss this point further at the end of this subsection.

This algorithm is as follows:

Let $\boldsymbol{\tau_0}$ be the cordon taxes calculated using Equation 7 (the second-best tax formula from the theory section) under current traffic conditions, and let $\boldsymbol{\phi_0}$ be the externalities under current conditions, as described in Section 8.

Repeat the following steps until the optimal cordon taxes calculated in any two subsequent iterations ($\boldsymbol{\tau_n}$ and $\boldsymbol{\tau_{n+1}}$) meet some arbitrary element-wise threshold for convergence:
$|\tau_n^h - \tau_{n+1}^h| < \epsilon$, where τ_n^h is element h of the tax vector calculated in step n.

In any iteration, n:

Step 1. *Use the NHTS dataset described in Section 8 to simulate driver choices under $\boldsymbol{\tau_{n-1}}$. In the first iteration, use $\boldsymbol{\tau_0}$, defined above.*

Step 2. *Re-scale the hourly sensor-level road densities by comparing the simulated number of trips that would pass over a given sensor in a given hour under the status quo to the number of trips that would pass over a given sensor in a given hour under the simulation from Step 1.*

Step 3. *Re-estimate the social damages associated with each trip according to the updated hourly traffic densities from Step 2. Call these updated damages $\boldsymbol{\phi_n}$. The details of assigning congestion externalities to routes are covered in Section 8.3.*

Step 4. *Apply Equation 7 (the second-best tax formula from the theory section), using the updated damages, $\boldsymbol{\phi_n}$. Define this tax vector as $\boldsymbol{\tau_n}$.*

Figure A16 plots the results of applying this algorithm to cordon pricing in San Francisco using a convergence threshold of \$0.05. The initial points (iteration one) are the taxes calculated with trip-level damages that reflect current traffic conditions, and are therefore equivalent to the results shown in Section 8 (see row 1 of Table 5). After 10 iterations of recalculating traffic density and taxes, the morning and evening converge to \$4.29 and \$5.90, respectively.

The fixed point from this exercise constitutes a lower bound because it ignores "induced demand," or "rebound," that is, marginal drivers who would have chosen not to take a trip in the absence of road pricing, but choose to take the trip under road pricing due to lower travel times. For any step $n > 1$ in the above algorithm, induced demand would imply traffic densities higher than those estimated by the discrete choice model (Duranton and Turner (2011)). Induced demand would therefore attenuate the difference in traffic conditions between taxed and untaxed equilibria. Optimal taxes that take into account endogenous externalities therefore lie between the results presented in Section 8 and the fixed point calculated in this Appendix.

Figure A16 — Bounding Equilibrium Effects

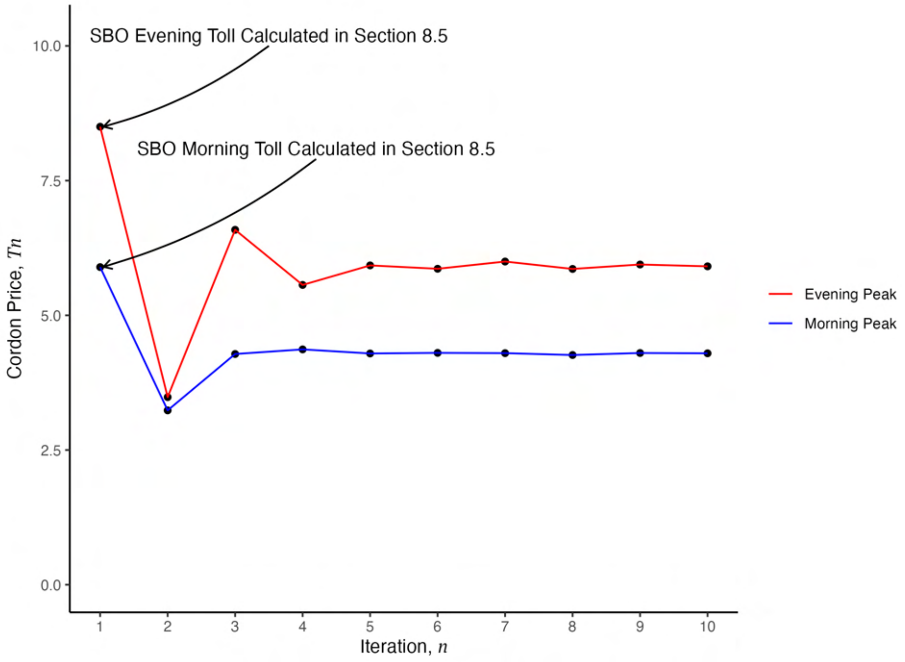

Figure A16: Per-mile driving externalities are larger under denser traffic conditions (Yang, Purevjav, and Li, 2020). As a result, trip-level traffic externalities calculated using untaxed traffic conditions may overestimate optimal taxes. This figure displays the results of the simulation exercise where I iteratively calculate traffic density, driver choices, and taxes until reaching a fixed point where driver's decisions under a given tax vector, τ^*, imply traffic densities (and associated externalities) such that applying Equation 7 yields τ^*. This optimal tax contains two elements: morning (blue) and evening (red) peak-hour prices. The fixed point in this exercise is a lower bound for the second-best peak-hour cordon prices in San Francisco because it ignores "rebound," or "induced demand" —– drivers adding other trips or shifting from other modes in response to the improved traffic conditions under taxation.

G. Congestion Pricing and Accidents

In a manner similar to congestion and pollution externalities, the decision to drive imposes external accident risk on other drivers. Anderson and Auffhammer (2014) show that this externality relies crucially on vehicle weight, and exceeds congestion and pollution externalities for the average US driver.

Large accident externalities for the average US driver, however, may not translate to higher optimal cordon prices because of differences in the risks of accidents in urban vs. rural areas. Empirical studies of the impact of congestion charges on accidents suggest that the value of accident reductions is several orders of magnitude smaller than pollution and congestion externalities. Green, Heywood, and Navarro (2016), for example, find that the London cordon zone reduced overall accidents by 35%, and fatal accidents by 25 to 35%. Because of the relatively low number of fatal auto-related deaths in London, however, the authors value these safety improvements at just £28 million annually. For comparison, Leape (2006) estimates the congestion benefits from London's cordon zone were estimated at £230 million annually. Similarly, Percoco (2016) finds that while Milan's Cordon Zone reduced overall traffic accidents by 16 to 18%, there was no detectable impact on fatal accidents. Valuations of associated benefits are therefore dominated by the roughly $3 billion in reduced pollution and congestion externalities (Gibson and Carnovale, 2015).

The relatively small impact of congestion pricing on severe accidents may reflect the fact that many of the main risk factors for severe traffic accidents — high traffic speeds, drinking and driving, and nighttime driving — are not well targeted by cordon zones. Relatedly, driving in cities in the US and Europe tends to be relatively safe overall, making it straightforward to put bounds on the accident-related benefits that may accrue from congestion pricing.

Together, these pieces of evidence suggest that it is unlikely that accounting for accident externalities would substantively change the conclusions in this paper.

H. Interactions with Existing Taxes and Revenue Requirements

In this Appendix, I cover the interaction between road pricing and existing environmental policies, as well as the literature on whether governmental revenue requirements impact the optimal Pigouvian tax.

H.1. Accounting for Existing Environmental Taxes

Broadly speaking, in the presence of existing Pigouvian taxes the optimal level for an *additional* tax covers the difference between the marginal damages associated with consumption and the existing corrective tax. It is therefore important to account for existing environmental policies that act as a tax on driving when calculating optimal Pigouvian road prices.

There are a number of State and Federal policies that regulate vehicle-related local pollution emissions in California. These policies largely fall into two categories: tailpipe regulations (e.g., catalytic converter requirements) and fuel content regulations (e.g., volatile organic compound regulations). Below, I use a simple model to demonstrate that these two types of policies have different implications for designing an additional tax to internalize the remaining externalities associated with driving. Regulations that impact vehicle costs should *not* be taken into account when calculating optimal road prices. The costs of fuel content regulations, however, should be subtracted from road prices to the extent that these regulations lead to higher per-mile prices.

Existing policies that impact vehicle cost: Consider a representative household with exogenous income I that consumes two goods, driving x and a quasilinear numeraire good z. Driving is associated with an externality, $\phi(a)$. The per-mile magnitude of this externality can be abated (a) on the assembly line at cost $c(a)$. I assume that ϕ_a and c_a are each differentiable, with $c'(a) > 0$ and $\phi'(a) < 0$. The planner's problem is to choose an abatement level, a, and a diving level x to maximize total welfare:

$$W = u(x) + z - \phi(a) \cdot x - c(a) \quad \text{s.t.} \quad I \geq z - p \cdot x$$

The Lagrangian associated with this maximization problem is:

$$\mathcal{L} = u(x) + z - \phi(a) \cdot x - c(a) + \lambda(I - z - p \cdot x)$$

The first-order conditions for an interior solution to this problem are:

$$\lambda = 1$$
$$u'(x) = \phi(a) + p$$
$$\phi'(a)x = c'(a)$$

These conditions imply that the planner equates marginal abatement costs and marginal abatement benefits, and (separately) equates marginal driving costs and marginal driving benefits. The fact that abatement costs do not enter directly into the first order condition for x implies that if a is set at some exogenous level, the policymaker would ignore the abatement cost when choosing the optimal level of driving, only weighing the utility of driving against the externalities that remain after abatement. I therefore ignore the costs of environmental policies that impact vehicle prices (e.g., requirements for catalytic converters) when calculating the level of "unpriced" externalities for drivers.

Existing policies that impact fuel cost: Now consider the same consumer model, but the per-mile magnitude of this externality can be abated by altering fuel content at cost $c(a) \cdot x$. That is, the total abatement cost now depends on the amount of driving, x.

Again consider a policymaker who maximizes total social welfare, W:

$$W = u(x) + z - (\phi(a) - c(a)) \cdot x; \qquad \text{s.t.} \qquad I \geq z - p \cdot x$$

The Lagrangian associated with this maximization problem is:

$$\mathcal{L} = u(x) + z - (\phi(a) - c(a)) \cdot x + \lambda(I \geq z - p \cdot x)$$

The first-order conditions with respect to x and a are:

$$\lambda = 1$$
$$u'(x) = \phi(a) + c(a) + p$$
$$\phi'(a) = c'(a)$$

As above, these first-order conditions imply that the planner equates marginal abatement costs and marginal abatement benefits, and equates marginal driving costs and marginal driving benefits. The crucial difference in this case is that the marginal cost of driving now includes abatement costs. As a result, the social planner will still weigh these costs when setting optimal road prices.

The results in the body of this paper are not adjusted for existing environmental policies that impact the variable cost of driving, namely fuel content regulation. Auffhammer and Kellogg (2011) estimate that fuel content regulations in California cost roughly 12 cents (in 2020 dollars) per gallon. If an average trip crossing San Francisco's cordon boundary travels roughly 10 miles per hour and has a fuel efficiency of 20 miles per gallon, the second-best optimal prices in this paper adjusted for pre-existing fuel regulation would be roughly \$0.06 lower than the results shown in Section 8.

H.2. Accounting for Government Revenue Requirements

The stylized models above raise the question of whether *any* policy that increases the per-mile cost of driving about the competitive equilibrium should be accounted for when calculating optimal road prices. Work by Kopczuk (2003) and Jacobs and De Mooij (2015) suggests that optimal taxation and Pigouvian taxation are separable problems: The calculation of optimal road prices should not take into account taxes that exist as a result of governments balancing the distortions of various revenue sources.

As noted by Jacobs and De Mooij (2015), however, this argument relies on the fact that the marginal cost of public funds is one in an optimal tax system. If the marginal cost of public funds is *not* one, then the optimal second-best Pigouvian tax could be higher or lower than a tax set equal to marginal social damages. Absent strong evidence that the marginal cost of public funds is above or below one, I assume that the marginal cost of public funds is one in the San Francisco Bay Area, and therefore do not adjust optimal road prices to reflect their interactions with the tax system.

I. Assessing External Validity with the NHTS

The appropriateness of using the driving demand model estimated using data from the San Francisco Bay Area (see Section 7) to cordon pricing in other cities depends on whether trips taken in other cities are similarly substitutable, and whether similar correlations between trip-level externalities and price responsiveness are present. In this Appendix, I use data from the 2017 National Household Travel Survey (NHTS) to investigate these relationships for two other US cities — New York and Los Angeles — that are currently considering implementing congestion pricing. I further investigate external validity in Appendix J, where I use public transit data from the Bay Area to examine whether the price-responsiveness of driving trips differs based on the availability of public transit.

Broadly, NHTS data suggest that the relevant relationships in each of these cities are similar to those in San Francisco. Drivers appear similarly able to shift trips temporally. Figure A17, for example, shows that similar fractions of drivers report flexible work schedules in each of these cities. Figure A18 shows that the likelihood of a given trip being flexible varies in New York and Los Angeles in a manner similar to the within-day variation in San Francisco. Figures A19 through A21 provide suggestive evidence that the way that externalities generated by driving — congestion and pollution — vary with price responsiveness in New York and Los Angeles is similar to the way that these externalities vary with price responsiveness in San Francisco. In each city, drivers who "agreed" or "strongly agreed" that gasoline prices impacted their decision to drive were modestly more likely to drive an older, more polluting vehicle. Similarly, drivers who report being more responsive to gas prices report driving along more congested routes, measured as the difference in reported commute time with vs. without traffic.

It is worth noting that these proxies for idiosyncratic externalities and price-responsiveness suggest a weak *positive* correlation, which differs from the results I estimate using FasTrak data. This could result from differences in sample or differences between groups in the mapping between actual actions and responses on the Likert scale.

Figure A17 — Schedule Flexibility by Metro Area

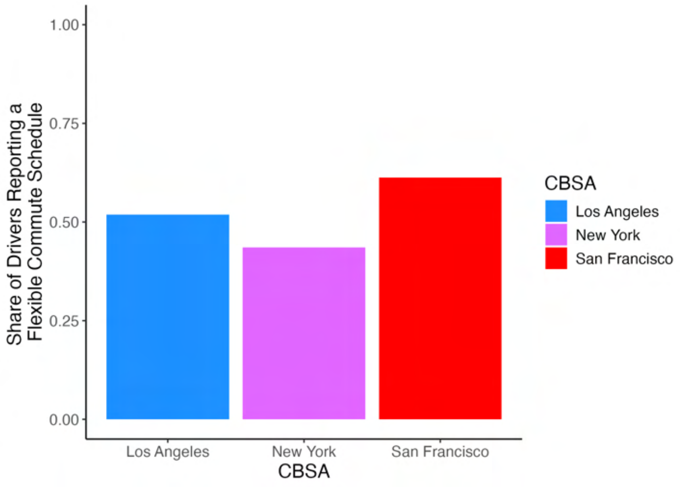

Figure A17: This figure plots the share of drivers who report having a flexible work schedule by metro area, according to the 2017 National Household Travel Survey.

Figure A18 — Schedule Flexibility by Time of Day

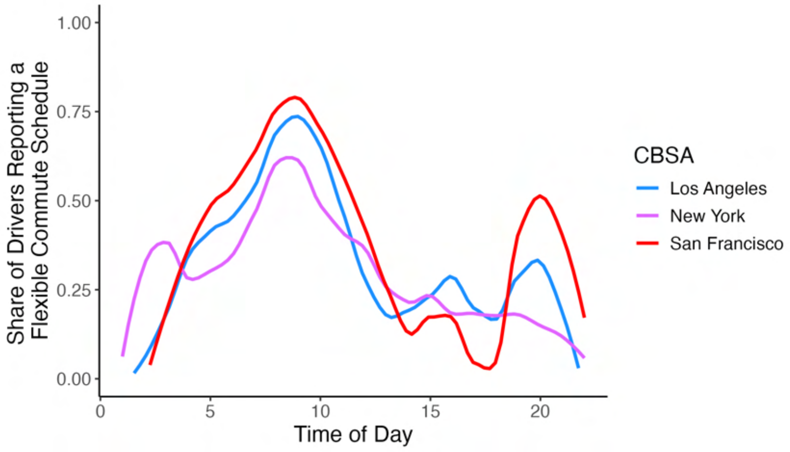

Figure A18: This figure plots the share of drivers who report having a flexible work schedule by time of day and metro area, according to the 2017 National Household Travel Survey.

Figure A19 — Emissions Factors vs. Gas Price Responsiveness

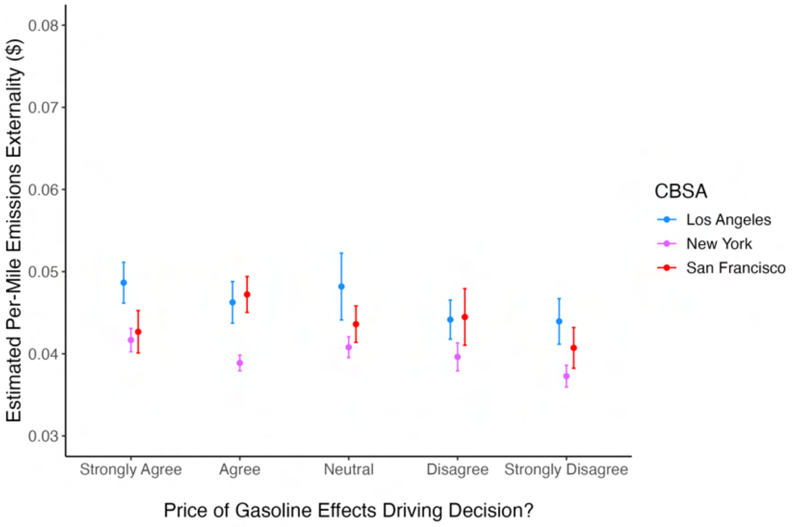

Figure A19: This figure plots estimates emissions factors of vehicles in the 2017 National Household Travel Survey against vehicle owners' self-reported responsiveness of driving demand with respect to gasoline prices. Emissions factors reflect vehicle age and fuel type.

Figure A20 — Vehicle Age vs. Gas Price Responsiveness

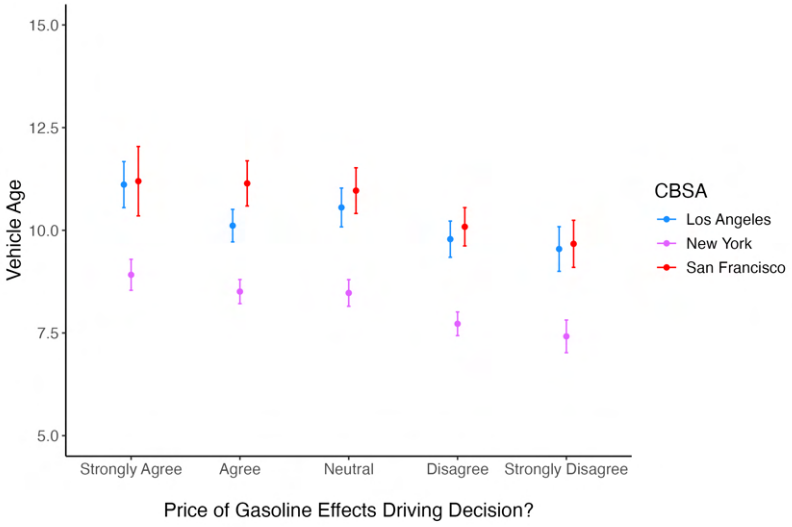

Figure A20: This figure plots vehicle age against vehicle owners' self-reported responsiveness of driving demand with respect to gasoline prices using data from the 2017 National Household Travel Survey.

Figure A21 — Congestion vs. Gas Price Responsiveness

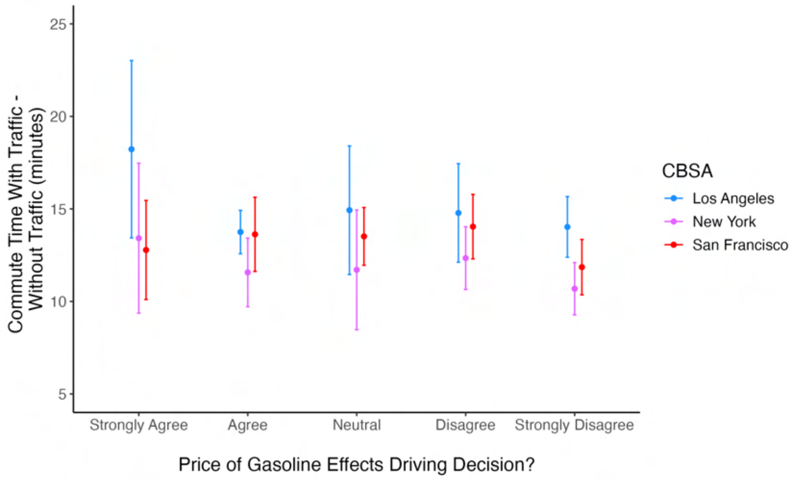

Figure A21: This figure plots self-reported gasoline price responsiveness against the amount of time a driver reports losing to traffic during their commute for drivers in the 2017 National Household Travel Survey.

J. Public Transit

As outlined in Section 2, optimal cordon prices are determined in part by the unpriced social cost of substitutes to peak-hour cordon trips. Understanding how substitution to the outside option (any non-driving activity, including not traveling, or public transit) differs with access to public transportation is therefore crucial for applying the discrete choice model estimated in the Bay Area to other cities.

In this Appendix, I first use data from the Bay Area Rapid Transit system to estimate the magnitude of substitution to public transportation in response to the 2010 change in toll prices on Bay Area Bridges. I then estimate an alternative specification of the logit model presented in Section 7 to test whether drivers with FasTrak devices registered in zip codes with easy walking access to public transit are more price responsive than are drivers who live in areas without access to public transit.

J.1. Public Transit in the San Francisco Bay Area

The Bay Area Rapid Transit (BART) system is a light rail network that connects the eastern Bay Area to the San Francisco Peninsula. BART is the most commonly used public transportation system in the Bay Area and the only rail system with trans-bay lines. The 46 stations that comprise the BART system are plotted in Figure A23. Riders are charged based on the length of their trip; in 2010 the minimum price for a BART trip was $1.75, and most trans-bay trips cost between $3 and $6. Prices for the BART system did not change between July 2009 and July 2012.

BART publishes monthly ridership at the station level. Table A6 and Figure A22 show the change in BART ridership estimated using a regression discontinuity design around the July 1, 2010 change in bridge prices. In my preferred specification (column 2), I estimate that the increase in toll prices on the Bay Area bridges increased BART ridership by an average of 148 weekday rides per station per month. This point estimate corresponds to a 1.8% increase relative to baseline ridership levels. Multiplying this estimate by the number of BART stations (46) implies an estimate of 6,808 additional weekday BART trips per month, or 324 additional BART trips per weekday following the increase in bridge toll prices.

These point estimates suggest that while some drivers switched to public transit, the drivers who switched to public transit represent a small fraction of the total number of drivers who substituted away from driving. For reference, Foreman (2016) finds that the average change in hourly trips following the July 2010 price increases on the Bay, San Mateo, and Dumbarton Bridges were -87, -14, and -48, respectively, implying a total decrease of 3,576 driving trips *per day* on these three bridges. Taking both of these estimates at face value implies that only 9% of the decrease in trans-bay trips were replaced by BART trips.

J.2. Price Responsiveness and Public Transit Access

In Table A7, I re-estimate Equation 9, allowing price-responsiveness to vary with access to public transportation. Specifically, I interact the *price* variable with an indicator variable for whether there is a BART station within 20 minutes walking distance of a given driver's zip code.[16] Point estimates suggest that drivers living in zip codes with transit stops nearby are slightly more price-responsive than are those without transit stops nearby, but this difference is not statistically significant.

In summary, although some Bay Area drivers responded to the increase in bridge tolls by shifting to public transit, the overall share of drivers who switched modes is quite low, and price sensitivity does not vary significantly based on public transit access. A possible explanation for the similarity in price responsiveness across drivers with different access to transit is that unobservable characteristics may determine selection into driving. Put differently, the people who live in transit-rich neighborhoods but nonetheless still choose to drive may have idiosyncratic preferences or pressures that lead them to be reluctant to switch modes, even though they happen to live near transit stations.

While these findings generally support the application of the discrete choice model estimated in San Francisco to areas with different public transit systems, several caveats bear mentioning. First, the BART system is a relatively expensive public transportation system. The magnitude

[16] According to the 2017 NHTS, roughly 90% of respondents who report taking public transit to work walk 20 minutes or fewer to the transit station.

of price-induced substitution away from roads and toward transit undoubtedly depends on the price differential between modes. Conditional on the other attributes of transit trips, cities that have cheaper public transit (e.g., New York) may experience higher cross-price elasticities between vehicle transportation and public transit. Second, the results in this Appendix (and this paper more generally) rely on short-term elasticity estimates, i.e., estimates of substitution elasticities holding fixed housing and work locations, as well as vehicle purchases. As firms and individuals sort in response to cordon prices, public transit access may lead to different long-run elasticities across regions where short-run elasticities look similar. While a full hedonic sorting model is beyond the scope of this paper; one would expect that cities with more connected and cheaper public transit systems would experience more drivers shifting to these modes. All else equal, this would (a) reduce leakage, and (b) increase second-best cordon prices relative to a city with poor public transit options.

Table A6 — Changes Public Transit Ridership

	(1)	(2)	(3)
Post	513^{***}	148^{**}	143
	(37)	(74)	(132)
Station FE	✓	✓	✓
Month of Year FE	✓	✓	✓
Bridge Closure Dummy	✓	✓	✓
Linear Trend in Months		✓	✓
Second-Degree Trend in Months			✓

$^{***}p < 0.01$; $^{**}p < 0.05$; $^{*}p < 0.1$

Table A6: This table displays the results of three regression discontinuity designs estimating the change in public transit ridership in the Bay Area following the July 2010 increase in driving tolls on trans-bay bridges. The *Post* variable is the reported change in monthly rides BART rides at the Station level; there are 46 Stations in the BART system. All regressions include station fixed effects, month-of-year (i.e., calendar month) fixed effects, and a dummy for September 2009, when the Bay Bridge was temporarily closed. Standard errors clustered at the month level are shown in parentheses. In columns (2) and (3), the linear and second-degree trends are fully interacted with the *post* variable. The data run from September 2009 to June 2012 and contain 1,462 station-month observations.

Figure A22 — Public Transit Ridership Regression Discontinuity Plots

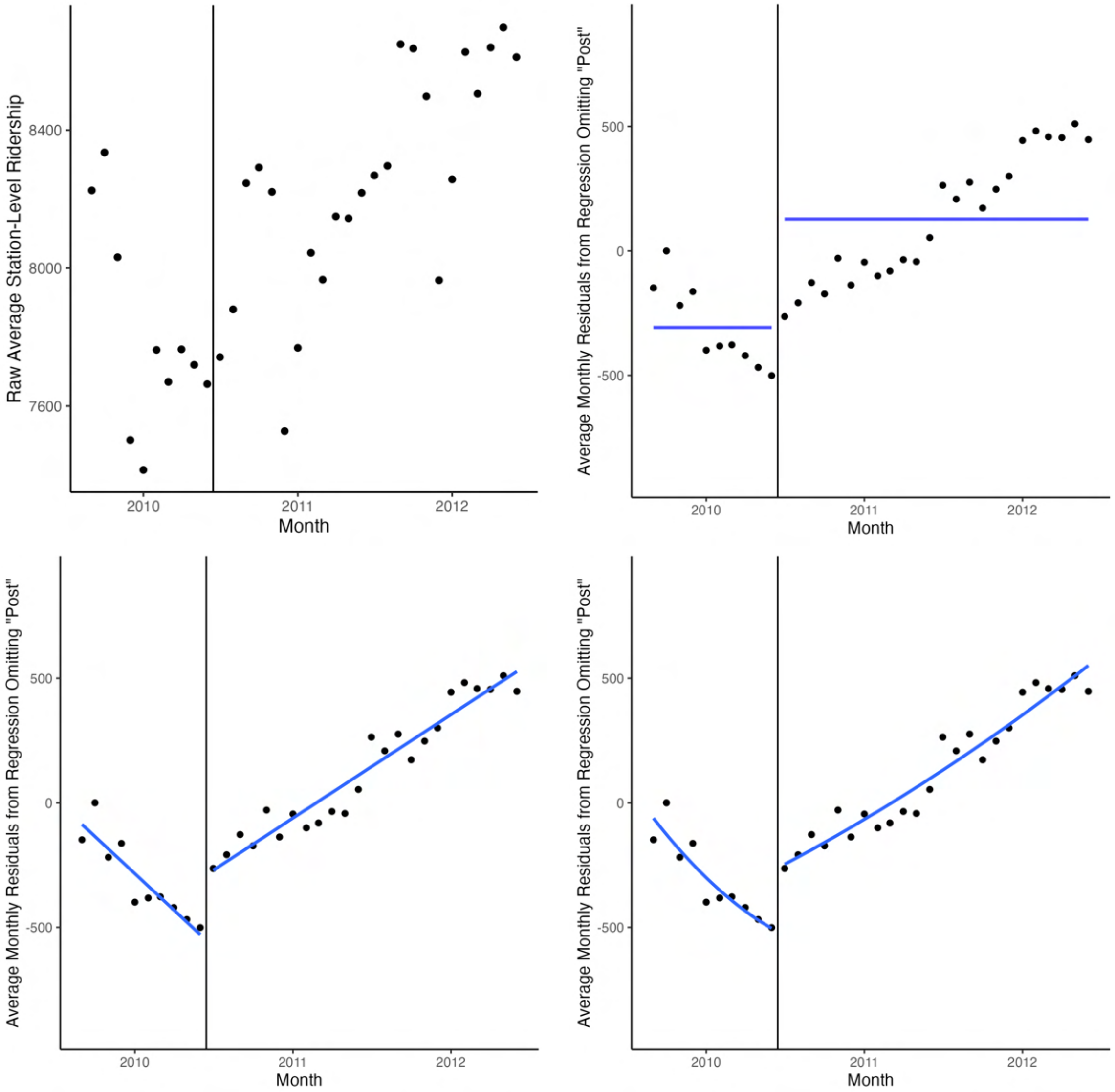

Figure A22: The first pane in this figure plots the monthly station-level turnstile exits averaged across the 46 stations on the Bay Area Rapid Transit (BART) system. The data run from September 2009 to June 2012, and contain 1,462 station-month observations. Panes 2 through 4 plot average monthly residuals from a regression of station-level exist on a set of station fixed effects, month-of-year fixed effects, and a dummy for months where there was a closure on the Bay Area's trans-bay bridges. Pane 2 fits a simple average to the pre vs. post residuals; pane 3 plots the pre and post residuals with a linear fit; pane 4 fits a second-degree polynomial to the pre and post residuals. The discontinuity between the fitted lines in these plots corresponds to the treatment effects in specifications (1) through (3) in Table A6, respectively.

Figure A23 — Access to Public Transit in the San Francisco Bay Area

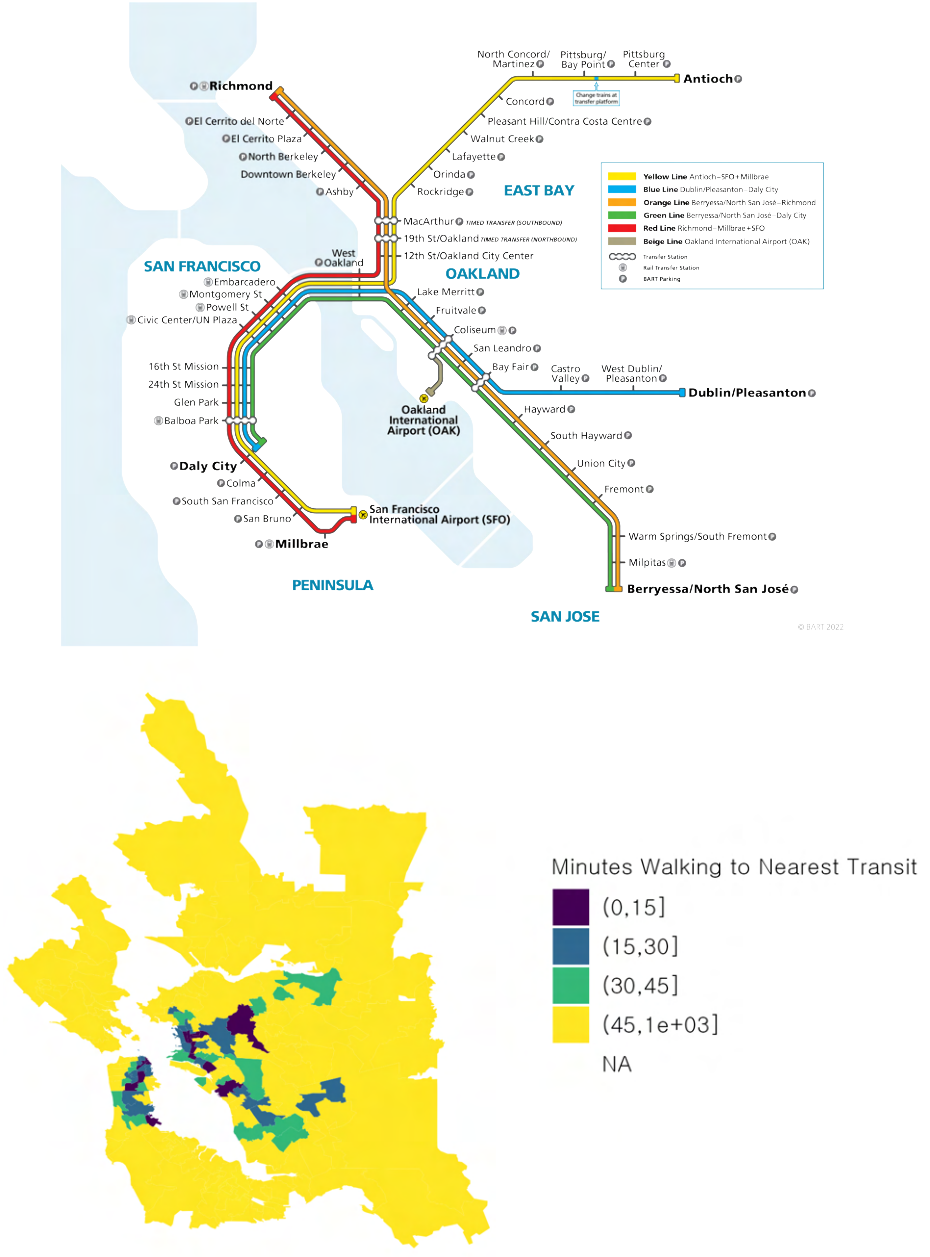

Figure A23: The top panel shows Bay Area Rapid Transit (BART) light rail stations along with Bay Area bridges. The bottom panel plots the estimated walking time (as per Google Maps) from the Google-registered address associated with a given Bay Area zip code (roughly the zip code centroid) to the nearest BART station.

Table A7 — Discrete Choice Model with Price Responsiveness by Transit Access

	Multinomial Logit	Multinomial Logit w/ Price*Transit
Travel Time	-3.69^{***}	-3.69^{***}
	(0.01)	(0.01)
Time Early	-2.55^{***}	-2.55^{***}
	(0.01)	(0.01)
Time Tate	-1.88^{***}	-1.88^{***}
	(0.01)	(0.01)
Price	-0.16^{***}	-0.15^{***}
	(0.02)	(0.02)
Price	-0.16^{***}	-0.15^{***}
	(0.02)	(0.02)
*Price * Nearby Transit*		-0.04
		(0.03)
Peak x Bridge FE	✓	✓

$^{***}p < 0.01$; $^{**}p < 0.05$; $^{*}p < 0.1$

Table A7: Results from a variation of Equation 9, a discrete choice model where drivers choose over routes and times of day, estimated in a two-stage process (multinomial logit and mean utility decomposition) described in Section 6. This model is estimated using FasTrak tolling microdata from the San Francisco Bay Area, as described in Section 5. The dependent variable is whether an individual i elects to take a trip on route r at time of day h. *Travel time* is the travel time (in hours) that driver i would incur by traveling via route r at time h. *Time early* is the number of hours that driver i would arrive before their ideal arrival time if they were to travel via route r at hour h. *Time late* is analogously defined. *Price* is the toll that driver i would incur by traveling via router at hour h. Column (1) is identical to column (1) of Table 3. In Column (2), I interact price with *transit access*, an indicator for whether a BART train station is within 20 minutes walking distance of a given driver's zip code.

K. Low-Income Exemptions

While road pricing can increase economic efficiency, concerns about regressivity have prompted planners in many cities to consider road pricing schemes specifically designed to reduce the incidence on low-income road users. In San Francisco, for example, a majority of the congestion pricing proposals under consideration include some level of income-based exemption (San Francisco County Traffic Authority, 2021). New York's Congestion Pricing Program, if allowed to continue, will partially refund congestion tolls for drivers who make under $60,000 per year (Regional Plan Association (2021)).

Table A8 compares predicted reductions in pollution, congestion, and deadweight loss in San Francisco under (a) the second-best peak hour cordon prices estimated using Equation 7, and (b) the same policy where drivers from low-income households (those with self-reported household income below $75,000 in the NHTS) are exempt from cordon fees. This exercise suggests that the efficiency costs of these exemptions are modest: exempting low-income drivers from cordon pricing in San Francisco would generate reductions in pollution and congestion externalities that are 2-3 percentage points smaller than under an optimal no-exemption policy. These efficiency costs are substantially smaller than my estimates of the efficiency costs that reflect other imperfections in cordon pricing, like charging peak-only vs. hour-specific cordon prices.

The relatively small efficiency cost of exemptions reflects the low proportion of low-income drivers among trips that use the cordon. In the sample of 1,891 trips from the California NHTS with the fastest routes that pass through California's cordon zone, just 9% are taken by drivers from houses with a total annual income of less than $75,000.

Table A8 — Second-Best Cordon Pricing with Low-Income Exemptions

	Performance Relative to the First-Best (%)	
Outcome	Second-Best Peak Hour	With Low Income Exemption
Welfare Gain	0.411	0.407
Congestion	0.406	0.394
Pollution	0.379	0.371

Table A8: Column (1) of this table reproduces the results from Table 6, which compares outcomes under second-best optimal peak hour cordon pricing to outcomes under Pigouvian pricing. The second column in this table compares the first-best policy to the cordon pricing scheme that is identical to the scheme column (1), except that households making less than $75,000 per year are exempt from cordon fees. Income data reflect self-reported household income from the 2017 National Household Travel Survey.

Appendix References

Auffhammer, Maximilian and Ryan Kellogg. 2011. "Clearing the air? The effects of gasoline content regulation on air quality." *American Economic Review* 101 (6):2687–2722.

Duranton, Gilles and Matthew A Turner. 2011. "The fundamental law of road congestion: Evidence from US cities." *American Economic Review* 101 (6):2616–52.

Green, Colin P, John S Heywood, and Maria Navarro. 2016. "Traffic accidents and the London congestion charge." *Journal of Public Economics* 133:11–22.

Heo, Jinhyok, Peter J Adams, and H Oliver Gao. 2016. "Public health costs of primary PM2. 5 and inorganic PM2. 5 precursor emissions in the United States." *Environmental Science & Technology* 50 (11):6061–6070.

Jacobs, Bas and Ruud A De Mooij. 2015. "Pigou meets Mirrlees: On the irrelevance of tax distortions for the second-best Pigouvian tax." *Journal of Environmental Economics and Management* 71:90–108.

Kopczuk, Wojciech. 2003. "A note on optimal taxation in the presence of externalities." *Economics Letters* 80 (1):81–86.

Percoco, Marco. 2016. "The impact of road pricing on accidents: a note on Milan." *Letters in Spatial and Resource Sciences* 9 (3):343–352.

Regional Plan Association. 2021. "Congestion Pricing in New York City." Tech. rep., Regional Plan Association.